TURUN
YLIOPISTO
UNIVERSITY
OF TURKU

# BROWN AND WHITE ADIPOSE TISSUE METABOLISM IN OBESITY

## Stimulation by Cold and Meal Ingestion

Teemu Saari

TURUN YLIOPISTON JULKAISUJA – ANNALES UNIVERSITATIS TURKUENSIS
SARJA – SER. D OSA – TOM. 1637 | MEDICA – ODONTOLOGICA | TURKU 2022

TURUN
YLIOPISTO
UNIVERSITY
OF TURKU

# BROWN AND WHITE ADIPOSE TISSUE METABOLISM IN OBESITY

## Stimulation by Cold and Meal Ingestion

Teemu Saari

TURUN YLIOPISTON JULKAISUJA – ANNALES UNIVERSITATIS TURKUENSIS
SARJA – SER. D OSA – TOM. 1637 | MEDICA – ODONTOLOGICA | TURKU 2022

## University of Turku

Faculty of Medicine
Clinical Physiology and Nuclear Medicine
Doctoral Programme in Clinical Research
Turku PET Centre

## Supervised by

Associate Professor
Kirsi A. Virtanen, MD, PhD
Turku PET Centre
Turku University Hospital and
University of Turku, Turku, Finland

Doctor Mueez U-Din, PhD
Turku PET Centre
Turku University Hospital and
University of Turku, Turku, Finland

## Reviewed by

Docent Tiina Ikäheimo, PhD
Center for Environmental and
Respiratory Health Research
Faculty of Medicine
University of Oulu, Oulu, Finland

Assistant Professor
Maria Chondronikola, PhD, RDN
Department of Nutrition
University of California, Davis, USA

## Opponent

Associate Professor, Jonatan Ruiz
Department of Physical Education and Sport
University of Granada, Granada, Spain

The originality of this publication has been checked in accordance with the University of Turku quality assurance system using the Turnitin OriginalityCheck service.

ISBN 978-951-29-8883-9 (PRINT)
ISBN 978-951-29-8884-6 (PDF)
ISSN 0355-9483 (Print)
ISSN 2343-3213 (Online)
Painosalama, Turku, Finland 2022

UNIVERSITY OF TURKU
Faculty of Medicine
Clinical Physiology and Nuclear Medicine
Turku PET Centre
TEEMU SAARI: Brown and white adipose tissue metabolism in obesity: stimulation by cold and meal ingestion
Doctoral Dissertation, 123 pp.
Doctoral Programme in Clinical Research
April 2022

## ABSTRACT

Adipose tissue (AT) metabolism is dysregulated in obesity. Reduced brown adipose tissue (BAT) glucose uptake during cold exposure is associated with obesity and insulin resistance, but the role of fatty acids in human BAT metabolism is unclear. Rodent BAT is activated by meal ingestion, in humans it is unclear if BAT is stimulated by meal. Increased subcutaneous adipose tissue (SAT) perfusion after a meal is reduced in obesity, leading to the accumulation of ectopic fat, increasing the risk of type 2 diabetes (T2D). Visceral adipose tissue (VAT) accumulation is considered more detrimental to metabolic health compared to SAT. Discovering what changes occur in VAT metabolism in obesity, and after weight loss, could help elucidate the role of VAT in metabolic disease.

Using positron emission tomography (PET) BAT fatty acid uptake (FAU) and perfusion were investigated in lean and subjects with obesity during stimulation by cold exposure or meal ingestion and at basal state. The effects of meal ingestion and the gut hormone glucagon-like peptide (GIP-infusion on SAT and VAT perfusion were studied using PET in subjects with obesity prior to and after bariatric surgery, as well as in healthy control subjects.

Cold stimulated BAT FAU and perfusion were blunted in subjects with obesity compared to controls. In subjects with obesity BAT FAU was lower already at basal state, resembling SAT FAU. Meal stimulation increased BAT perfusion similarly to cold exposure, showing that meal ingestion activates BAT. Meal and GIP-induced increase of SAT perfusion were blunted in subjects with obesity prior to bariatric surgery. Bariatric surgery normalizes SAT perfusion response to a meal, but not to GIP stimulation. VAT perfusion after a meal or GIP stimulation was similar between controls and subjects with obesity and was unaffected by bariatric surgery, however after surgery VAT blood flow response to a meal was seen already at 20 min after a meal, compared to 50 min before bariatric surgery.

This thesis work shows that obesity has a blunting effect on BAT FAU during cold exposure and at basal level. Meal activates BAT: postprandial BAT perfusion was similar to cold exposure perfusion. Additionally, bariatric surgery was shown to normalize postprandial SAT blood flow response.

KEYWORDS: adipose tissue, cold exposure, meal stimulation, obesity, bariatric surgery, perfusion, metabolism, positron emission tomography

TURUN YLIOPISTO
Lääketieteellinen tiedekunta
Kliininen fysiologia ja isotooppilääketiede
Turun PET-keskus
TEEMU SAARI: Ruskean ja valkoisen rasvan aineenvaihdunta lihavuudessa: kylmäaltistuksen ja ruokailun vaikutukset
Väitöskirja, 123 s.
Turun kliininen tohtoriohjelma
Huhtikuu 2022

## TIIVISTELMÄ

Lihavilla henkilöillä rasvakudoksen aineenvaihdunta on häiriintynyt. Vähentynyt ruskean rasvan (BAT) toiminta on yhdistetty ylipainoon ja insuliiniresistenssiin. Kylmäaltistus lisää BAT:n glukoosin sisäänottoa, mutta on epäselvää, mikä on vapaiden rasvahappojen rooli ihmisen BAT:n aineenvaihdunnassa. Jyrsijöillä BAT aktivoituu ruokailun jälkeen, mutta vielä ei ole selvää, aktivoiko ruokailu myös ihmisen BAT:a. Ruokailu lisää ihonalaisen rasvakudoksen (SAT) verenkiertoa. Lihavilla tämä vaikutus on heikentynyt, mikä lisää rasvan varastoitumista muihin kudoksiin. Tämä lisää riskiä sairastua tyypin 2 diabetekseen. Vatsaontelon sisäistä rasvaa (VAT) pidetään terveydelle haitallisempana kuin SAT:tä. VAT:n roolista aineenvaihdunnallisissa sairauksissa voidaan saada lisää tietoa tutkimalla lihavuuden ja lihavuusleikkauksen siihen aiheuttamia muutoksia.

Tutkimuksen tavoitteena oli selvittää lihavuuden vaikutuksia BAT:n rasvahappoaineenvaihduntaan ja verenkiertoon kylmäaltistuksessa positroniemissiotomografiaa käyttäen. Lisäksi tavoitteena oli tutkia ruokailun BAT:ta aktivoivaa vaikutusta. Lisäksi tutkittiin ruokailun ja glucose-dependent insulinotropic polypeptiden (GIP) vaikutusta SAT:n ja VAT:n verenkiertoon lihavilla henkilöillä ennen lihavuusleikkausta ja sen jälkeen, sekä verrokeilla.

Kylmäaltistus lisää BAT:n rasvahappojen sisäänottoa ja verenkiertoa normaalipainoisilla henkilöillä, mutta ei lihavilla. Lihavilla BAT:n rasvahappojen sisäänotto oli jo huoneenlämmössä matalampi kuin normaalipainoisilla henkilöillä. Ruokailu lisäsi BAT:n verenvirtausta samalle tasolle kuin kylmäaltistus, mikä osoittaa ruokailun aktivoivan BAT:ta.

SAT:n verenkierto ruokailun ja GIP-infuusion jälkeen oli ylipainoisilla matalampi kuin normaalipainoisilla. Lihavuusleikkaus normalisoi ylipainoisten henkilöiden SAT:n ruokailun jälkeisen vasteen, mutta ei vaikuttanut GIP:n aiheuttamaan aktiivisuuteen. VAT:n verenkierto lisääntyi ruokailun ja GIP-infuusion jälkeen samankaltaisesti normaalipainoisilla ja ylipainoisilla. Lihavuusleikkauksen jälkeen ruokailun aiheuttama VAT:n verenkierron lisääntyminen nähtiin jo 20 min ruokailun jälkeen, kun ennen lihavuusleikkausta vaste oli nähtävissä vasta 50 min ruokailun jälkeen. GIP:n aiheuttamaan vasteeseen lihavuusleikkauksella ei ollut vaikutusta.

Tässä tutkimuksessa osoitettiin, että BAT:n rasvahappojen sisäänotto on heikentynyt lihavilla kylmäaltistuksessa ja huoneenlämmössä. Ruokailu aktivoi BAT:ta, sillä ruokailun jälkeinen BAT:n verenkierto oli samalla tasolla kuin kylmäaltistuksessa. Lisäksi osoitettiin, että lihavuusleikkaus normalisoi ruokailun aiheuttaman verenkierron lisääntymisen SAT:ssa.

AVAINSANAT: rasvakudos, kylmäaltistus, ruokailu, lihavuus, lihavuusleikkaus, verenkierto, aineenvaihdunta, lihavuus, postitroniemissiotomografia

# Table of Contents

# Abbreviations

| | |
|---|---|
| $^{18}$F-FDG | $^{18}$F-2-fluoro-2-deoxy-D-glucose |
| $^{18}$F-FTHA 14(*R,S*)- | $^{18}$F-fluoro-6-thia-heptadecanoic acid |
| $^{1}$H MRS | Proton magnetic resonance spectroscopy |
| $A_{2A}R$ | Adenosine receptor $A_{2A}$ |
| AC | Adenylyl cyclase |
| ACSL | Long-chain acyl-CoA synthetase |
| ATP | Adenosine triphosphate |
| AUC | Area under the curve |
| BAT | Brown adipose tissue |
| BMI | Body mass index |
| CAC | Citric acid cycle |
| cAMP | 3'-5'-cyclic adenosine monophosphate |
| $CB_1R$ | Cannabinoid receptor type 1 |
| CNS | Central nervous system |
| CoA | Coenzyme A |
| CT | Computed tomography |
| Dio2 | Deiodinase 2 |
| EE | Energy expenditure |
| FABPpm | Plasma membrane fatty acid binding protein |
| FASN | Fatty acid synthase |
| FATP | Fatty acid transport protein |
| FAU | Fatty acid uptake |
| FFA | Free fatty acid |
| FOV | Field of view |
| GCP | Good clinical practice |
| GIP | Glucose dependent insulinotropic peptide |
| GIPR | Glucose dependent insulinotropic peptide receptor |
| GLP-1 | Glucagon-like peptide-1 |
| GLUT1 | Glucose transporter 1 |
| GLUT4 | Glucose transporter 4 |
| HDL | High density lipoprotein |

| | |
|---|---|
| $HOMA_{IR}$ | Homeostasis model assessment of insulin resistance |
| HU | Hounsfield unit |
| $K_i$ | Net influx rate |
| LD | Laser doppler |
| LDL | Low density lipoprotein |
| LPL | Lipoprotein lipase |
| MRI | Magnetic resonance imaging |
| Myf5 | Myogenic factor 5 |
| OGTT | Oral glucose tolerance test |
| PET | Positron emission tomography |
| PKA | Protein kinase A |
| RARE | Retinoic acid responsive element |
| ROS | Reactive oxygen species |
| SAT | Subcutaneous adipose tissue |
| SUV | Standardized uptake value |
| T2D | Type 2 diabetes |
| T3 | Triiodothyronine |
| T4 | Thyroxin |
| TAC | Time activity curve |
| TG | Triglyceride |
| TRE | Thyroid hormone responsive element |
| TSH | Thyroid stimulating hormone |
| UCP1 | Uncoupling protein 1 |
| VAT | Visceral adipose tissue |
| VEGF | Vascular endothelial growth factor A |
| VLDL | Very low density lipid |
| VOI | Volume of interest |
| WAT | White adipose tissue |

# List of Original Publications

This dissertation is based on the following original publications, which are referred to in the text by their Roman numerals:

I Saari TJ, Raiko J, U Din M, Niemi T, Taittonen M, Laine J, Savisto N, Haaparanta-Solin M, Nuutila P, Virtanen KA. Basal and cold-induced fatty acid uptake of human brown adipose tissue is impaired in obesity. *Scientific Reports*, 2020 Sep 1;10(1):14373. doi:10.1038/s41598-020-71197-2

II U Din M*, Saari T*, Raiko J, Kudomi N, Maurer SF, Lahesmaa M, Fromme T, Amri EZ, Klingenspor M, Solin O, Nuutila P, Virtanen KA. Postprandial Oxidative Metabolism of Human Brown Fat Indicates Thermogenesis. *Cell Metabolism*. 2018 Aug 7;28(2):207–216.e3. doi:10.1016/j.cmet.2018.05.020

III Saari T, Koffert J, Honka H, Kauhanen S, U Din M, Wierup N, Lindqvist A, Groop L, Virtanen KA, Nuutila P. Obesity associated blunted subcutaneous adipose tissue blood flow after meal is improved after bariatric surgery. *The Journal of Clinical Endocrinology & Metabolism*, 2022;, dgac191, https://doi.org/10.1210/clinem/dgac191

* Equal contribution

# 1 Introduction

Worldwide obesity increases each year, with over 1.9 billion overweight and 650 million adults with obesity around the world (Abelson and Kennedy, 2004; WHO, 2019), and 1 in 4 of adults in Finland with obesity (Koponen et al., 2018). Obesity increases the risk for metabolic disorders, cardiovascular disease as well as other non-communicable diseases. Obesity is characterized by increased accumulation of adipose tissue (AT), and AT dysfunction. Different AT depots have been shown to contribute differently to obesity-related metabolic dysfunctions (Zwick et al., 2018).

AT has a role in energy storage as well as acting as an endocrine organ. Postprandially AT takes up lipids and they are stored within the cell (Frayn, 2002). Dysfunction in AT metabolism and blood flow decreases this fat storage and the lipids are instead stored in other tissues such as muscles and the liver. Accumulation of lipids in other tissues (ectopic fat) leads to dysfunctions in these tissues, eventually causing adverse effects on insulin sensitivity, glucose homeostasis, and lipid metabolism.

Bariatric surgery induces rapid weight loss and improvement of metabolic health (Adams et al., 2017). AT mass decreases rapidly and changes in its substrate uptake, as well as blood flow, are seen after bariatric surgery. It is not yet clear how these changes are mediated. AT blood flow is closely related to its metabolism, and blood flow regulation is an essential part of its function (Frayn et al., 2003). There are changes in incretin secretion rates seen after bariatric surgery (Nauck and Meier, 2018). However, it is not clear how and if increased incretin secretion contributes to metabolic improvement after bariatric surgery. Since AT plays a vital role in postprandial lipid handling, any of its dysfunction is reflected in other tissues, causing further harm. It is vital to understand changes caused by obesity and weight loss in different AT depots.

Brown adipose tissue (BAT) is a thermogenic AT type, which expends energy to produce heat in response to cold stimulation (Cannon and Nedergaard, 2004). The discovery of active BAT in adult humans increased the interest in its function and potential role as a therapeutic target to combat obesity, since BAT metabolism is reduced in humans with obesity (Orava et al., 2013), and increased BAT activity is related to improved insulin sensitivity (Chondronikola et al., 2014). In rodents, BAT

ablation leads to obesity (Himms-Hagen, 1979; Lowell et al., 1993). Most human studies focus on BAT glucose metabolism to assess BAT activity (Virtanen et al., 2009), but rodent BAT utilizes free fatty acids (FFA) more than glucose in heat production (Ma and Foster, 1986). In addition to cold exposure, meal ingestion stimulates rodent BAT thermogenesis, however, the evidence of human meal-induced thermogenesis is sparse. Improving our understanding of human BAT metabolism and how this tissue is activated is important to assess its potential role as a therapeutic target. Increasing BAT activity could increase energy expenditure, and therefore, remains an interesting and potential treatment option for weight reduction or maintenance as well as for improving insulin sensitivity.

AT depots play an important role in obesity-related metabolic changes. Understanding which stimulators of AT activity are dysfunctional in obesity would help us understand changes in its function in obesity. Positron emission tomography (PET) enables the study of different AT depots in humans non-invasively. This thesis aimed to investigate the effects of obesity on the metabolism of different AT depots (BAT, SAT, and VAT) during stimulated states.

# 2 Review of the Literature

## 2.1 Adipose tissue

### 2.1.1 White adipose tissue

The primary function of white adipose tissue (WAT) is to store energy within the adipocytes, as a single lipid droplet in the form of triglycerides (TG). WAT depots can be categorized by anatomical location; SAT, intra-abdominal or VAT, bone marrow adipose tissue, epicardial adipose tissue, perirenal adipose tissue, periadventitial adipose tissue (Ibrahim, 2010). The most prominent depots are SAT and VAT. SAT comprises over 80% of total WAT and VAT around 15% (Walker et al., 2014). Different AT depots are metabolically distinct. Changes in fat distribution, cell size, and dysregulation of WAT metabolism are linked to increased risk of metabolic disease (Guilherme et al., 2008, 2019; Morigny et al., 2021; Ouchi et al., 2011a, 2011b). While the release and storage of energy remains the principal function of WAT, it also has a role in whole-body glucose and lipid metabolism (Morigny et al., 2021). The excess accumulation of adipose tissue can lead to insulin resistance and reduced AT glucose clearance. WAT acts as an endocrine organ, secreting leptin, adiponectin, and fatty acids, as well as other adipokines, to regulate metabolic homeostasis (Kim and Moustaid-Moussa, 2000; Singla, 2010).

### 2.1.2 Brown adipose tissue

BAT is a thermogenic tissue, and the main function of BAT is to generate heat without muscle shivering. Brown adipocytes contain multiple small lipid droplets and more mitochondria compared to WAT. The mitochondria of brown adipocytes have a unique protein located on the inner membrane, uncoupling protein 1 (UCP1) (Cannon and Nedergaard, 2004; Ricquier, 2005). UCP1 enables the thermogenic capacity of BAT, by uncoupling mitochondrial respiration from adenosine triphosphate (ATP) synthesis (Nicholls and Locke, 1984). Instead of ATP heat is produced. BAT is activated by exposure to cold, via the sympathetic nervous system (SNS). BAT plays an important role in the thermal regulation of small animals such as mice and rats (Cannon and Nedergaard, 2004).

BAT was thought to play an important role in heat production of infants since skeletal muscles are still undeveloped and lack the capacity to maintain body heat (Aherne and Hull, 1966). BAT mass in infants can be 1–5% of their body weight (Cannon and Nedergaard, 2004). It was thought that BAT activity diminishes during adolescence when hormonal changes occur (Nedergaard et al., 2010), however, there were reports of human BAT depots based on postmortem analysis of infants and adults showing BAT depots in the cervical or axillary depot, perirenal/adrenal area, and along major blood vessels and arteries (Enerbäck, 2010; Heaton, 1972). It was also suggested that BAT was more prominent in adult humans who had been exposed to cold while working in outdoor conditions (Hassi, 1977; Huttunen et al., 1981). There was no evidence that these BAT depots were metabolically active. Several reports of symmetrical uptake patterns in the neck area of $^{18}$F-2-fluoro-2-deoxy-D-glucose ($^{18}$F-FDG) during PET studies were published, but it was not confirmed that the area of activation was indeed BAT (Barrington and Maisey, 1996; Engel et al., 1996; Hany et al., 2002; Nedergaard et al., 2007; Yeung et al., 2003). Combining PET imaging with anatomical reference obtained by computed tomography (CT) led to three simultaneous reports in 2009 which concluded that BAT was indeed metabolically active in human adults (van Marken Lichtenbelt et al., 2009; Saito et al., 2009; Virtanen et al., 2009).

### 2.1.3 Beige adipose tissue

Beige adipocytes, also referred to as brite adipocytes (”**br**own **i**n whi**te**”), are the third type of adipocyte, which exist within WAT. Beige adipose tissue expresses high levels of UCP1, and it is capable of producing heat, similarly to BAT (Lidell et al., 2013, 2014). Beige adipose tissue is activated during prolonged cold exposure, to increase heat production (Cannon and Nedergaard, 2004; Waldén et al., 2012; Zingaretti et al., 2009). Before beige adipose tissue was characterized, it was thought that most murine WAT could differentiate into BAT, during prolonged exposure to high levels of intracellular cyclic AMP (cAMP), caused by cold exposure or by adrenergic stimulation (Cannon and Nedergaard, 2004). However, while they share a similar function, brown adipocytes originate from progenitor cells expressing myogenic factor 5 (Myf5) and beige adipocytes do not (Xue et al., 2007). It has also been shown that the UCP1-expression of brown and beige adipocytes is controlled by separate routes (Xue et al., 2005, 2007).

Human BAT is thought to resemble rodent beige adipose tissue more closely, than rodent ‘classical’ BAT, (Lidell et al., 2013; Sharp et al., 2012; Wu et al., 2012), although it does share molecular signatures with both (Cypess et al., 2013; Jespersen et al., 2013; Lidell et al., 2013). These differences need to be considered when attempting to translate results from rodents to humans. Feeding mice a high-energy

diet and housing them in thermoneutral conditions has been shown to reduce the thermogenic potential of beige adipose tissue in middle-aged mice, where only BAT retained its' thermogenic potential (de Jong et al., 2019).

## 2.2 Adipose tissue metabolism

In the postprandial state, the fatty acids received from food are transported from the small intestine to circulation in the form of chylomicrons and very-low-density lipoproteins (VLDL). When TGs stored in chylomicron form and VLDL reach adipose tissue, they are hydrolyzed into FFAs by lipoprotein lipase (LPL), which is located on the capillary endothelium (Figure 1). FFAs are taken up by the cell by the action of a fatty acid translocase CD36, plasma membrane fatty acid binding protein (FABPpm), fatty acyl CoA synthetases (FATP and ACSL) or caveolin-1. A portion of LPL-derived FFA is not taken up by the cell and instead binds to albumin and is transported via circulation to other tissues. FFA taken up into the tissue can either be used as energy by beta-oxidation or converted back to TG and stored within the cell (Morigny et al., 2021).

Both LPL and CD36 are stimulated by insulin, increasing the storage of fatty acids into adipose tissue after meal ingestion (Fielding and Frayn, 1998). Insulin also stimulates the esterification of FFAs within the tissue, via action by acyl-CoA synthetase, leading to increased TG storages within the cells' lipid droplet(s). LPL is essential in the clearance of TG from circulation (Kersten, 2014). The deletion of AT-specific LPL genes in mice leads to an inability to store exogenous FFAs as TGs in adipose tissue, and *de novo* lipogenesis was markedly increased (Weinstock et al., 1997).

Adipocytes also use glucose to synthesize TGs, by *de novo* lipogenesis (Collins et al., 2011). In this process, glucose is first taken up by the cell via glucose transporters (GLUT1 and GLUT4). Glucose is metabolized in the cell through glycolysis to produce pyruvate, which is converted to acetyl-CoA and incorporated into the citric acid cycle (CAC) (also known as Krebs' cycle) to produce citrate, or ATP via oxidation of glucose. Citrate is further processed towards acetyl-CoA and malonyl-CoA, which are used by the fatty acid synthase (FASN) to produce palmitate, which is converted into TG and stored within the adipocyte.

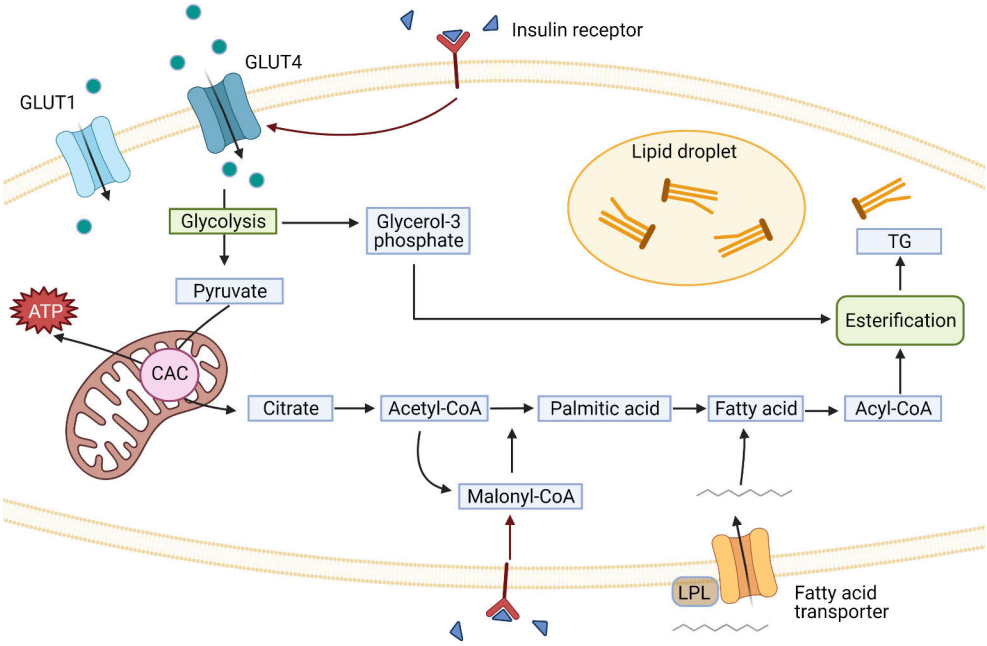


**Figure 1.** Principles of adipose tissue glucose and fatty acid uptake and the process of storing triglycerides (TG) in lipid droplets inside the adipocyte. Modified from (Lafontan and Langin, 2009; Morigny et al., 2021). Adenosine triphosphate (ATP); coenzyme A (CoA); citric acid cycle (CAC); lipoprotein lipase (LPL); fatty acid (FA); glucose transporter 1 (GLUT1); glucose transporter type 4 (GLUT4).

Energy stored as TG within adipocytes can be broken down to glycerol and FFAs, by a process called lipolysis (Zechner et al., 2012). Lipolysis is most active when there is a need for energy, for example during exercise and fasting conditions. During the postprandial state, lipolysis is inhibited by insulin.

The blood flow of AT is closely related to its' metabolism (Frayn and Karpe, 2014; Samra et al., 1996). AT metabolism is quickly changed from fat release to fat storage after meal ingestion (Coppack et al., 1992; Summers et al., 1996), and the reverse is true after stimulation in response to exercise (Heinonen et al., 2012). Since TGs and FFAs are not water-soluble, and cannot freely diffuse between cells, the blood flow of AT plays an important role in the mobilization and storage of fat. While the increased need for fat storage plays a role in increased postprandial AT perfusion, it is likely not the only contributing factor. Postprandial AT perfusion is increased even after ingestion of a meal composed entirely of glucose, but not after intravenous infusion of glucose and insulin mimicking the achieved plasma glucose and insulin levels in oral glucose administration (Karpe et al., 2002a). An increase in AT blood flow after a meal is seen after 30-60 minutes, but the peak of circulating

chylomicrons occurs after around 3 hours (Frayn and Karpe, 2014). It is possible that increased blood flow is required for signaling as well as substrate mobilization in AT.

### 2.2.1 AT metabolism during glucose-dependent insulinotropic peptide stimulation

GIP is a hormone secreted by K cells located in the proximal small intestine, and this hormone is released in response to the ingestion of a meal containing either glucose or fat (Falko et al., 1975). GIP increases insulin release after meal ingestion. GIP receptors (GIPR) are expressed in the pancreas, AT, gut, bone, and trachea (Thondam et al., 2020; Yip et al., 1998) However, the increase of insulin secretion caused by GIP only occurs in the presence of glucose (Kim and Egan, 2008). GIP secretion after meal ingestion is not impaired in subjects with T2D (Calanna et al., 2013), but the effects of GIP seem blunted (Nauck et al., 1993).

GIP increases SAT blood flow, in the presence of insulin (Asmar et al., 2010, 2016a). This response is blunted in obesity (Asmar et al., 2014), and partially normalized after conventional weight loss (Asmar et al., 2016b; Nauck and Meier, 2018). In mice, GIP has a role in increased fat accumulation when insulin effects are blunted (Zhou et al., 2005).

GIP increases FFA esterification and the storage of TAG into AT (Thondam et al., 2020). In vitro and in rodents GIP has been shown to increase LPL activity and expression, increasing TG clearance (Eckel et al., 1979; Knapper et al., 1995). However, there is no human evidence of increased LPL activity by GIP (Thondam et al., 2017).

### 2.2.2 BAT metabolism during cold exposure

When exposed to cold, most mammals rely on skeletal muscles and BAT to generate heat. BAT thermogenesis is regulated by the central nervous system (CNS) and more specifically in the preoptic area of the hypothalamus (Morrison and Nakamura, 2019; Morrison et al., 2012). Cold temperature is detected by thermoreceptors located on the skin and various areas of the body core, sending afferent signals to the hypothalamus, where they are processed together with signals from thermosensitive neurons in the brain (Morrison and Nakamura, 2019; Morrison et al., 2012; Nakamura and Morrison, 2007). This causes efferent neural signals to increase BAT sympathetic nerve activity, increasing heat production. Noradrenaline is released by the SNS, binding to adrenergic receptors on the surface of brown adipocytes (Figure 2). Rodent BAT expresses alpha-1, alpha-2, beta-1, beta-2, and

beta-3 adrenoceptors (Cannon and Nedergaard, 2004). The beta-3 adrenergic receptors have been regarded as the essential receptors regulating BAT thermogenesis. While BAT is producing heat plasma noradrenaline levels are elevated. Administration of noradrenaline or adrenaline increases BAT metabolism similarly to cold exposure. Adrenergic stimulation caused by cold exposure has both acute and chronic effects. In mice, adrenergic stimulation causes the release of adenosine in BAT, which increases beige adipocyte recruitment and energy expenditure via adenosine receptor $A_{2A}$ ($A_{2A}R$) activation (Gnad et al., 2014). In humans, the administration of adenosine increased BAT perfusion and additionally cold exposure decreased the density of $A_{2A}R$ in BAT (Lahesmaa et al., 2018a). This shows that adenosine has a prominent role in increasing human BAT oxidative metabolism and that in humans, cold exposure increases the production of adenosine in BAT. Murine brown adipocytes themselves do not possess beta-2 adrenoceptors (Bengtsson et al., 2000), but they are present in the tissue (Revelli et al., 1992; Rothwell et al., 1985), possibly predominantly located in the vasculature (Cannon and Nedergaard, 2004). Recently it was shown that human BAT thermogenesis is not activated by mirabegron, a beta-3-adrenoceptor agonist, indicating that beta-2 might have a more prominent role in human BAT compared to rodents (Blondin et al., 2020). Cold stimulation causes the activation of adenylyl cyclase (AC), which is responsible for converting ATP into 3'-5'-cyclic adenosine monophosphate (cAMP). cAMP activates protein kinase A (PKA), leading to conformation changes in the lipid droplet coating protein perilipin. This allows hormone-sensitive lipase (HSL), which is also activated by PKA, to hydrolyze the TGs stored in the lipid droplets, releasing FFAs. These released FFAs activate UCP1.

The ability of BAT to produce heat is enabled by UCP1, a protein located on the inner membrane of the mitochondria (Figure 2) (Cannon and Nedergaard, 2004). During heat production, UCP1 enables protons to move against the electrochemical gradient, and instead of ATP heat is produced (Cannon and Nedergaard, 2004; Ravussin and Galgani, 2011). UCP1 activity is regulated in several different ways; peroxisome proliferator responsive element (PPRE), thyroid hormone responsive element (TRE), and retinoic acid responsive element (RARE) are all thought to be regulators of UCP1 transcription (Yao et al., 2011). UCP1 activity is also regulated by reactive oxygen species (ROS) (Mills et al., 2018). ROS production in respiratory complex I is stimulated by succinate (Murphy and O'Neill, 2018).

The thyroid hormone signaling chain, which is regulated by deiodination, has a role in BAT adrenergic signaling (Bianco and McAninch, 2013). Thyroxin (T4), produced by the thyroid gland, is converted to its' active form triiodothyronine (T3) by deiodinase 2 (Dio2). Stimulation of beta-3 adrenergic receptors increases

Dio2 expression in BAT. T3 upregulates UCP1 expression, increasing the thermogenic potential of BAT (Lee et al., 2012). T3 -/- mice have a reduced ability to maintain their body temperature and they are not able to reduce the amount of excess energy received from food (Cannon and Nedergaard, 2004; Nedergaard and Cannon, 2010).

BAT relies on glucose, fatty acids, and intracellular TGs for its' primary energy sources in heat production. In rodents, BAT relies on fatty acids up to 90% over glucose to generate heat (Ma and Foster, 1986). Their primary source of fatty acids for oxidation in BAT is thought to be the intracellular lipid pool (Ma and Foster, 1986), but it is unclear if BAT substrate utilization is similar in humans and rodents. In mice when a BAT-specific gene involved in lipolysis was knocked out BAT function remained even at a fasting state (Shin et al., 2017). When lipolysis was defective in both BAT and WAT the mice were sensitive to cold during fasting state, but not when food was available. It is possible that in rodents BAT can function even without lipolysis of internal TG stores.

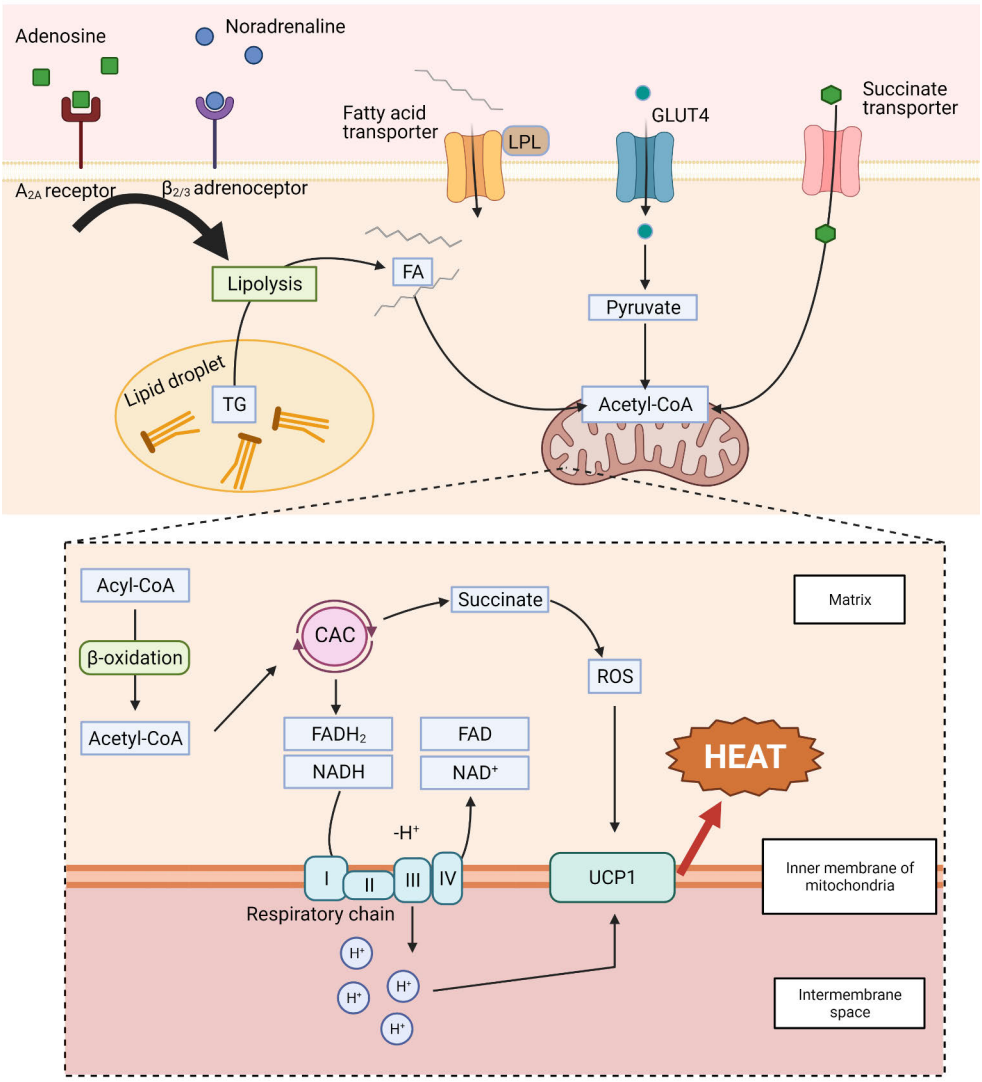


**Figure 2**. Figure showing the principles of BAT activation during cold exposure and heat production by respiratory uncoupling by uncoupling protein 1 (UCP1), located in the inner membrane of mitochondria. Modified from (Morigny et al., 2021; Murphy and O'Neill, 2018). Coenzyme A (CoA); citric acid cycle (CAC); flavin adenine dinucleotide hydroquinone form ($FADH_2$); flavin adenine dinucleotide (FAD); nicotinamide adenine dinucleotide (NADH); oxidized nicotinamide adenine dinucleotide ($NAD^+$); reactive oxygen species (ROS); lipoprotein lipase (LPL); fatty acid (FA); glucose transporter type 4 (GLUT4).

#### 2.2.2.1 Cold exposure studies in humans

Cold exposure is commonly used as a stimulus in studies investigating BAT. Cold exposure methods can be roughly divided into acute and chronic cold exposure.

Chronic cold exposure is characterized as being prolonged and/or occurring recurrently (Blondin et al., 2014; Labbé et al., 2015) and causing cold acclimation (Castellani and Young, 2016). Acute cold exposure is often shorter in duration but can also be more severe. Acute cold exposure methods vary between studies in terms of used clothing, type of exposure (air, water, ice-packs, temperature-adjustable blankets or suits), an area which is exposed (whole body or local cooling) (van Marken Lichtenbelt et al., 2009; Nedergaard et al., 2007; Orava et al., 2013; U Din et al., 2016; Virtanen et al., 2009).

Previous reports have shown symmetrical $^{18}$F-FDG uptake patterns in the neck and supraclavicular area (Cohade et al., 2003; Nedergaard et al., 2007; Yeung et al., 2003). While it was suggested that BAT could be responsible for this phenomenon, the site of this increased radiotracer uptake was not confirmed to be BAT. Instead, the first confirmed reports of BAT activity in the supraclavicular area in adults were published in 2009 (Cypess et al., 2009; van Marken Lichtenbelt et al., 2009; Virtanen et al., 2009). Cold exposure increased BAT GU by 15-fold in lean healthy subjects and its existence was confirmed by analysis of samples of the supraclavicular fat depot, which expressed several BAT mRNA markers (Virtanen et al., 2009).

In humans, BAT GU rate is increased by acute cold exposure (Orava et al., 2011, 2013; Ouellet et al., 2012; Virtanen et al., 2009). BAT GU is related to its blood flow during cold exposure (Orava et al., 2011). Insulin stimulation also increases BAT GU but does not affect its perfusion (Orava et al., 2011). This would indicate that stimulation by cold and insulin are regulated differently. BAT GU measured during acute cold exposure did not increase from baseline after subjects underwent a 4-week cold acclimation protocol (Blondin et al., 2014).

Cold exposure induces upregulation of genes involved in lipid metabolism in human BAT (Chondronikola et al., 2016). In lean subjects BAT FAU measured by $^{18}$F-FTHA PET is higher compared to some skeletal muscles and SAT during cold exposure (Ouellet et al., 2012). The same study shows that oxidative metabolism, measured by increased uptake of $^{11}$C-acetate, increases during cold exposure. An earlier study has shown that BAT oxidative metabolism is related to FAU during cold exposure (U Din et al., 2016). As mentioned above, while cold acclimation over 4 weeks did not increase BAT GU, it augmented the oxidative capacity of BAT (Blondin et al., 2014). Suppression of lipolysis of intracellular TG stores using nicotinic acid reduces BAT oxidative metabolism in human BAT, showing that intracellular lipids are an integral part of BAT metabolism (Blondin et al., 2017). It should be mentioned that nicotinic acid reduces lipolysis in all adipocytes, both brown and white, by inhibiting adenylate cyclase activity (Lule et al., 2016).

The prevalence of BAT in humans is not well known because of difficulties in BAT detection, as well as varying methods of employing cold exposure and considerable inter-individual variation in the activation of BAT. A previous study showed

that subjects demonstrating no supraclavicular BAT activation in $^{18}$F-FDG PET scans still showed expression of BAT-specific genes (Lee et al., 2011). The expression levels were lower compared to subjects with detectable BAT activity in $^{18}$F-FDG PET scans. While there are no exact thresholds that define the presence of BAT, there have been efforts to produce guidelines for studying it in humans, to allow easier comparisons of results and standardizing methods (Chen et al., 2016). Muscle shivering thermogenesis has been reported to reduce human BAT energy metabolism (Ouellet et al., 2012), which might also affect BAT detection. In rodents, BAT plays an important part in energy homeostasis and thermoregulation (Cannon and Nedergaard, 2004). However, compared to rodents the amount of BAT humans possess is significantly smaller (Carpentier et al., 2018). Related to this, while there is evidence that BAT contributes to increased energy expenditure and thermoregulation in humans, the contribution is relatively smaller compared to rodents, and skeletal muscles play a larger role in humans (Acosta et al., 2018; Brychta and Chen, 2017; van Marken Lichtenbelt, 2021; Ouellet et al., 2012).

### 2.2.3 BAT metabolism in postprandial state

In rodents, meal ingestion increases BAT respiratory rate (Glick et al., 1981, 1983, 1984, 1985). In addition, BAT UCP1 activation increases after a meal in rodents (Essen et al., 2017; Lupien et al., 1985), as well as BAT glucose metabolism and FA synthesis (Saito et al., 1989). It has been proposed that postprandial activation of BAT is mediated through the SNS (van Baak, 2008). Eating increases plasma glucose and insulin concentrations, which are sensed by the hypothalamus. Administration of insulin has been shown to increase BAT glucose uptake in lean subjects, however, there was no increase in perfusion (Orava et al., 2011). There is evidence of other pathways, which play a role in postprandial thermogenesis: administration of propranolol, a non-selective beta-adrenergic receptor agonist, did not influence postprandial thermogenesis in human males (Thörne and Wahren, 1989). Bile acids (BA) activate BAT G protein-coupled receptor TGR5, which results in increased cAMP levels, which in turn activates type 2 iodothyronine deiodinase (Dio2). As previously described Dio2 converts T4 to T3, enabling T3 to increase UCP1 expression in BAT, thus increasing thermogenic potential. BAs also act as ligands for the nuclear farnesoid X receptor (FXR), which when activated decreases the expression of cholesterol 7α-hydroxylase, which is the rate-limiting enzyme involved in BA synthesis, allowing for increased BA synthesis to occur (Kawamata et al., 2003; Parks et al., 1999). FXR agonist fexaramine increases the browning of white adipose tissue and thermogenesis in mice (Fang et al., 2015). Oral administration of BA che-

nodeoxycholic acid (CDCA) increased the energy expenditure of healthy human females and CDCA was shown to increase TGR5 signaling in vitro in human-derived brown adipocytes (Broeders et al., 2015).

#### 2.2.3.1 Postprandial BAT studies in humans

Meal-induced thermogenesis in humans has not been widely studied and the role of meal-induced thermogenesis may have in regulating energy homeostasis is not clear (Kozak, 2010; Peterson et al., 2017). In a retrospective study, it was shown that patients who were instructed to eat a high-fat, very-low-carbohydrate, protein-permitted diet on the night prior to an $^{18}$F-FDG PET-scan showed less BAT activity compared to patients who underwent the scans in a fasting state (Williams and Kolodny, 2008). A previous study also demonstrated that meal ingestion compared with fasting before cold exposure decreased BAT $^{18}$F-FDG standardized uptake value (SUV) (Vrieze et al., 2012). Furthermore, in lean subjects a carbohydrate-rich, high-calorie meal increased BAT GU compared to fasting, however cold exposure still increased BAT GU more than meal ingestion (Vosselman et al., 2013). Cold acclimation over 4 weeks did not increase dietary FAU or GU in BAT, however, its oxidative metabolism did increase (Blondin et al., 2017).

## 2.3 Effects of obesity on adipose tissue

### 2.3.1 WAT in obesity

Obesity is characterized by an excess of adipose tissue. Accumulation of VAT has been more strongly associated with obesity-related complications than SAT, such as type 2 diabetes (Cinti, 2005; Després and Lemieux, 2006; Fox et al., 2007; Gallagher et al., 2009; Ibrahim, 2010). Excess AT can lead to dysfunction of adipocytes, which contributes to metabolic disorders such as decreased insulin sensitivity, and an increase of circulatory lipids and glucose. The spillover resulting from reduced fatty acid storage of AT postprandially can lead to the accumulation of TGs in other tissues such as muscles and the liver (Frayn, 2002). Another contributing factor is that insulin-stimulated inhibition of FFA release from AT is reduced in obesity (Coppack et al., 1992). Excessive accumulation of this ectopic fat leads to insulin resistance (Hocking et al., 2013; Trouwborst et al., 2018).

AT secretes the hormone adiponectin, which is involved in stimulating fatty acid oxidation in skeletal muscle and inhibition of endogenous glucose production in the liver (Fang and Judd, 2018). Even though adiponectin is secreted by AT, obesity and T2D have been associated with decreased adiponectin levels in plasma (Arita et al., 1999). Additionally, decreased levels of adiponectin, caused by a polymorphism in

adiponectin encoding gene, are associated with an increased prevalence of diabetes (Kara et al., 2002; Stumvoll et al., 2002). Adiponectin is known to increase the hepatic insulin action, suppressing glucose production in the liver, and decreasing the flux of fatty acids into the liver, increasing insulin sensitivity (Berg et al., 2001; Yamauchi et al., 2003). Adiponectin also prevents ectopic lipid accumulation, the storage of lipids in the liver and muscles, by increasing lipid storage into adipocytes (Fu et al., 2005). The mechanism of insulin sensitivity action caused by adiponectin is thought to be the enhancement of AMPK activation (Wu et al., 2003; Yamauchi et al., 2002). Adiponectin also has anti-inflammatory effects, which may have a positive effect on insulin sensitivity (Holland et al., 2011; Ohashi et al., 2010; Turer and Scherer, 2012).

Leptin is released from adipose tissue into circulation. Leptin acts as a circulating factor, controlling for whole-body metabolism through hypothalamic regulation and as a paracrine factor activating adipose afferent fibers, which signal to CNS (Friedman and Halaas, 1998; Montez et al., 2005). Leptin controls the satiety signal: activation of leptin receptors in the hypothalamus suppresses food intake and increases energy expenditure (Tilg and Moschen, 2006; Valassi et al., 2008). In Vitro, leptin decreases lipogenesis, increases TG hydrolysis, and increases FA oxidation (William et al., 2002). Leptin increases the sympathetic signaling to WAT (Geerling et al., 2014) and BAT (Rezai-Zadeh and Münzberg, 2013), increasing lipolysis. Afferent fibers, which innervate WAT, express leptin receptors, and they are activated if leptin is injected into adipose tissue (Guilherme et al., 2019).

During expansion AT expresses vascular endothelial growth factor A (VEGF), which promotes vascularization. In obesity, AT is often hypoxic due to insufficient vascularization, which promotes fibrosis and inflammation (Sun et al., 2011). Vascularization and innervation of adipose tissue are closely connected (Carmeliet and Tessier-Lavigne, 2005; Slavin and Ballard, 1978) VEGF knockout mice have reduced vasculature, and increased hypoxia, increased inflammation, accelerated development of metabolic disease. Induced VEGF-expression in these knockout mice reverses the effects (Sung et al., 2013). VEGF increases adipose tissue innervation and increases nerve density and it has been shown that VEGF-A has a role in the control of adipose tissue function and in improving systematic energy metabolism and glucose homeostasis via increased adipose tissue vascularization (Park et al., 2017; Sun et al., 2012; Sung et al., 2013).

### 2.3.2 BAT in obesity

The role of BAT in human metabolism and maintenance of energy homeostasis is still unclear. Increased BAT activity measured by substrate uptake, blood flow, or

oxygen consumption has been linked to a more favorable metabolic profile in humans (Blondin et al., 2015; Hanssen et al., 2015; Lee et al., 2014; Orava et al., 2011, 2013; Saito et al., 2009). It is not clear whether decreased BAT activity is the result of obesity or one of the contributing factors of obesity.

In rodents, it has been shown that reduced BAT activity leads to obesity, and unfavorable glucose and lipid profiles (Bartelt et al., 2011; Berbée et al., 2015; Cannon and Nedergaard, 2004; Himms-Hagen, 1979). On the other hand, increasing BAT activation in rodents can lead to prevention or remission of metabolic disease or obesity (Ghorbani et al., 1997; Harms and Seale, 2013). Transplantation of functional BAT to Ob/Ob mice increased their energy expenditure and improved glucose homeostasis (Liu et al., 2015).

Increased BAT activation is an interesting and potential target for therapeutics to reduce obesity and increase insulin sensitivity. Earlier studies of potential BAT activators via beta3-adrenoceptor agonists proved difficult despite promising results in mice (Arch, 2002, 2008). Different routes of activation and recruitment of BAT may prove more favorable targets if tissue specificity of beta3-adrenoceptor activation cannot be solved.

### 2.3.3 Effects of bariatric surgery on WAT and BAT

Bariatric surgery is an effective way to achieve a relatively fast and sustained weight loss. Compared to conventional weight loss by calorie restriction, more rapid and greater weight loss and higher rates of remission are seen in subjects undergoing bariatric surgery (Gloy et al., 2013). Weight loss after bariatric surgery is also related to better glucose homeostasis, insulin sensitivity, and a healthier circulatory lipid profile (Buchwald et al., 2009). Bariatric surgery has been shown to prevent type 2 diabetes, and to increase remission from type 2 diabetes, with reported rates of 86.6% of cases showing improvement or remission of diabetes (Adams et al., 2012, 2017; Buchwald et al., 2009; Sjöström et al., 2004).

After bariatric surgery the volume of SAT is reduced more in comparison to VAT, but a larger portion of VAT is reduced, and the reductions are associated (Bazzocchi et al., 2015; Guiducci et al., 2007; Merlotti et al., 2017; Toro-Ramos et al., 2015). However, there is still a gap in our understanding of how the tissue-specific metabolism of SAT and VAT is affected by the weight loss due to bariatric surgery, particularly under stimulated conditions. Different adipose tissue depots have distinct responses to hormonal stimulation, and it has been shown that they can react differently to weight loss (Asmar et al., 2014; Frayn and Karpe, 2014).

BAT function is not completely lost in subjects with obesity (Hanssen et al., 2016; Mihalopoulos et al., 2020; Vijgen et al., 2011), and weight loss may even in-

crease its metabolism. After bariatric surgery BAT fatty acid uptake increases in basal conditions among morbidly obese women, measured by $^{18}$F-FTHA PET/CT (Dadson et al., 2018). In another study, BAT activity, measured by semi-quantitative SUV of $^{18}$F-FDG during cold exposure, increased in morbidly obese subjects after bariatric surgery (Vijgen et al., 2012).

## 2.4 In-vivo investigation methods of adipose tissue

### 2.4.1 Metabolism and substrate utilization

#### Positron emission tomography

PET imaging can be used to quantify tissue-specific metabolism in vivo (Krishnamoorthy et al., 2017). PET-imaging utilizes biologically active substances, like glucose, which are labeled with a radioactive component ($^{18}$F, $^{15}$O for example). Other substances, such as water or oxygen can also be labeled, to measure tissue blood flow or oxygen consumption. After administration, the radioactive components begin to decay, and positrons are released. The positron interacts with an electron leading to annihilation, causing two gamma photons to travel in opposite directions. These photons are then detected by the PET scanners, and these detection events are used to construct 3D images, where each voxel has a radioactivity/time value attached to it. PET data can be used in conjunction with CT or MRI images, which provide anatomical reference, and the exact site of activity seen in PET images can be pinpointed.

Data from PET images can be used to calculate tissue-specific uptake rates of substances that the tracer is mimicking. The most used radiotracer is $^{18}$F-FDG, a glucose analog, used for quantification of glucose uptake rate. Other radiotracers include $^{11}$C-acetate, which is used to assess oxidative metabolism, and $^{18}$F-FTHA, a palmitate analog, is used for tissue-specific fatty acid uptake quantification. Quantification of tissue-specific uptake rates requires the use of dynamic scanning, where the PET scan is performed at timed intervals. Arterial sampling is required if an image-derived arterial input function cannot be created. Image-derived input function requires the arch of the aorta, abdominal aorta, or iliac arteries to be visible in the PET image. Arterial sampling is also required if the tracer used is metabolized, to measure the amount of metabolized and un-metabolized tracer in the blood.

$^{18}$F-FTHA is a palmitate analog, which is taken up by the cell using the same mechanism as FFAs. $^{18}$F-FTHA contains a sulfur bridge, which causes the molecule to become trapped inside the cell after it has gone through the initial steps of β-oxidation (figure 3) (DeGrado et al., 1991, 2000; Guiducci et al., 2007). This allows

us to quantify tissue-specific fatty acid uptake rate using multiple time graphical analysis, also called Gjedde-Patlak-plot. In this method the amount of tracer accumulating in tissue over time is compared to the amount of tracer activity in plasma over time, producing net influx rate of tracer (Ki). Tissue-specific FAU can be calculated by multiplying the net influx rate of $^{18}$F-FTHA with plasma FFA concentration.

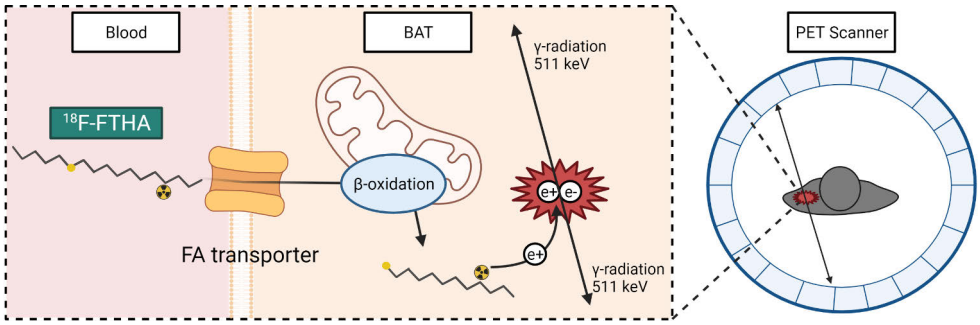


**Figure 3.** $^{18}$F-FTHA is taken up by the cell, after which it undergoes partial beta-oxidation, which is stopped due to the sulfur bridge (represented as the yellow dot on the carbon chain), trapping the tracer in the cell. Gamma radiation from the annihilation event is detected by the PET scanner. Modified from (Guiducci et al., 2007; Krishnamoorthy et al., 2017).

Inert substances such as water or oxygen can also be used as radiotracers. Tissue perfusion rates can be calculated by using radiolabeled water ($^{15}$O-$H_2O$) commonly referred to as radiowater. Radiowater is inert and freely diffusible and the method to calculate tissue perfusion is based on the principle of exchange of inert gas between blood and tissues and the Fick's principle (Kety, 1985; Kety and Schmidt, 1945; Oikonen, 2014). Inhalable radiotracers are also available, such as $^{15}O_2$, which can be used to measure BAT oxygen consumption (Muzik et al., 2012; U Din et al., 2016).

PET imaging can also be used to study receptor occupancy. For example, cannabinoid receptor type 1 ($CB_1R$) can be used to locate BAT in rodents (Eriksson et al., 2015), and in lean humans, $CB_1R$ is upregulated during acute cold exposure (Lahesmaa et al., 2018b).

Static image acquisition is used to provide a standardized uptake value (SUV). SUV is a semi-quantitative method; it shows the relation between activity in tissue compared to the amount of tracer injected in relation to the bodyweight of the subject. This technique is more commonly used than dynamic imaging, and it is useful in detecting tumors and cumulative tracer uptake, however, it does not allow for quantification of tracer influx rate.

PET imaging is not available everywhere, and it is an expensive method. Radiotracers are short living, rendering it difficult to transport them over long distances.

Optimally, radiotracer production should be in the vicinity of the research facilities. Subjects taking part in PET studies are exposed to radiation, which limits the number of scans per subject. The resolution of PET images is limited, partially due to the movement of positrons before annihilation occurs and limits caused by detector size, as well as several other factors that affect spatial resolution (Moses, 2011). This limit of resolution prevents the study of small BAT depots. The limited field of view of PET scanners restricts the area which can be studied simultaneously.

### 2.4.2 Physiological reference and tissue composition

#### X-ray computed tomography

X-ray computed tomography (CT) utilizes ionizing radiation coupled with an electronic detector array to produce cross-sectional images of the body. The images produced are based on tissue densities and they can be expressed in the Hounsfield unit scale (HU). HU describes the radiodensity based on comparative density to water, which is considered 0 HU. CT can be used to measure Hounsfield units of the BAT region, and the triglyceride contents of the measured area can be estimated (Blondin et al., 2017; Hanssen et al., 2015, 2016; Ouellet et al., 2012; U Din et al., 2017).

#### Magnetic resonance imaging

In addition to providing anatomical reference when used in conjunction with PET-imaging, MRI can be used for BAT fat fraction measurements and T2* relaxation times. Proton magnetic resonance spectroscopy ($^{1}$H MRS) has been used to measure BAT temperature and triglyceride content (Holstila et al., 2017; Koskensalo et al., 2017).

### 2.4.3 Other perfusion quantification methods

#### $^{133}$Xe washout

$^{133}$ Xenon ($^{133}$Xe) washout technique has been used to quantify adipose tissue blood flow since 1966, and it has been thought of as the gold standard (Goossens and Karpe, 2008; Larsen et al., 1966; Melvin and McQuaid, 2018). $^{133}$Xe is a lipophilic, gamma-emitting molecule that is injected in gaseous form into adipose tissue. When injected, it can be measured how much of $^{133}$Xe is in water phase and fat phase of adipose tissue. Fat content can be considered constant and changes in the water phase are modulated by blood flow. Radioactivity can be detected with a skin-mounted

detector or by a gamma camera. This method is relatively cheap, and the resulting quantified absolute flow is reproducible.

### Laser Doppler technique

Laser doppler (LD) ultrasound is a non-invasive method, which can be used to measure AT blood flow. LD monitors the movement of red blood cells in a large blood vessel, within the tissue. The blood vessels used in the analysis must be large enough to enable accurate measures of their volume, so this technique is not feasible with smaller blood vessels, such as the arteries/arterioles in adipose tissue. In the future, skin-mounted probes may be developed, which would allow LD to measure tissue blood flow in deeper tissues.

# 3 Aims

The general aim of this thesis was to investigate AT metabolism, focusing on BAT, SAT, and VAT metabolism under different stimulated conditions, and to investigate the effects of obesity on these AT depots. The specific aims of studies in this thesis were:

- To investigate how BAT FAU and perfusion are stimulated by cold exposure, and to learn if it is blunted in subjects with obesity. (I)

- To evaluate if meal ingestion stimulates BAT FAU and perfusion, how meal stimulation compares to stimulation by cold exposure, and if obesity has a blunting effect. (II)

- To investigate SAT and VAT perfusion under stimulated conditions, either after a mixed meal or during GIP-infusion, and explore differences in responses to stimulation between control and subjects with obesity. (III)

- To assess how bariatric surgery affects the responses of SAT and VAT perfusion to stimulation by meal ingestion or GIP infusion. (III)

# 4 Materials and Methods

## 4.1 Study subjects

For studies I and II healthy lean and obese subjects were recruited, both male and female, between ages 20–50 years. The general characteristics of study participants are provided in table 1.

Study III included 10 subjects with morbid obesity with T2D, who were scheduled for bariatric surgery (gastric bypass n=5, vertical sleeve gastrectomy n=5), and 10 healthy control subjects between ages of 18–60 years. The study was registered to the clinical trials database (clinicaltrials.gov), identifier number NCT01880827. The general characteristics of participants in study III are in table 1.

Exclusion criteria included smoking, use of medication potentially influencing study variables (a washout period of 24 hours for antihypertensives, 72 hours for anti-diabetic drugs except for long-acting GLP-1 receptor agonists 10 weeks), impaired glucose tolerance or lipid profile in subjects participating in study I and II as well as control subjects in study III, history of cardiovascular disease, food restrictions affecting the meal protocol, participation in other studies which involve radiation exposure, and pregnancy or lactation.

**Table 1.** General characteristics of study participants in studies I–III. Data presented as mean (SD).

| Study | Group | Age (years) | Gender (F/M) | BMI (kg/m$^2$) | Plasma glucose (mmol/l) | Plasma insulin (mU/l) |
|---|---|---|---|---|---|---|
| I-II | Control | 36.60 (10.50) | 18F / 11M | 25.09 (2.47) | 5.42 (0.47) | 7.17 (3.11) |
| I-II | Obese | 42.40 (8.68) | 6F / 4M | 33.56 (3.36) | 5.71 (0.65) | 12.83 (6.54) |
| III | Control | 46 (9.41) | 8F / 2M | 23.10 (2.41) | 5.1 (0.37) | 4.5 (2.1) |
| III | T2D Before Surgery | 51.7 (7.01) | 8F / 2M | 40.8 (5.92) | 6.53 (1.09) | 19.4 (9.35) |
| III | T2D After Surgery | 52.3 (6.73) | 8F / 2M | 35.15 (6.26) | 5.65 (0.72) | 12.2 (7.13) |

## 4.2 Study outlines

### 4.2.1 Studies I–II

To quantify BAT fatty acid uptake rate and perfusion during cold exposure and at room temperature, each subject underwent two PET/CT imaging sessions. The study outline is depicted in figure 4. One of the imaging sessions was conducted during acute cold exposure protocol, by using cooling blankets. The temperature of the cooling blankets was adjustable and could be increased to avoid shivering. The temperature of the blankets was increased if study subjects reported shivering to the investigators, or if shivering was observed by the investigators. After a two-hour cold exposure period, at the start of the scan, the average temperature of the water inside the blanket was 15.0 ± 2.0°C for lean subjects and 10.0 ± 4.8°C for subjects with obesity. Room temperature scans were conducted as a negative control, to assess the baseline BAT activity. They did not involve any cooling protocol and were conducted at approximately 22°C. Cold exposure and room temperature scans were conducted in a random order, and there was at least a 7-day interval between studies.

Study II was part of the same project as study I, but in this study, the focus was on postprandial BAT fatty acid uptake and blood flow, with cold exposure studies acting as positive controls. The study procedure is depicted in figure 4. Each study subject was imaged using PET/CT once at room temperature after receiving a mixed meal containing a standardized meal and secondly during acute cold exposure. The standardized meal contained 542 kcal (58% carbohydrates, 25% fat, and 17% protein). The cold exposure was conducted as described in study I, using cooling blankets. Cold exposure and postprandial scans were conducted in a random order, with a minimum of 7 days between the study visits.

To quantify tissue-specific perfusion, an intravenous injection of $^{15}O$-$H_2O$ and a dynamic emission scan of the thoracic region was performed (frames: 6 × 5 sec, 6 × 15 sec, 8 × 30 sec). Radiowater was produced using Hidex Radiowater Generator (Hidex Oy, Turku, Finland).

To quantify tissue-specific FAU $^{18}F$-FTHA, a palmitate analog, was used. After $^{15}O$-$H_2O$ had sufficiently decayed (i.e. 10 minutes), an intravenous injection of $^{18}F$-FTHA was given and a dynamic emission scan was performed (frames: 1 × 60 sec, 6 × 30 sec, 1 × 60 sec, 3 × 300 sec, 2 × 600 sec) on the same area as with radiowater. $^{18}F$-FTHA was produced as previously described (Degrado, 1991; Savisto et al., 2018).

All scans in studies I–II were performed with the same PET/CT scanner (Discovery 690 PET-CT scanner; General Electric Medical Systems, Milwaukee, WI, USA). After the acquisition of scanning data computerized reconstruction was carried out. Quantitative corrections were applied to PET image data, including detector

normalization, dead-time, radioactive decay, randoms, attenuation and scatter. Images were reconstructed using iterative 3D-OSEM (GE Vue Point HD-S) reconstruction using 24 subsets and 2 iterations. All images were filtered using a 6.4 mm Gaussian post-filter.

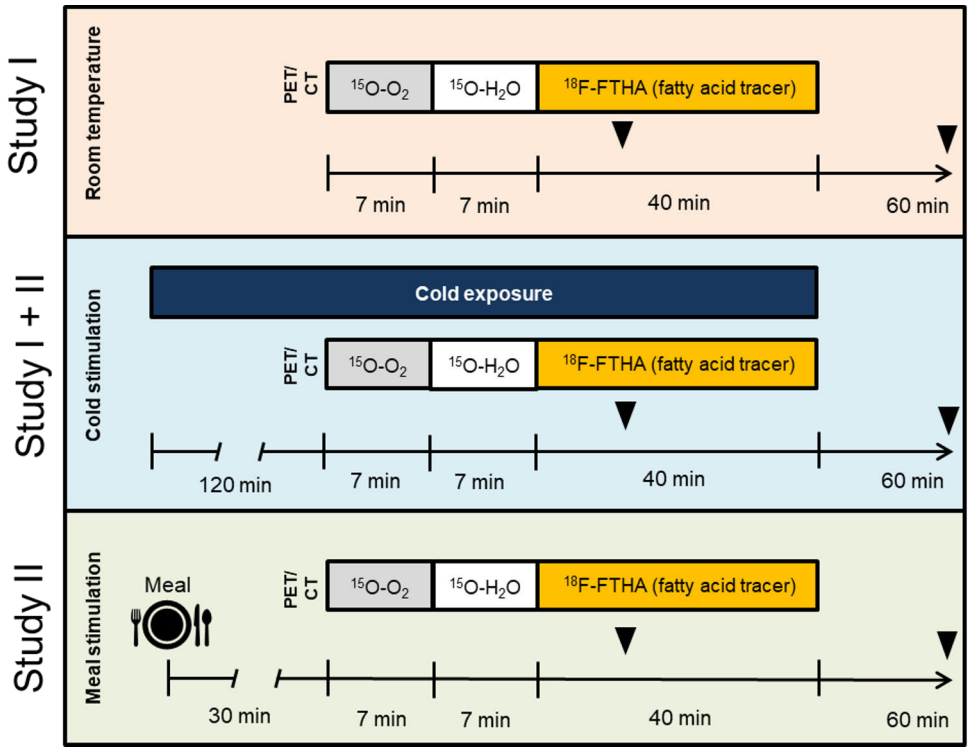


**Figure 4.** Outline of studies I and II. The cold stimulation protocol was identical in both studies. Times are indicated related to the first tracer injection, which is at 0 min. Triangles indicate blood sampling times, additional blood sample was collected before scanning. Cold exposure and room temperature control scan were performed after an overnight fast. Modified from original publications I and II.

### 4.2.2 Study III

Study III included two scanning protocols, one conducted with GIP-infusion and the other after receiving a mixed meal. The studies were conducted on separate days, in random order. The subjects were imaged using a combined PET/MRI scanner to investigate the changes in AT blood flow after a mixed-meal or GIP infusion (Figure 5). The blood flow to the adipose tissue depots was measured using $^{15}$O-H$_2$O PET radiotracer. Blood flow measurements were conducted at three time points; baseline before stimulation, and at 20-minutes and 50-minutes after mixed meal ingestion or the start of GIP infusion.

In the mixed meal procedure subjects ingested a 250-kcal liquid meal (Nutridrink, Nutricia Advanced Medical Nutrition, Amsterdam, Netherlands) consisting of 40 grams of carbohydrates, 6 grams of fat, and 9 grams of protein in 10 minutes. The dose was selected to enable the ingestion of the meal in a 10-minute timeframe during the scanning episodes. For the subjects who underwent bariatric surgery the mixed-meal experiment was repeated (55–97) days post-surgery.

During the GIP infusion procedure, a constant infusion of GIP1–42 (Bachem Holding AG, Bubendorf, Switzerland) at the rate of 4.0 pmol/kg/min was initiated. After 15 min, the rate was halved to 2.0 pmol/kg/min to reproduce GIP excretion seen after the ingestion of a mixed meal (Christensen et al., 2011). During the scanning sessions plasma levels of glucose, insulin, GIP, and glucagon-like peptide-1 (GLP-1) were measured at time points 0, 15, 30, 45, 60, and 90 minutes. The subjects with T2D underwent bariatric surgery and after approximately two months the PET-MRI scanning with the same protocol as described above was repeated. The GIP infusion experiment was repeated 69 ± 25 days after s and mixed meal scans 77 ± 27 days after bariatric surgery (mean ± SD).

Tissue-specific perfusion was quantified using an intravenous injection of $^{15}O$-$H_2O$, after which a dynamic emission scan (frames: 20 × 5 sec, 3 × 10 sec, 4 × 20 sec, 4 × 30 sec) of the abdomen was performed. PET scans were performed at three time points, to assess perfusion at baseline and twice after the stimulation.

PET and MRI scans were performed using a combined PET/MRI–scanner Philips Ingenuity (Philips Healthcare, Cleveland, OH). All data were corrected for dead time, decay, and measured photon attenuation and reconstructed in a 256 x 256 matrix.

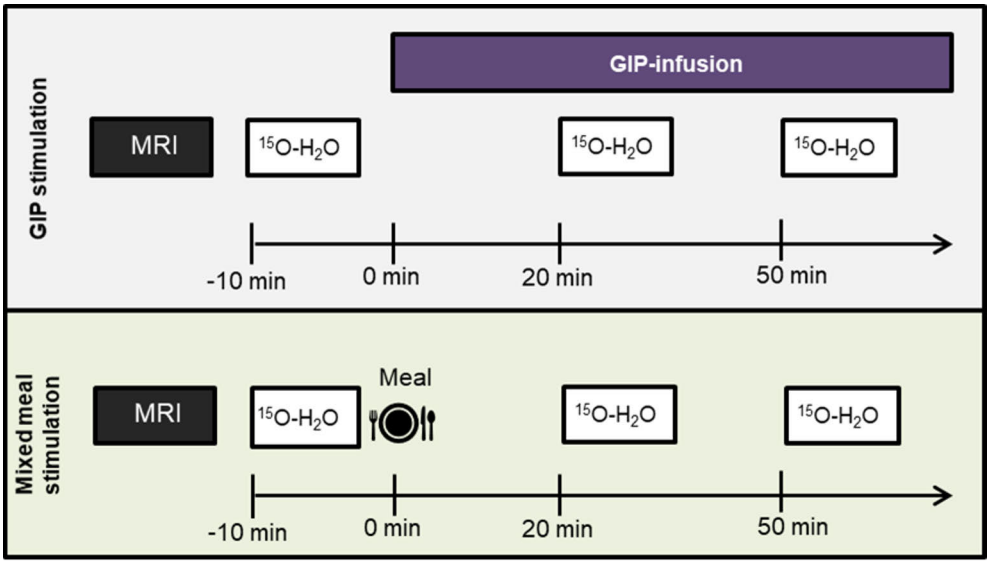


**Figure 5.** Timeline of the study protocol. All subjects were scanned after an overnight fast. All subjects were first scanned with MRI, followed by three PET scans using $^{15}O$-$H_2O$ at three time points: baseline, 20 minutes, and 50 minutes after stimulation by meal ingestion or GIP-infusion. GIP infusion was started at 4 pmol/kg/min and halved after 15 minutes to reproduce physiological concentrations of GIP after a meal. Timepoints indicated from the start of stimulation at 0 minutes. Modified from original publication III.

## 4.3 PET data analysis

### 4.3.1 Volume of interest

In studies I and II volumes of interest (VOI) were drawn manually using fused dynamic PET-CT images. VOIs were drawn in the supraclavicular fat depots (typical BAT area), the lateral part of the deltoid muscles, and SAT in the posterior area of the neck. Input functions for modeling calculations were derived from the images by drawing a VOI into the arch of the aorta. Examples of typical VOIs are shown in figure 6. In study III VOIs were drawn manually, using MRI images as an anatomical reference. VOIs were drawn on the subcutaneous adipose tissue, visceral adipose tissue, and to obtain image-derived input function, on the abdominal aorta.

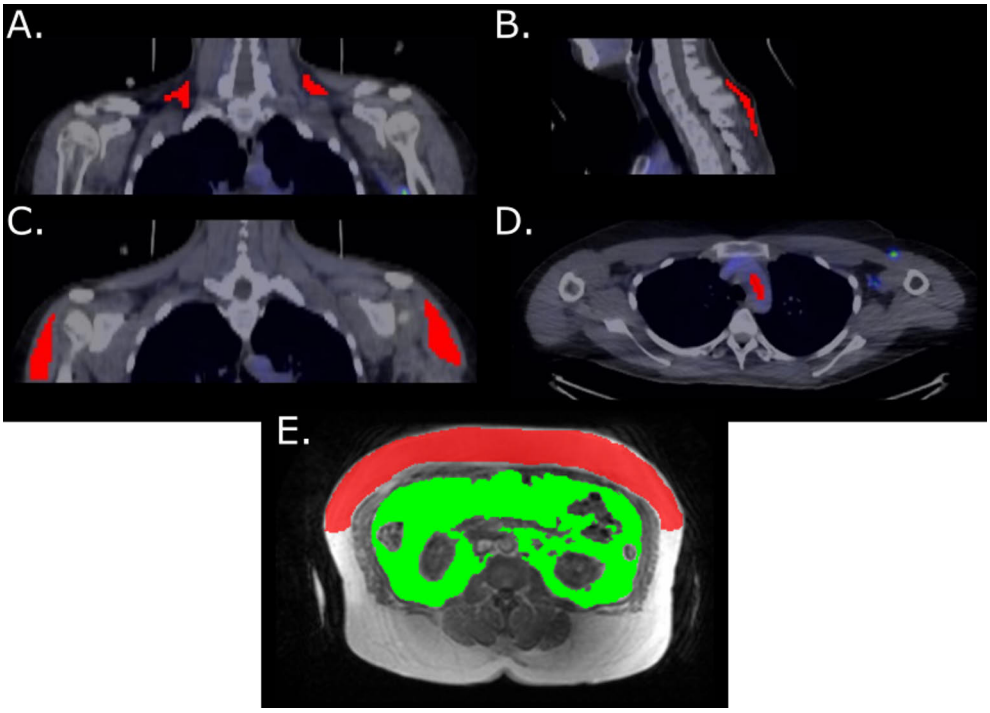


**Figure 6.** Fused PET/CT (A-D) and PET/MRI (E) images with examples of VOIs used to measure tissue activity. A. Supraclavicular BAT depot B. SAT region, in some cases SAT data was analyzed from the chest SAT if the neck depot was too small. C. Deltoid muscles. D. Arch of the aorta E. SAT area in red, VAT area in green, drawn on MRI images.

### 4.3.2 Tissue-specific fatty acid uptake rate

Tissue-specific FAU was calculated using multiple-time graphical analysis (Gjedde, 1982; Patlak et al., 1983; Rutland, 1979). Plasma input functions were corrected for metabolites which were measured from plasma samples acquired during the scanning. Image-derived blood time-activity curve (TAC) was corrected from blood activity to plasma activity, since FFAs in plasma are bound 99.99% to circulating plasma proteins, using b2plasma software (b2plasma 0.6.16 Turku PET Centre, Turku, Finland) and measured hematocrit. The net influx rate ($K_i$) of $^{18}$F-FTHA from the graphical analysis was multiplied by plasma FFA concentrations measured during the scans to calculate tissue-specific FAU. All analysis of PET-CT images was done using Carimas software (Turku PET Centre, Turku, Finland) (Harms et al., 2014; Nesterov et al., 2014, 2015).

### 4.3.3 Tissue-specific perfusion

Tissue-specific perfusion was calculated using the 1-tissue compartment model, a method based on the principle of exchange of inert gas between blood and tissues (Kety and Schmidt, 1945). Input functions were derived from the images, by drawing a VOI in the arch of the aorta in studies I and II, and to the descending aorta in study III. The descending aorta was used in study III, because the arch of the aorta was not visible, since the focus was on the abdominal area. The same VOIs used to acquire TACs in FAU calculations were used in perfusion analysis in studies I and II. Radiowater was produced using Hidex Radiowater Generator (Hidex Oy, Turku, Finland). Analysis of PET images was done using Carimas software (Turku PET Centre, Turku, Finland) (Nesterov et al., 2014, 2015).

## 4.4 Other measurements/calculations

#### $^{1}$H-MRS (Study I-II)

$^{1}$H-MRS was performed using a pointed-resolved spectroscopy (PRESS) sequence with a repetition time (TR) of 3000 ms, an echo time (TE) of 25 ms, and a number of signal averages (NSA) of 4. A sample frequency of 1000 was used with 2048 samples. T2 correction was not applied. The size of the voxel was optimized and adjusted for each subject to avoid surrounding muscles, and 4 saturation bands were used. The typical voxel size was 10 mm x 10 mm x 12 mm. Scout images with good resolution were acquired for the placement of the spectroscopy voxel. An expert physician specialized in BAT imaging located the BAT, based on previous PET studies and general knowledge of BAT anatomy. Great care was taken to place the voxel inside the fat deposit and to avoid all contamination by muscle tissue or vessels. The obtained $^{1}$H-MRS data were analyzed using the LCModel.

#### Tissue-specific oxygen consumption (Study I–II)

Tissue-specific oxygen consumption was calculated from tissue-specific TACs acquired from $^{15}O$-$O_2$ PET scans, using a 1-tissue compartment model which incorporated perfusion values (Kudomi et al., 2013; U Din et al., 2016). Carimas software (Turku PET Centre, Turku, Finland) was used for PET image analysis (Nesterov et al., 2014, 2015)

### Indirect calorimetry (Study I–II)

Whole-body energy expenditure (EE) and whole-body substrate utilization rates were measured using the indirect respiratory calorimetry technique (Deltatrac II, Datex-Ohmeda) performed during scanning sessions for approximately 100–120 minutes. Measurements were excluded from analyses if they deviated more than 1.5 SD from the mean $vO_2$, $vCO_2$, EE, or respiratory quotient values, caused by irregular breathing. The first 30 minutes of the calorimetry data were also excluded. Whole-body energy expenditure, respiratory quotient, and substrate utilization rates were calculated using $vO_2$ and $vCO_2$ according to the Weir equation (Weir, 1949) and manufacturer's equations (Meriläinen, 1987) using Matlab (Version: R2011a). Protein oxidation was accounted for in the equations by considering urinary nitrogen to be 13 g/24 h. Whole-body energy expenditure and substrate oxidation rates were divided by fat-free mass to compare different subjects; the percentage of fat (%) was measured with a bioimpedance-based method (Omron BF400, Omron Healthcare).

### Blood measurements

Plasma insulin, TSH, free plasma T4, and free plasma T3 concentrations were measured using the electrochemiluminescence immunoassay technique (Modular E180 automatic analyzer, Roche Diagnostics GmbH). The plasma concentrations of total cholesterol, high-density lipoprotein (HDL) cholesterol, and triglycerides were measured photometrically (Modular P800, Roche Diagnostics GmbH). The plasma concentration of low-density lipoprotein (LDL) was calculated using the Friedewald equation (Friedewald et al., 1972). Serum FFA concentration was determined photometrically (NEFA C, ACS-COD, Wako Chemicals GmbH; Modular P800, Roche Diagnostics GmbH). The plasma glucose concentration was determined by a glucose oxidase method (Analox GM9 Analyzer, Analox Instruments).

### Adipose tissue biopsies (I–II)

Biopsies were obtained from the supraclavicular region of 31 subjects. The site of the biopsy was determined by imaging data of the area ($^{18}$F-FTHA PET/CT or MRI). The procedure was carried out by a plastic surgeon at room temperature (~22 °C) under local anesthesia. SAT sample was collected from the same incision. The samples were fixed in formalin after extraction. BAT was defined based on morphology by an experienced pathologist, and samples designated as BAT positive showed cells with multilocular lipid droplets.

### Adipose tissue depot volumes (III)

Volumes of SAT and VAT depots were calculated using predictive equations by Schweitzer et al. by first measuring SAT and VAT volumes from a single slice at the level of L3 vertebrae (Schweitzer et al., 2015).

### Insulin sensitivity

Whole-body insulin sensitivity (M-value) was calculated from hyperinsulinemic-euglycemic clamp study results (DeFronzo et al., 1979; Schlichtkrull et al., 1965). Insulin resistance ($HOMA_{IR}$) was calculated using the homeostasis model assessment method (Matthews et al., 1985). In studies I and II oral glucose tolerance test (OGTT) results were used to calculate the Matsuda index and insulinogenic index (Matsuda and DeFronzo, 1999; Seltzer et al., 1967). Matsuda index represents insulin sensitivity and the insulinogenic index is an indicator of impaired insulin secretion (Hanson et al., 2000).

## 4.5 Statistical analysis I–III

For studies I-II power calculations and the number of subjects were determined based on previous studies using $^{18}$F-FDG and previous unpublished $^{18}$F-FTHA data (Orava et al., 2011, 2013; Virtanen et al., 2009). Statistical analyses were performed using IBM SPSS Statistics (version 22). Comparison of means was performed with a two-way Student's t-test. Correlations between variables were calculated using Pearson's, Spearman's rank correlation, and point-biserial correlation when correlating categorical and continuous variables. Multiple linear regression analysis was performed to evaluate associations between variables and to adjust for confounding factors. P-value of less than 0.05 was considered statistically significant. Data are presented as mean ± SD unless stated otherwise. N represents the number of subjects; details of groups and statistical parameters can be found in the figure legends.

In study III the comparison of means was performed with a two-way Student's t-test, ANOVA, or Wilcoxon rank-sum test. Associations between variables are calculated using Pearson's or Spearman's rank-sum test. Changes over time and between groups were tested with repeated-measures analyses using linear mixed models, and the Tukey-Kramer method was used to adjust the P values of pairwise comparisons. P-value of less than 0.05 was considered statistically significant. Data are presented as mean and SD if not stated otherwise. Normality of distribution was checked visually together with the Shapiro-Wilk test of normality and Q-Q plot. Statistical analyses were performed using IBM SPSS Statistics (version 25) or SAS JMP Pro 25.

## 4.6 Ethics

The study protocol was reviewed by the local ethical committee of the Hospital District of Southwest Finland and the study was carried out according to the principles of the Declaration of Helsinki and GCP guidelines. Written informed consent was signed by all study subjects before any study procedures and inclusion in the study.

# 5 Results

## 5.1 AT FAU and perfusion during cold and meal stimulation (I–II)

General characteristics of subjects participating in studies I and II are provided in table 2.

**Table 2.** General characteristics of subjects participating in studies I and II. p-value for independent samples *t*-test, Fisher's exact test for gender. Modified from original publication I. Data are presented as mean (SD).

| | Lean group n=29 | Obese group n=10 | Lean vs Obese p-value |
|---|---|---|---|
| **Age (years)** | 36.60 (10.50) | 42.40 (8.68) | 0.1 |
| **Gender (F/M)** | 18F / 11M | 6F / 4M | 1.0 |
| **BMI (kg/m$^2$)** | 25.09 (2.47) | 33.56 (3.36) | 0.0001 |
| **Height (cm)** | 171.4 (10.1) | 170.0 (9.3) | 0.69 |
| **Weight (kg)** | 74.0 (11.5) | 97.8 (18.9) | 0.003 |
| **Waist circumference (cm)** | 88.04 (13.10) | 106.45 (16.65) | 0.007 |
| **Fat percentage of weight (%)** | 30.08 (8.18) | 38.61 (7.72) | 0.009 |
| **HDL cholesterol (mmol/l)** | 1.64 (0.39) | 1.43 (0.32) | 0.15 |
| **LDL cholesterol (mmol/l)** | 2.76 (0.79) | 2.84 (0.73) | 0.8 |
| **Triglycerides (mmol/l)** | 0.79 (0.29) | 1.41 (0.97) | 0.11 |
| **HbA1c (mmol/mol)** | 35.01 (4.43) | 31.91 (5.63) | 0.97 |
| **Plasma glucose (mmol/l)** | 5.42 (0.47) | 5.71 (0.65) | 0.24 |
| **Plasma insulin (mU/l)** | 7.17 (3.11) | 12.83 (6.54) | 0.045 |
| **Plasma C-peptide (nmol/l)** | 0.63 (0.19) | 0.96 (0.34) | 0.03 |
| **HOMA-IR** | 2.01 (0.89) | 1.54 (0.77) | 0.16 |
| **M-value (mg/kg/min)** | 8.38 (2.85) | 5.64 (3.87) | 0.03 |
| **Matsuda index** | 6.05 (2.85) | 7.34 (2.51) | 0.22 |
| **Insulinogenic index** | 0.88 (0.48) | 0.85 (0.43) | 0.84 |

As expected, subjects in the obese group had higher BMI, weight, waist circumference and body fat percentage compared to lean subjects. Subjects in the obese group also had elevated plasma insulin and C-peptide levels compared to lean subjects indicating a level of insulin resistance, however, there was no difference in HOMA-IR. Lean subjects M-value was lower compared to the obese group, indicating a difference in control of blood glucose homeostasis. Subjects in the obese group tended to be older, however, there was no significant difference between the groups.

### 5.1.1 Effects of cold exposure

During cold exposure BAT, FAU was higher compared to room temperature ($p<0.02$). There was no difference in SAT FAU ($p=0.66$) between exposure to cold and room temperature. Cold exposure increased supraclavicular BAT perfusion compared to room temperature ($p<0.02$). SAT ($p=0.873$) perfusion was similar during cold exposure and at basal state. Supraclavicular BAT FAU was positively associated with increased BAT perfusion during cold exposure (rho=0.62, $p=0.003$) and at basal state (rho=0.51, $p=0.03$).

Plasma FFA levels increased from baseline as a result of cold exposure ($p<0.0001$), while they remained unchanged at room temperature. Plasma triglyceride levels increased from baseline during cold exposure ($p=0.01$).

The area under the curve (AUC) of plasma triglycerides during cold exposure was significantly higher compared to room temperature ($p=0.04$). However, no significant differences were seen in other AUC values (Table 3).

**Table 3.** Changes in skin temperature and several biochemical characteristics during cold exposure. Modified from the original publication I. Data are presented as mean (SD).

| | Cold Exposure AUC | Room temperature AUC | ΔAUC | p-value |
|---|---|---|---|---|
| Skin temperature (°C) | 66.20 (2.80) | 68.90 (1.19) | − 1.78 (2.62) | 0.08 |
| Plasma TSH (mU/l) | 2.89 (1.18) | 2.75 (1.31) | 0.15 (0.81) | 0.44 |
| Plasma T3 (mU/l) | 8.78 (1.07) | 8.45 (1.06) | 0.34 (0.91) | 0.11 |
| Plasma T4 (mU/l) | 26.53 (3.57) | 26.97 (4.27) | − 0.42 (2.52) | 0.48 |
| Plasma insulin (mU/l) | 12.69 (7.38) | 11.51 (6.64) | 0.88 (4.59) | 0.44 |
| Plasma TG (mmol/l) | 2.17 (0.87) | 1.78 (0.97) | 0.39 (0.77) | 0.04 |
| Plasma glucose (mmol/l) | 10.54 (1.22) | 10.78 (0.66) | 0.19 (0.57) | 0.61 |
| Plasma FFA (mmol/l) | 1.58 (0.47) | 1.48 (0.40) | 0.13 (0.33) | 0.12 |

### 5.1.2 Effects of meal ingestion (II)

BAT FAU after meal ingestion was lower compared to cold exposure ($p<0.001$). SAT FAU also decreased after a meal, compared to cold exposure ($p<0.001$). Perfusion of supraclavicular BAT increased similarly after meal ingestion as it did after cold exposure (14.3±5.2 vs. 12.7±7.4 ml/100g/min, $p=0.5$). SAT perfusion remained similar during both cold exposure and meal ingestion.

Calculation of FAU requires the use of circulating plasma FFA, which are suppressed after a meal due to an increase in plasma insulin levels (figure 7), causing postprandial FAU values to be significantly lower compared to room temperature and cold exposure. Net influx rate $K_i$ represents the uptake rate of $^{18}$F-FTHA into the tissue, independent of plasma FFA concentrations. This allows us to compare the uptake of our fatty acid tracer between cold exposure and postprandial states without the effects of lowered FFA levels. BAT $K_i$ was significantly higher after meal ingestion compared to cold exposure (0.013±0.008 vs. 0.023±0.02 $min^{-1}$, $p<0.02$). Similarly, SAT (0.003±0.001 vs. 0.009±0.005 $min^{-1}$, $p<0.001$) $K_i$ was higher after meal ingestion compared to cold exposure. BAT $K_i$ correlated negatively with baseline plasma FFA concentrations (rho=-0.54, $p=0.032$).

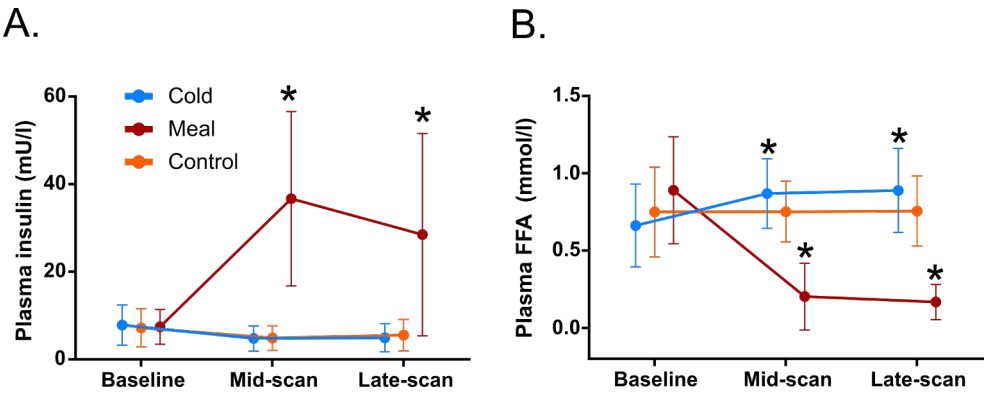


**Figure 7.** Plasma insulin and FFA concentrations measured during scans. An increase of plasma insulin and a decrease of FFAs can be seen after meal ingestion. Data presented as mean and SD. * indicates a significant change from baseline. Modified from original publications I and II.

### 5.1.3 Effects of obesity on BAT FAU and perfusion (I–II)

BAT FAU was twice as high among lean compared to subjects with obesity during cold exposure ($p<0.02$) (Figure 8). Obesity seemed to blunt supraclavicular BAT FAU already at room temperature and it was two times higher among lean subjects ($p<0.01$).

Among lean subjects cold exposure increased BAT FAU ($p<0.03$) and perfusion ($p< 0.04$) (Figure 8), whereas this effect could not be observed in subjects with obesity.

Meal ingestion increased BAT perfusion in lean subjects similarly to cold exposure ($p=0.8$) (Figure 8). However, in subjects with obesity postprandial BAT perfusion was lower compared to cold exposure ($p<0.013$). SAT perfusion increased in lean subjects after a meal, compared to cold exposure ($p<0.01$). Also, the tracer influx rate into BAT ($p<0.03$) and SAT ($p<0.006$) increased after a meal in lean subjects.

BAT FAU measured during cold exposure correlated negatively with several obesity-related variables (figure 10): BMI ($r=-0.39$, $p<0.02$), waist circumference ($r=-0.34$, $p<0.04$), M-value ($rho=0.39$, $p<0.02$), as well as age ($r=-0.51$, $p=0.001$). Increased plasma HDL concentrations were related to higher BAT FAU during cold exposure ($r=0.45$, $p=0.006$). Single linear regression was calculated to predict BAT FAU during cold exposure. A significant regression equation was found with BAT perfusion ($F(1, 34)=11.95$, $p=0.001$), subjects predicted BAT FAU was equal to -1.103 + 0.913(BAT Perfusion). Another significant regression equation was found with BAT radiodensity ($F(1, 36) = 9.16$, $p = 0.005$), predicted BAT FAU was equal to 1.344 + 0.017(BAT HU). To assess the relationship of each of these parameters as a predictor of BAT FAU multiple regression analysis was performed. A significant regression equation was found $F(5, 27)=6.60$, $p<0.0005$, adjusted $R^2=0.47$. However, only age ($p=0.029$) and BAT perfusion ($p=0.043$) added statistically to the prediction. There was no significant colinearity in this model, and none of the variance inflation factors (VIF) were above 10. To further check for confounding factors, the relationships of age, BMI, and M-value using multiple linear regression were analyzed. Age ($p=0.004$) and BMI ($p=0.028$) predicted BAT FAU during cold exposure, but M-value was not a significant predictor ($p=0.91$) when corrected for age and BMI.

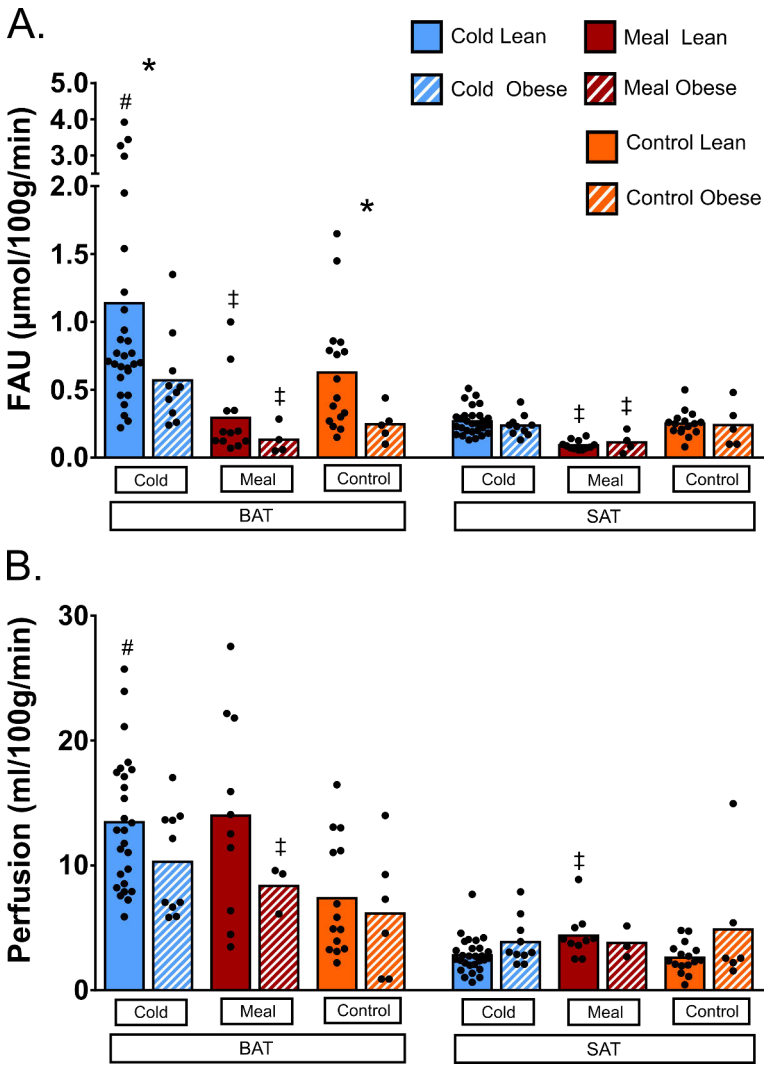


**Figure 8.** **A.** FAU of BAT and SAT measured with $^{18}$F-FTHA during cold exposure, room temperature fasting state (control), and at postprandial state (meal). **B.** Tissue-specific perfusion of BAT and SAT measured with $^{15}O$-$H_2O$ during cold exposure, room temperature fasting state (control), and at postprandial state (meal). Results are presented as mean and individual data points. * indicates $p<0.05$ individual samples t-test comparing lean and obese. # indicates $p<0.05$ paired t-test comparing cold vs control. ‡ indicates $p<0.05$ paired t-test comparing cold vs meal results. Modified from original publications I and II.

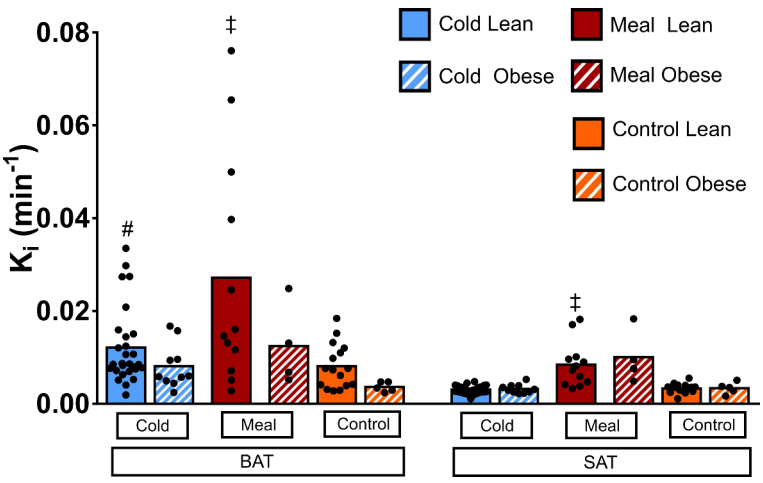


**Figure 9.** Net influx rates ($K_i$) uptake rates of $^{18}$F-FTHA into BAT and SAT during cold exposure, at postprandial state (meal), and at room temperature (control). Results are presented as mean and individual data points. # indicates p<0.05 paired t-test comparing cold vs control. ‡ indicates p<0.05 paired t-test comparing cold vs meal results. Modified from original publications I and II.

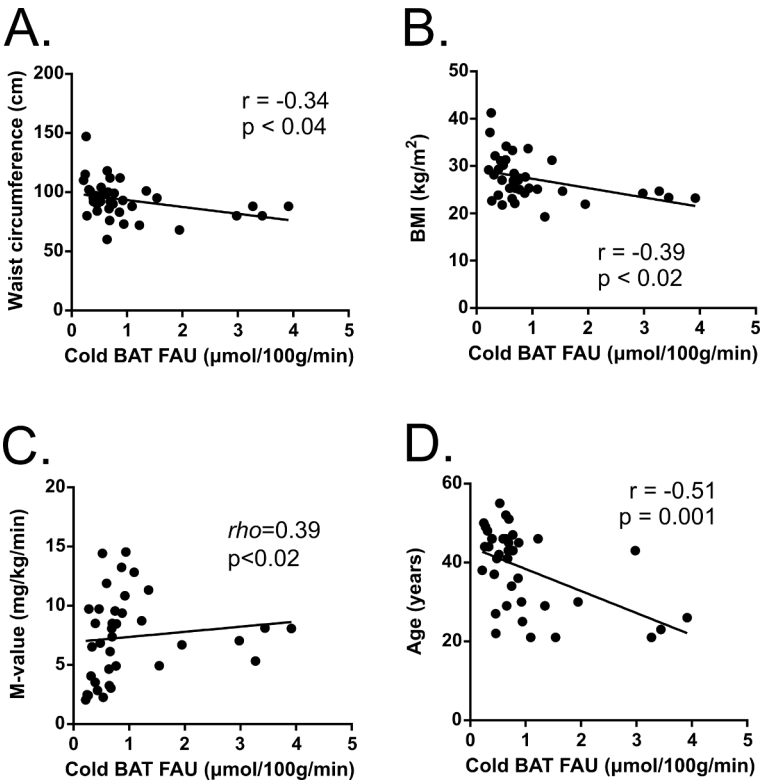


**Figure 10.** Associations between supraclavicular BAT FAU during cold exposure and several obesity-related parameters and age. Modified from original publication I.

### 5.1.4 BAT FAU and perfusion of subjects with histologically detected BAT (I–II)

A subgroup of study participants (n=31) volunteered for a supraclavicular adipose depot sample. Subjects were categorized into high or low BAT groups, based on the morphology of the sample. Using this method a total of 7 subjects were found to possess histological evidence of BAT. Figure 11 illustrates two high BAT subjects during exposure to cold and room temperature. The general characteristics of these subjects can be found in table 4.

Subjects with identifiable BAT were in general younger compared to low BAT subjects. There was no difference between the groups in several variables related to BAT activity, such as BMI, waist circumference, or M-value. Running a point-biserial correlation between high and low BAT subjects, subjects with no histological evidence of BAT did not show an increase in BAT FAU in cold ($r_{pb}$=-0.862, $p < 0.001$) or room temperature ($r_{pb}$=-0.775, $p < 0.001$) as well as moderate negative correlation with BAT perfusion in cold ($r_{pb}$=-0.384, $p = 0.021$), but no significant correlation with room temperature BAT perfusion ($r_{pb}$=-0.175, $p = 0.8$) was seen.

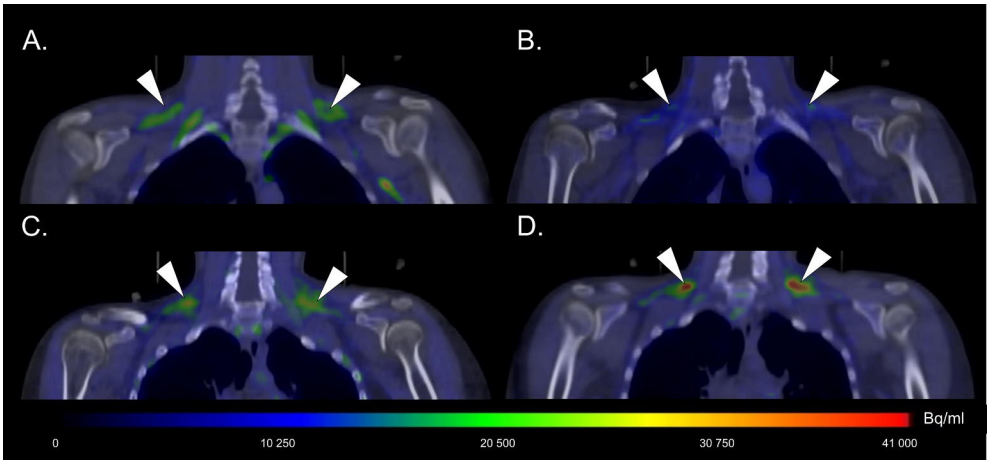


**Figure 11.** $^{18}$F-FTHA PET/CT fusion images, all PET and CT images are in the same scale, PET images are sums of final frames 10–13. Triangles indicate the location of supraclavicular BAT depots. A. high BAT subject in cold exposure. Symmetrical activation of BAT can be seen in the supraclavicular adipose deposits. B. Same high BAT subject as in figure A in room temperature. C. high BAT subject in cold exposure. D. The same high BAT subject as in figure C after meal ingestion, showing increased tracer uptake in the supraclavicular area. Modified from original publication I.

**Table 4.** General characteristics of subjects with or without histological evidence of BAT. Data are presented as mean (SD), p values provided for unpaired comparison between high BAT and low BAT subjects. Modified from original publication I.

| | | High BAT n=7 | Low BAT n=24 | p-value |
|---|---|---|---|---|
| | Age (years) | 27.57 (7.7) | 40.52 (10.68) | 0.004 |
| | Gender (M/F) | 4F / 3M | 12F / 12M | |
| | BMI (kg/m$^2$) | 24.8 (3.0) | 28.11 (5.05) | 0.05 |
| | Waist circumference (cm) | 85.71 (10.87) | 94.98 (18.86) | 0.13 |
| | M-value (mg/kg/min) | 7.35 (2.14) | 6.34 (3.92) | 0.4 |
| | Fat percentage of weight (%) | 30.26 (9.37) | 30.55 (8.60) | 0.5 |
| | HDL cholesterol (mmol/l) | 1.74 (0.42) | 1.49 (0.39) | 0.207 |
| | LDL cholesterol (mmol/l) | 2.71 (0.95) | 2.84 (0.67) | 0.76 |
| | Triglycerides (mmol/l) | 0.81 (0.21) | 1.05 (0.71) | 0.205 |
| | $HbA_{1c}$ (mmol/mol) | 33.19 (4.21) | 35.47 (4.50) | 0.248 |
| **COLD** | BAT FAU (µmol/100g/min) | 2.64 (1.01) | 0.54 (0.24) | 0.001 |
| | BAT Perfusion (ml/100g/min) | 16.56 (5.80) | 11.06 (4.96) | 0.051 |
| | BAT Ki | 0.025 (0.007) | 0.008 (0.004) | 0.0003 |
| | WAT FAU (µmol/100g/min) | 0.31 (0.12) | 0.22 (0.067) | 0.079 |
| | WAT Perfusion (mL/100g/min) | 2.44 (1.22) | 2.84 (0.96) | 0.45 |
| | WAT Ki | 0.003 (0.001) | 0.003 (0.001) | 0.7 |
| **POSTPRANDIAL** | BAT FAU (µmol/100g/min) | 0.59 (0.49) | 0.15 (0.09) | 0.3 |
| | BAT Perfusion (ml/100g/min) | 24.67 (4.06) | 8.24 (3.49) | 0.06 |
| | BAT Ki | 0.05 (0.03) | 0.01 (0.02) | 0.2 |
| | WAT FAU (µmol/100g/min) | 0.08 (0.05) | 0.09 (0.03) | 0.8 |
| | WAT Perfusion (ml/100g/min) | 4.7 (0.85) | 3.69 (0.98) | 0.3 |
| | WAT Ki | 0.008 (0.001) | 0.008 (0.005) | 0.7 |
| **CONTROL** | BAT FAU (µmol/100g/min) | 1.19 (0.43) | 0.36 (0.22) | 0.025 |
| | BAT Perfusion (ml/100g/min) | 6.38 (4.25) | 7.02 (4.74) | 0.83 |
| | BAT Ki | 0.013 (0.005) | 0.005 (0.003) | 0.03 |
| | WAT FAU (µmol/100g/min) | 0.32 (0.13) | 0.22 (0.10) | 0.22 |
| | WAT Perfusion (mL/100g/min) | 1.95 (0.44) | 3.52 (3.80) | 0.19 |
| | WAT Ki | 0.004 (0.001) | 0.003 (0.001) | 0.6 |

## 5.2 Effects of bariatric surgery on stimulated AT perfusion (III)

### 5.2.1 AT blood flow before bariatric surgery

The general characteristics of subjects participating in study III are found in table 5. At basal state, there was no difference in SAT or VAT perfusion rates between subjects with obesity and controls (Figure 12).

Mixed meal ingestion increased SAT perfusion in controls (p=0.012) (measured 20 minutes after meal ingestion), but not in subjects with obesity (p=0.46). 50 minutes after a meal the control subjects' SAT perfusion was still elevated compared to baseline (p=0.004). Subjects with obesity also showed an increase in perfusion from baseline 50 minutes after eating (p=0.004). SAT perfusion after a meal was higher in controls compared to subjects with obesity over time (p=0.041). However, no such difference was observed for VAT perfusion (p=0.23).

SAT perfusion increased 20 minutes after GIP infusion both in controls (p=0.001) and subjects with obesity (p=0.001). Equally, VAT perfusion was also higher 20 minutes after GIP infusion both in controls (p=0.0001) and subjects with obesity (p=0.003). Both SAT and VAT perfusion increased from baseline 50 minutes following a GIP infusion in controls (p=0.0002 and p=0.006, SAT and VAT respectively), as well as subjects with obesity (p=0.03 and p=0.02, SAT and VAT respectively). Even though GIP infusion increased SAT perfusion in both groups, the change of SAT perfusion over time was lower in subjects with obesity compared to controls (p=0.002). However, there was no statistically significant difference in VAT perfusion over time between controls and subjects with obesity (p=0.051)

### 5.2.2 Changes after bariatric surgery

After bariatric surgery, the subjects with obesity lost weight, and there was an improvement in insulin sensitivity as measured by $HOMA_{IR}$ as well as fasting plasma glucose levels and insulin levels. Both SAT and VAT mass had decreased significantly. Changes in general characteristics, as well as several biochemical variables, can be seen in table 5.

Basal SAT and VAT perfusion were not affected by bariatric surgery (Figure 13). Likewise SAT and VAT perfusion were similar between controls and subjects with obesity after bariatric surgery.

Following bariatric surgery, ingesting a meal increased SAT perfusion significantly after 20 minutes (p=0.009) compared to basal conditions. An increase in perfusion was also seen for VAT (p=0.008) 20 minutes after a meal. The effects of meal

ingestion remained for 50 minutes as both SAT (p=0.028) and VAT (p=0.005) perfusion were higher compared to the basal state. The change over time in SAT perfusion after meal ingestion was similar between controls and subjects with obesity following bariatric surgery (p=0.46). The meal-induced change in VAT perfusion over time remained similar to control subjects after bariatric surgery.

Resembling results observed before bariatric surgery, SAT blood flow was increased after 20 (p=0.003) and 50 minutes (p=0.028) of the GIP infusion. The GIP-induced increase of VAT perfusion was observed 20 (p=0.0001) and 50 minutes (p=0.005) after the start of the infusion. The change of SAT perfusion over time after the GIP infusion remained higher in controls compared to subjects with obesity even after undergoing bariatric surgery (p=0.002). The change of VAT blood flow over time did not differ between controls and post-surgery subjects after GIP infusion (p = 0.49) or GIP-infusion (p = 0.57).

**Table 5.** General characteristics of study participants of study III. Data are presented as mean (SD). * indicates p < 0.05 controls vs subjects with obesity before surgery. # indicates p < 0.05 controls vs subjects with obesity after surgery. The significance of paired comparison of subjects with obesity before and after bariatric surgery is provided in the last column. Modified from original publication III.

| | Controls n=10 | Before Surgery n=10 | After Surgery n=10 | Before vs After Surgery |
|---|---|---|---|---|
| **Age (years)** | 46 (9.41) * | 51.7 (7.01) | 52.3 (6.73) # | 0.005 |
| **Gender (F/M)** | 8F / 2M | 8F / 2M | 8F / 2M | 1.0 |
| **BMI (kg/m$^2$)** | 23.10 (2.41) * | 40.8 (5.92) | 35.15 (6.26) # | < 0.0001 |
| **Height (cm)** | 165.75 (10.5) | 167.74 (12.85) | 167.49 (12.99) | 0.094 |
| **Weight (kg)** | 63.65 (13.68) * | 114.63 (18.89) | 98 (16.25) # | < 0.0001 |
| **Waist circumference (cm)** | 80.65 (10.08) * | 121.05 (7.57) | 109.56 (9.67) # | 0.001 |
| **Fat percentage of weight (%)** | 25.62 (5.91) * | 45.98 (9.71) | 40.92 (13.53) # | 0.007 |
| **HDL cholesterol (mmol/l)** | 1.89 (0.52) * | 1.249 (0.34) | 1.29 (0.38) # | 0.593 |
| **LDL cholesterol (mmol/l)** | 2.57 (0.82) | 2.4 (1.12) | 1.92 (0.66) # | 0.061 |
| **Total cholesterol (mmol/l)** | 4.82 (1.08) | 4.49 (1.38) | 3.72 (0.87) # | 0.01 |
| **Triglycerides (mmol/l)** | 0.78 (0.39) * | 1.86 (0.66) | 1.1 (0.49) | 0.005 |
| **HbA1c (mmol/mol)** | 32.07 (3.58) * | 39.73 (4.03) | 35.93 (2.81) # | 0.014 |
| **Plasma glucose (mmol/l)** | 5.1 (0.37) * | 6.53 (1.09) | 5.65 (0.72) # | 0.008 |
| **Plasma insulin (mU/l)** | 4.5 (2.1) * | 19.4 (9.35) | 12.2 (7.13) # | 0.026 |
| **Plasma C-peptide (nmol/l)** | 0.52 (0.15) * | 1.219 (0.30) | 1.001 (0.37) # | 0.025 |
| **HOMA-IR** | 1.04 (0.52) * | 5.87 (3.4) | 3.11 (1.89) # | 0.019 |
| **SAT mass (kg)** | 14.7 (3.7) * | 39.68 (6.61) | 31.98 (8.41) # | <0.0001 |
| **VAT mass (kg)** | 1.6 (0.6) * | 6.38 (1.40) | 4.92 (1.30) # | <0.001 |

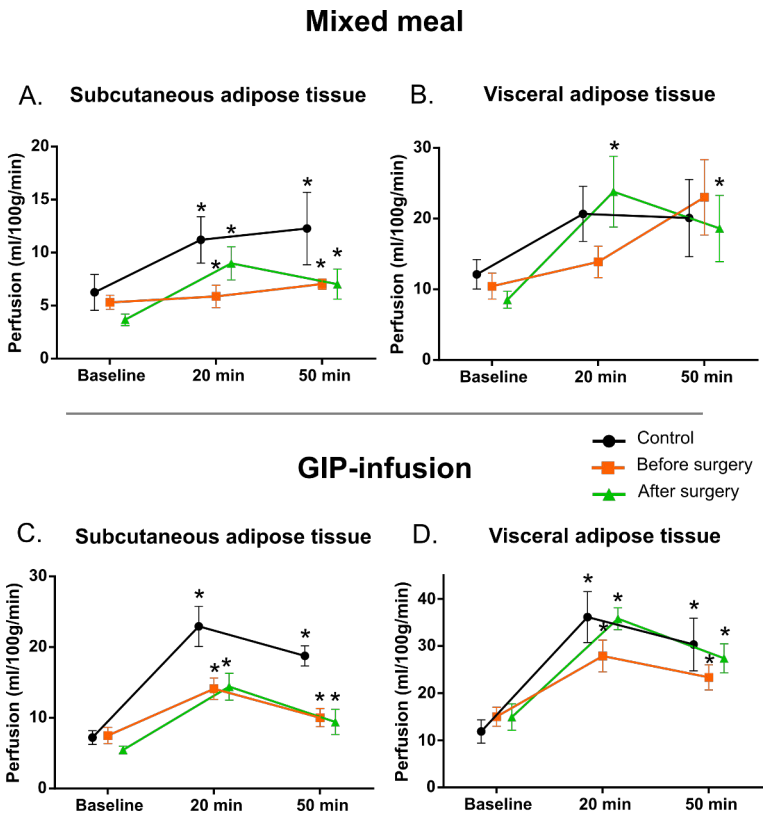


**Figure 12.** SAT and VAT blood flow at baseline, 20-min and 50-min after a mixed meal or start of GIP-infusion. Statistical comparison was done using linear mixed models, and the Tukey-Kramer method was used to adjust the P values of pairwise comparisons. Data presented as mean ± SEM. * indicates a significant change from baseline. Modified from original publication III.

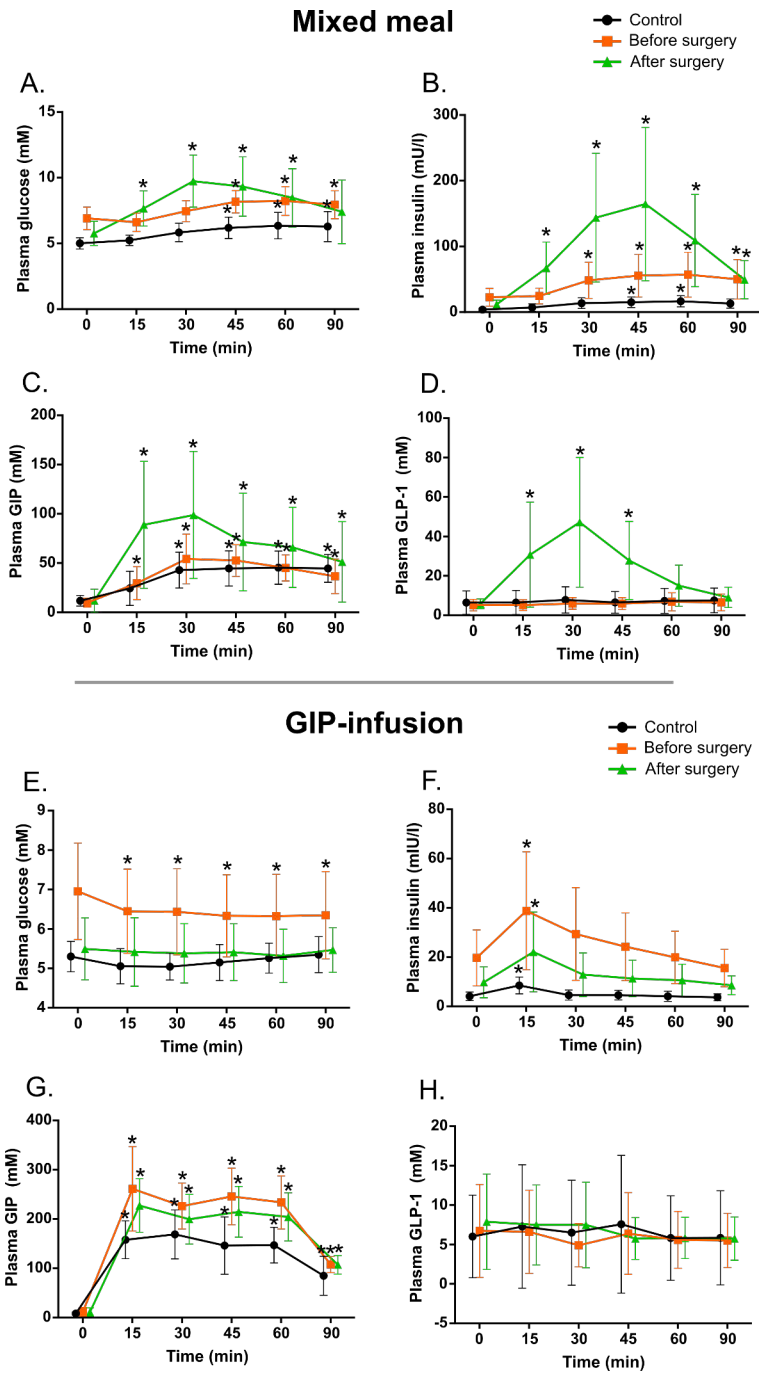


**Figure 13.** Changes in glucose, insulin, and incretin levels in response to a mixed meal and GIP infusion. Data presented as mean ± SD. * indicates significant change ($p < 0.05$) from baseline. Modified from original publication III.

Plasma concentrations of glucose, insulin, GIP, and GLP-1 during scanning are provided in figure 13.

Meal ingestion induced changes in AUC of plasma glucose ($p=0.035$), insulin ($p<0.001$), c-peptide ($p<0.001$), and GLP-1 ($p<0.01$) increased significantly after bariatric surgery compared to pre-surgery values. Postprandial GIP AUC was significantly higher in subjects with obesity after bariatric surgery compared to controls ($p=0.03$) but did not differ significantly compared to pre-surgery values ($p=0.07$). Following bariatric surgery, the increased SAT blood flow after meal ingestion was associated with higher plasma GIP AUC ($rho=0.95$, $p<0.00001$).

Plasma glucose AUC was lower in subjects with obesity after bariatric surgery: in addition, no decrease of plasma glucose from baseline was observed in subjects with obesity as was detected before surgery. GIP infusion increased plasma insulin concentrations in subjects with obesity before and after bariatric surgery. During GIP infusion there was a negative correlation between SAT perfusion AUC and plasma insulin AUC ($rho=-0.83$, $p=0.005$) in subjects with obesity before bariatric surgery and the increased SAT perfusion correlated with higher plasma glucose AUC ($rho=0.73$, $p=0.03$) (Figure 14). After bariatric surgery the correlation between plasma insulin AUC and SAT perfusion during GIP-infusion was positive ($rho=0.91$, $p=0.002$) in subjects with obesity.

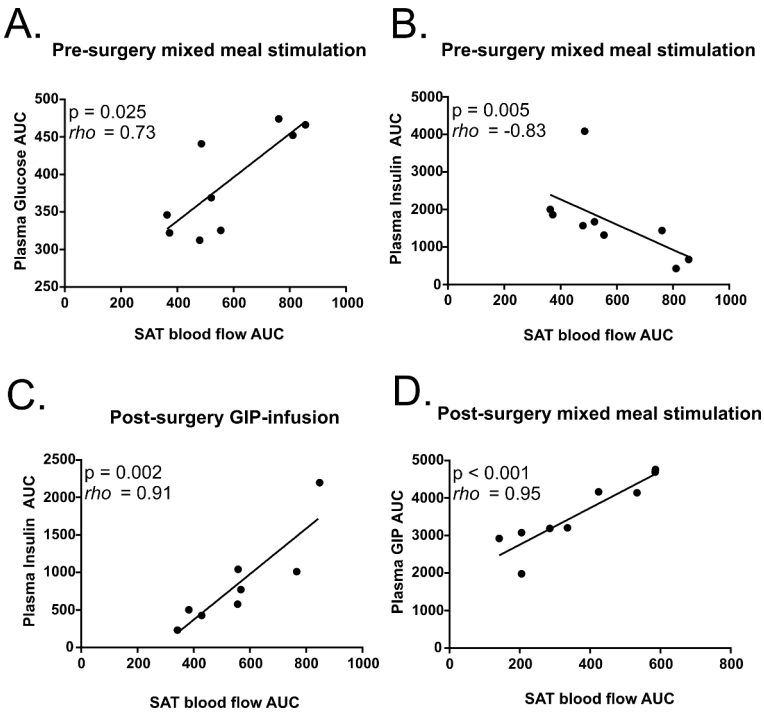


**Figure 14.** Associations between AT blood flow AUC and measured plasma variable AUCs, calculated using Spearman's rank correlation coefficient. Modified from original publication III.

# 6 Discussion

## 6.1 Obesity has a blunting effect on BAT FAU and perfusion during cold exposure

In study I BAT FAU was two-fold higher during cold exposure compared to basal conditions in lean subjects. Cold exposure has been shown to increase BAT GU and perfusion in lean subjects (Orava et al., 2013; Virtanen et al., 2009). BAT FAU has been previously reported, but there were no comparisons between stimulated and unstimulated results as well as no comparisons between lean and subjects with obesity (Blondin et al., 2015). In addition to FAU, there was also an increase in BAT perfusion in lean subjects after cold exposure, similar to previous reports (Orava et al., 2011, 2013).

Cold exposure did not increase BAT FAU or perfusion in subjects with obesity. This would indicate that subjects with obesity have a reduced amount of BAT or that its activation is dysregulated in subjects with obesity. BAT FAU during cold exposure was associated with obesity (waist circumference, BMI) and markers of metabolic syndrome (M-value and plasma HDL-cholesterol concentration) as well as age. Obesity has been previously linked to reduced BAT glucose uptake during cold exposure in several studies (Cypess et al., 2009; Orava et al., 2013; Saito et al., 2009; Zingaretti et al., 2009). It has been suggested that obesity causes the reduced capacity to recruit adipocytes with thermogenic potential, or it might cause a dysfunction in the regulation of BAT activity, or that subjects with obesity simply have less BAT in their depots (Bartelt and Heeren, 2014; Carpentier et al., 2018; Ouellet et al., 2012). Age was the strongest predictor of reduced BAT FAU during cold exposure in multivariate regression analysis when comparing the different predictors. This would indicate that while obesity does have a blunting effect on BAT metabolism, BAT activity also diminishes with aging. Aging is related to diminished UCP1 activity, mitochondrial dysfunction, changes in SNS, and hormonal changes, which could all contribute to the loss of BAT function (Bahler et al., 2016; Lenaz, 1998; Zoico et al., 2019). Subjects with histological evidence of BAT have several folds higher FAU in BAT compared to those with no detected BAT. While in the whole group cold exposure BAT FAU was associated with BMI, waist circumference, and

M-value, there was no difference between high BAT and low BAT subjects, however, subjects with histological evidence of BAT were younger compared to low BAT subjects. As would be expected, there was an association between having histological evidence of BAT and higher BAT FAU and perfusion. Since this distinction between high and low BAT subjects was based solely on histological evidence, including other markers of BAT could have revealed additional study subjects with lesser amounts of BAT, which were not detected here.

Increased perfusion was associated with increased FAU during cold exposure and at basal state. Perfusion has been previously shown to be positively associated with BAT GU, as well as BAT oxygen consumption (Orava et al., 2011; U Din et al., 2016). BAT FAU is also related to BAT oxygen consumption (U Din et al., 2016). It is important to note that, using our method of $^{18}$F-FTHA PET/CT-imaging, does not directly measure fatty acid metabolism, since it is not certain what happens to FFAs after uptake into tissue (Guiducci et al., 2007). Inhibition of lipolysis by nicotinic acid decreases BAT GU and oxidative metabolism during cold exposure (Blondin et al., 2017; Labbé et al., 2015), showing that internal TG storages are essential for BAT metabolism. While $^{18}$F-FTHA uptake does not measure FA metabolism directly, the association between FAU and oxygen consumption of BAT would indicate that it is related to the metabolism of BAT, and not only replenishment of TG stores.

## 6.2 BAT FAU is blunted in obesity already at basal level

In addition to a blunted cold exposure effect in obesity, in study I lean subjects BAT FAU was two-fold higher compared to subjects with obesity even at basal conditions. In subjects with obesity at basal state, there was no difference between BAT and SAT FAU. However, in lean subjects, BAT FAU at basal state was over two-fold higher compared to SAT values. This indicates that subjects with obesity have a reduced amount of BAT in their supraclavicular region and that the tissue would consist more of white than brown adipocytes. Reduced BAT GU in subjects with obesity at basal state has not been reported, however, BAT glucose metabolism is more active than WAT at basal level (Weir et al., 2018). It is possible that glucose does not play a prominent role in BAT metabolism during basal conditions and GU increases during an acute need for energy, such as during cold exposure.

While increased BAT activity, as measured by several variables, has been linked to a more favorable metabolic profile and reduced fat mass in humans, it is still unclear what role BAT plays in energy homeostasis. In rodents, BAT increases energy expenditure significantly, since the amount of tissue is relatively large (Cannon and

Nedergaard, 2004). Cold exposure increases BAT substrate uptake and oxygen consumption significantly also in humans; however, the amount of BAT is smaller, and the contribution of BAT to total energy expenditure is comparably smaller (Carpentier et al., 2018). BAT activity has been associated with increased thermogenesis during cold exposure (Chen et al., 2013; Ouellet et al., 2012), but humans most likely rely on other means of heat production such as skeletal muscles (Brychta and Chen, 2017). So, while BAT has a role in human metabolism, it is uncertain how much it can contribute by itself and the interactions between BAT and other tissues warrants further investigation.

## 6.3 Mixed meal increases BAT perfusion similarly to cold exposure, but reduces BAT fatty acid uptake

Mixed meal ingestion increased BAT perfusion as much as cold exposure. Blood flow also plays an important role in substrate mobilization and transportation in AT (Frayn et al., 2003). This is an important indicator of increased BAT activation after a mixed meal. A carbohydrate-rich meal does not seem to stimulate BAT FAU. FAU of all measured tissues decreased after having a meal compared to cold and room temperature. After meal ingestion plasma FFA levels are reduced due to the effects of rising insulin levels (Czech et al., 2013; Holm et al., 2000; Stahl et al., 2002). As briefly mentioned in the methods and the results sections, FAU values are calculated using plasma FFA concentrations. This causes the postprandial FAU levels to be significantly lowered, compared to results from results recorded at a fasting state at room temperature or cold exposure. FAU is calculated using the net influx rate of the tracer ($K_i$). $K_i$ is independent of available plasma FFAs and is a quantity of fractional uptake rate of the tracer, $^{18}$F-FTHA, while FAU is dependent on plasma FFAs telling us the absolute net FFA uptake per minute. In lean subjects, postprandial BAT $K_i$ was higher than at room temperature or even cold exposure $K_i$. Having a mixed meal did not increase $K_i$ in subjects with obesity as it did in lean subjects; in subjects with obesity BAT $K_i$ was similar after cold exposure and meal ingestion. Increased BAT $K_i$ was related to lower plasma FFA concentrations. FFA transport activity may increase in response to lower plasma FFA concentrations because the brown adipocytes are attempting to retain a certain rate of FFA uptake into the cell, even when the available FFAs decrease. Insulin stimulation increases BAT GU in humans (Orava et al., 2011). So, while BAT attempts to increase FAU during the postprandial state, it is likely that glucose and internal TG stores are the primary energy source postprandially since circulatory FFAs are not available. BAT GU could be more detectable compared to FAU in a postprandial state. It is increased after a high-calorie carbohydrate-rich meal compared to SAT and VAT (Vosselman et al., 2013).

Cold exposure increased BAT GU more than meal ingestion, and it was proposed that this could be due to increased GU seen in skeletal muscles following meal ingestion, which leads to decreased substrate availability for BAT. Insulin stimulation increases BAT GU even at room temperature, however not to the extent seen during cold exposure (Orava et al., 2011). Increased SNS activity after a meal (van Baak, 2008) increases BAT activity, however, the substrate utilization seems to be dependent on meal composition.

## 6.4 Effects of bariatric surgery on SAT and VAT blood flow

Perfusion plays an integral part in regulating AT metabolism (Frayn and Karpe, 2014). In study III it was shown that stimulation of SAT blood flow by GIP or a mixed meal is blunted in subjects with obesity with T2D. The response of SAT perfusion towards a mixed meal is normalized in subjects with obesity two months after bariatric surgery. Bariatric surgery did not induce any substantial changes in GIP-induced increase of perfusion in SAT or VAT of subjects with obesity.

## 6.5 Bariatric surgery normalizes SAT blood flow response to a mixed meal

In the postprandial state, insulin increases adipose tissue blood flow (Baron, 1994; Lambadiari et al., 2015). This effect is reduced in subjects with obesity (Ardilouze et al., 2012; Coppack et al., 1996; Jansson et al., 1998), and subjects with insulin resistance, even independent of weight (Karpe et al., 2002b). The response of SAT perfusion to a mixed meal normalized after bariatric surgery. There was no change in VAT perfusion over time to meal stimulation. However, after bariatric surgery VAT perfusion increased already 20 minutes after a meal in subjects with obesity, whereas this increase occurred only after 50 minutes before bariatric surgery. This shows that there was some improvement in the responsiveness of VAT to a meal. This faster increase of perfusion after a meal could contribute to the ability of AT to store lipids after a meal into VAT, decreasing lipid accumulation into other tissues.

There was a positive correlation between SAT perfusion AUC and plasma GIP concentration AUC in subjects with obesity after bariatric surgery, so while GIP induced perfusion response did not change after bariatric surgery, GIP does seem to play some role in postprandial SAT perfusion response after bariatric surgery.

## 6.6 GIP induced blood flow increase is reduced in obese subject SAT, but not VAT

GIP has been shown to increase SAT blood flow in the presence of insulin (Asmar et al., 2016a). Effects of GIP on AT blood flow are blunted in subjects with obesity, presumably due to decreased insulin sensitivity. GIP-infusion increased SAT and VAT perfusion in lean and subjects with obesity. GIP-infusion induced a higher increase of SAT perfusion over time in control compared to subjects with obesity before or after bariatric surgery. Indeed, bariatric surgery had no effect on SAT perfusion over time in response to GIP infusion.

In VAT GIP-infusion induced an increase of perfusion in all subjects. There was no difference in GIP-induced increase of perfusion between control or subjects with obesity before or after bariatric surgery. It seems that in VAT the blood flow increasing effects of GIP are not blunted in obesity.

Bariatric surgery did not induce any change in VAT or SAT regarding GIP signaling. Previously it has been shown that SAT perfusion response to GIP-infusion increases after weight loss by caloric restriction over 16 weeks (Asmar et al., 2016b). SAT blood flow response to GIP may normalize after a longer period after bariatric surgery. However, the pre-surgery weight and the degree of weight loss were lesser in study III compared to the study by Asmar et al. Subjects in study III were still obese and in the weight loss phase at the time of follow-up scans, and the average weight loss was 17 kg at that time point. If the blunted effects of GIP are indeed related to insulin resistance in subjects with obesity, there should be some improvement as insulin sensitivity has been shown to increase as early as 6 days preceding bariatric surgery (Ballantyne et al., 2006; Wickremesekera et al., 2005). In addition, insulin sensitivity improved in study III as well, indicated by lower $HOMA_{IR}$ in subjects with obesity after bariatric surgery.

There was a robust increase in GLP-1 levels in subjects with obesity after bariatric surgery in response to mixed meal stimulation. This response was far greater than control subjects. GLP-1 secretion after a meal increases following bariatric surgery (Jirapinyo et al., 2018). This increase is thought to be due to the more rapid delivery of nutrients into the gastrointestinal tract, but the mechanism is not completely understood. GLP-1 has several functions, including functions related to insulin secretion and appetite decreasing effects (Müller et al., 2019; Nauck and Meier, 2018). It is thought that increased postprandial GLP-1 secretion is a major contributor to improved metabolic health after bariatric surgery, however not all mechanisms are well understood (Grill, 2020; Nannipieri et al., 2013). GLP-1 increases SAT and VAT blood flow in healthy individuals (Asmar et al., 2017; Müller et al., 2019). However, there was no association between SAT perfusion AUC and plasma GLP-1 AUC after a mixed meal in subjects with obesity after bariatric surgery. So, while

increased GLP-1 secretion is likely a contributor to improved metabolic health after bariatric surgery, it was not directly associated with SAT perfusion improvements.

Obesity-related complications are connected to the accumulation of VAT more than that of SAT (Cinti, 2005; Gallagher et al., 2009). It has been shown that bariatric surgery reduces both VAT and SAT, however, a larger portion of VAT is reduced (Bazzocchi et al., 2015; Guiducci et al., 2007; Merlotti et al., 2017; Toro-Ramos et al., 2015). In study III bariatric surgery reduced both SAT and VAT mass in subjects with obesity. A mixed meal and GIP-infusion induced similar responses in VAT blood flow of subjects with obesity before and after bariatric surgery and control subjects, indicating that VAT perfusion is not blunted in obesity as SAT perfusion is.

## 6.7 Strengths and limitations

PET/CT imaging is a non-invasive method, which is highly sensitive. Using dynamic PET image acquisition tissue-specific tracer uptake can be quantified. In studies I and II the same subjects were imaged twice, which allowed for pairwise comparisons. In study I the room temperature scans worked as a negative control for cold exposure scans, and in study II cold exposure scans acted as a positive control when compared to postprandial activation. In study III SAT and VAT perfusion was measured under non-stimulated and stimulated conditions both in lean and obese – as well as before-and-after bariatric surgery-associated weight loss. Since the same subject was imaged at basal conditions and at two time points after stimulation this allowed a pair-wise comparison of the results, as well as observing the interaction over time. The same limitations apply to all studies; PET scanners used in these studies only had a limited FOV not allowing for the simultaneous dynamic image acquisition of more tissues, the resolution of images limits the quantification of tracer uptake of smaller areas, and since subjects are exposed to radiation it decreases the number of times each subject can be imaged.

A limiting factor in the BAT studies (I-II) was the low number of subjects who demonstrated histological evidence of BAT (7 out of 31 that volunteered for biopsy), making statistical comparison difficult in some cases. Merely the histology of the tissue samples has been studied, and differentiation between BAT and SAT can be challenging based on histology alone. Further, due to the small sample size and inter-individual variability of FAU in BAT, it is not possible to suggest a FAU value cutoff point for a subject to be likely possessing histologically evident BAT. The groups in studies I-II differed in terms of age, with subjects with obesity tending to be older on average (not significantly, $p=0.1$). The number of subjects with obesity was also lower compared to lean subjects. In multiple linear regression analysis, no confounding factors were found. When comparing cold exposure and room temperature values

paired t-tests were performed, to reduce the effect of interindividual variation. Additionally, BAT FAU measured with PET merely tells us the tissue intake of fatty acids. This method cannot reveal the subsequent post-uptake fate of fatty acids i.e., whether they are utilized for mitochondrial oxidative metabolism, or intracellular lipid storage. Spillover from other tissues is also an issue when analyzing smaller depots, which might cause an overestimation of activity. This is the reason why the focus of these studies is on the supraclavicular BAT depot since they are the largest "uniform" depot of BAT in humans. In postprandial study II, the use of FAU to compare activity proved difficult, since its calculation is dependent on plasma FFA levels, which are greatly suppressed in the postprandial state. This causes postprandial FAU levels to be low. To avoid this, the net influx rate was used in these comparisons, since it is unaffected by plasma FFA levels. While this does not reflect the actual FAU, it does tell us of the potential of FAU.

The follow-up time after bariatric surgery (study III) was relatively short, the mixed meal test was repeated on average 69 days, and the GIP-infusion test 80 days following the surgery. Since the subjects with obesity were still in the process of rapid weight loss, it is possible that more pronounced changes in AT blood flow could be seen at a later time point after surgery. However, this can also be considered a strength of the study, since the rapid changes in AT perfusion under stimulation can already be seen shortly after bariatric surgery. In study III there was no statistically significant difference in visceral AT blood flow between controls and subjects with obesity, which could be due to high inter-individual variation, where a larger study cohort could have helped. It is difficult to determine whether the changes are more dependent on changes in insulin sensitivity and glucose homeostasis or weight loss.

# 7 Conclusions

I. Cold exposure increases BAT FAU in lean subjects, but this effect is blunted in subjects with obesity. Lower BAT FAU is related to obesity and several obesity-related parameters, as well as age. In subjects with obesity, BAT metabolism is not only lower during cold stimulation but also at the basal level. This suggests that supraclavicular fat depots of subjects with obesity mostly consist of WAT. The increased BAT FAU at basal state compared to SAT in lean subjects shows that BAT is somewhat active even at basal state, implying an increased fatty acid metabolism or increased lipid turnover.

II. A mixed meal increased BAT perfusion similarly to cold exposure, indicating that BAT is activated by meal ingestion as well as cold exposure. BAT FAU was reduced by meal ingestion in all tissues, due to reduced plasma FFA concentrations by insulin action. The net influx rate of the palmitate analog $^{18}$F-FTHA into BAT increased in lean but not in subjects with obesity after meal ingestion. In lean subjects, this increase was even more pronounced than during cold exposure. However, it seems that obesity has a blunting effect on $^{18}$F-FTHA uptake in both stimulated conditions. It is possible that lower plasma FFA concentrations increased BAT fatty acid transport increasing the influx rate. This shows that BAT metabolism increases after meal ingestion and since FFAs are less available during postprandial state, intracellular TGs or glucose may be the most important energy sources for BAT after a meal.

III. SAT blood flow of subjects with obesity following a meal or GIP infusion is blunted. After bariatric surgery meal ingestion elicits a normalized response in SAT, increasing perfusion similarly to control subjects. Normalization of postprandial SAT perfusion may contribute to the improved metabolic condition induced by bariatric surgery. Postprandial normalization of WAT blood flow would reduce lipid overflow, reducing ectopic fat accumulation. VAT perfusion remained similar after bariatric surgery, showing that VAT function is at least somewhat retained in obesity. Since GIP induces an increase in blood flow to SAT and VAT even before bariatric surgery, the normalized meal response seen in SAT after bariatric surgery could be mediated via other regulators than GIP, such as other gut hormones.

# 8 Acknowledgements

This study was conducted at the Turku PET Centre, University of Turku, and Turku University Hospital.

I wish to thank my supervisors associate professor Kirsi Virtanen and Dr. Mueez U Din. Thank you, Kirsi for introducing me to PET imaging and brown adipose tissue research and for giving me this opportunity to take part in several projects over the years. I have learned innumerable things during my time working at Turku PET Centre. I'm grateful for your guidance and patience with me. Thank you, Mueez, you have been an important part of my Ph.D. journey, your support and collaboration over the years have been remarkable.

I also wish to thank the reviewers of this work docent Tiina Ikäheimo and assistant professor Maria Chondronikola for their valuable and constructive feedback, which helped me improve the thesis. I also wish to thank associate professor Jonatan Ruiz for accepting the role of dissertation opponent. Thank you to docent Jarna Hannukainen and professor Eriika Savontaus, members of my Ph.D. follow-up committee, for their support.

I am very grateful for all my excellent collaborators and co-authors in these projects. I have learned a lot from all of you and your expertise, support and knowledge are very much appreciated. I wish to thank Juho Raiko for his important role in the studies, I also always admired your confidence when writing and making it look easy. Jukka Koffert and Henri Honka thank you for your role in acquiring, and your support in analyzing, the bariatric surgery data. Thank you, Janne Orava, for teaching me the analysis of PET images and helping me with all my questions at the beginning. I am grateful for the guidance and support professor Pirjo Nuutila has provided. I wish to thank my co-workers at Turku PET Centre Miikka Honka, Minna Lahesmaa, Prince Dadson, Piryanka Motiani, Kumail Motiani, Kalle Koskensalo, and Francisco Acosta for always keeping up a good atmosphere and good discussions, work-related or not. Thank you to all the staff at Turku PET Centre whose work and efforts allowed us to carry out these studies. Thank you to Rami Mikkola and Marko Tättäläinen for providing IT support as well as Sauli Pirola and Timo Laitinen for their help with Carimas. Thanks to all the volunteers who participated in these studies, this work would not be possible without them.

Thank you to my parents Asmo and Marjut for supporting me. I also wish to thank Helena and Väinö for all the support over the years. Thank you to all my friends who have had the patience to listen to my jabbering about my work over the years after making the mistake of asking “Mites väikkäri?”. Special thanks to Siiri, Niitti, Kipi, Toki, and Tyrni for always bringing me joy. Finally, I wish that thank my wife Elina for her support and love during this project, you have always encouraged me to keep going.

# References


Abelson, P., and Kennedy, D. (2004). The Obesity Epidemic. Science (1979) *304*, 1413–1413. https://doi.org/10.1126/science.304.5676.1413.

Acosta, F.M., Martinez-Tellez, B., Sanchez-Delgado, G., Alcantara, J.M.A., Acosta-Manzano, P., Morales-Artacho, A.J., and Ruiz, J.R. (2018). Physiological responses to acute cold exposure in young lean men. PLoS ONE *13*. https://doi.org/10.1371/JOURNAL.PONE.0196543.

Adams, T.D., Davidson, L.E., Litwin, S.E., Kolotkin, R.L., LaMonte, M.J., Pendleton, R.C., Strong, M.B., Vinik, R., Wanner, N.A., Hopkins, P.N., et al. (2012). Health benefits of gastric bypass surgery after 6 years. JAMA - Journal of the American Medical Association *308*, 1122–1131. https://doi.org/10.1001/2012.jama.11164.

Adams, T.D., Davidson, L.E., Litwin, S.E., Kim, J., Kolotkin, R.L., Nanjee, M.N., Gutierrez, J.M., Frogley, S.J., Ibele, A.R., Brinton, E.A., et al. (2017). Weight and Metabolic Outcomes 12 Years after Gastric Bypass. New England Journal of Medicine *377*, 1143–1155. https://doi.org/10.1056/nejmoa1700459.

Aherne, W., and Hull, D. (1966). Brown adipose tissue and heat production in the newborn infant. J Pathol Bacteriol *91*, 223–234. https://doi.org/10.1002/PATH.1700910126.

Arch, J.R.S. (2002). β3-Adrenoceptor agonists: potential, pitfalls and progress. European Journal of Pharmacology *440*, 99–107. https://doi.org/10.1016/S0014-2999(02)01421-8.

Arch, J.R.S. (2008). The discovery of drugs for obesity, the metabolic effects of leptin and variable receptor pharmacology: perspectives from β3-adrenoceptor agonists. Naunyn-Schmiedeberg's Archives of Pharmacology 2008 378:2 *378*, 225–240. https://doi.org/10.1007/S00210-008-0271-1.

Ardilouze, J.-L., Sotorník, R., Dennis, L.A., Fielding, B.A., Frayn, K.N., and Karpe, F. (2012). Failure to increase postprandial blood flow in subcutaneous adipose tissue is associated with tissue resistance to adrenergic stimulation. Diabetes Metab *38*, 27–33. https://doi.org/10.1016/j.diabet.2011.06.005.

Arita, Y., Kihara, S., Ouchi, N., Takahashi, M., Maeda, K., Miyagawa, J.I., Hotta, K., Shimomura, I., Nakamura, T., Miyaoka, K., et al. (1999). Paradoxical decrease of an adipose-specific protein, adiponectin, in obesity. Biochemical and Biophysical Research Communications *257*, 79–83. https://doi.org/10.1006/bbrc.1999.0255.

Asmar, A., Asmar, M., Simonsen, L., Madsbad, S., Holst, J.J., Hartmann, B., Sorensen, C.M., and Bülow, J. (2017). Glucagon-like peptide-1 elicits vasodilation in adipose tissue and skeletal muscle in healthy men. Physiological Reports *5*. https://doi.org/10.14814/phy2.13073.

Asmar, M., Simonsen, L., Madsbad, S., Stallknecht, B., Holst, J.J., and Bülow, J. (2010). Glucose-Dependent Insulinotropic Polypeptide May Enhance Fatty Acid Re-esterification in Subcutaneous Abdominal Adipose Tissue in Lean Humans. Diabetes *59*, 2160–2163. https://doi.org/10.2337/db10-0098.

Asmar, M., Simonsen, L., Arngrim, N., Holst, J.J., Dela, F., and Bülow, J. (2014). Glucose-dependent insulinotropic polypeptide has impaired effect on abdominal, subcutaneous adipose tissue metabolism in obese subjects. International Journal of Obesity *38*, 259–265. https://doi.org/10.1038/ijo.2013.73.

Asmar, M., Simonsen, L., Asmar, A., Holst, J.J., Dela, F., and Bülow, J. (2016a). Insulin Plays a Permissive Role for the Vasoactive Effect of GIP Regulating Adipose Tissue Metabolism in Humans. The Journal of Clinical Endocrinology & Metabolism *101*, 3155–3162. https://doi.org/10.1210/jc.2016-1933.

Asmar, M., Arngrim, N., Simonsen, L., Asmar, A., Nordby, P., Holst, J.J., and Bülow, J. (2016b). The blunted effect of glucose-dependent insulinotropic polypeptide in subcutaneous abdominal adipose tissue in obese subjects is partly reversed by weight loss. Nutrition and Diabetes *6*. https://doi.org/10.1038/nutd.2016.15.

van Baak, M.A. (2008). Meal-induced activation of the sympathetic nervous system and its cardiovascular and thermogenic effects in man. Physiology & Behavior *94*, 178–186. https://doi.org/https://doi.org/10.1016/j.physbeh.2007.12.020.

Bahler, L., Verberne, H.J., Admiraal, W.M., Stok, W.J., Soeters, M.R., Hoekstra, J.B., and Holleman, F. (2016). Differences in Sympathetic Nervous Stimulation of Brown Adipose Tissue Between the Young and Old, and the Lean and Obese. J Nucl Med *57*, 372–377. https://doi.org/10.2967/jnumed.115.165829.

Ballantyne, G.H., Farkas, D., Laker, S., and Wasielewski, A. (2006). Short-term Changes in Insulin Resistance following Weight Loss Surgery for Morbid Obesity: Laparoscopic Adjustable Gastric Banding versus Laparoscopic Roux-en-Y Gastric Bypass. Obesity Surgery 2006 16:9 *16*, 1189–1197. https://doi.org/10.1381/096089206778392158.

Baron, A.D. (1994). Hemodynamic actions of insulin. Am J Physiol *267*, E187-202. https://doi.org/10.1152/ajpendo.1994.267.2.E187.

Barrington, S.F., and Maisey, M.N. (1996). Skeletal Muscle Uptake of Fluorine-18-FDG: Effect of Oral Diazepam. Journal of Nuclear Medicine *37*, 1127 LP – 1129.

Bartelt, A., and Heeren, J. (2014). Adipose tissue browning and metabolic health. Nature Reviews Endocrinology *10*, 24–36. https://doi.org/10.1038/nrendo.2013.204.

Bartelt, A., Bruns, O.T., Reimer, R., Hohenberg, H., Ittrich, H., Peldschus, K., Kaul, M.G., Tromsdorf, U.I., Weller, H., Waurisch, C., et al. (2011). Brown adipose tissue activity controls triglyceride clearance. Nature Medicine *17*, 200–205. https://doi.org/10.1038/nm.2297.

Bazzocchi, A., Ponti, F., Cariani, S., Diano, D., Leuratti, L., Albisinni, U., Marchesini, G., and Battista, G. (2015). Visceral Fat and Body Composition Changes in a Female Population After RYGBP: a Two-Year Follow-Up by DXA. Obesity Surgery *25*, 443–451. https://doi.org/10.1007/s11695-014-1422-8.

Bengtsson, T., Cannon, B., and Nedergaard, J. (2000). Differential adrenergic regulation of the gene expression of the beta-adrenoceptor subtypes beta1, beta2 and beta3 in brown adipocytes. Biochemical Journal *347*, 643.

Berbée, J.F.P., Boon, M.R., Khedoe, P.P.S.J., Bartelt, A., Schlein, C., Worthmann, A., Kooijman, S., Hoeke, G., Mol, I.M., John, C., et al. (2015). Brown fat activation reduces hypercholesterolaemia and protects from atherosclerosis development. Nature Communications *6*, 6356. https://doi.org/10.1038/ncomms7356.

Berg, A.H., Combs, T.P., Du, X., Brownlee, M., and Scherer, P.E. (2001). The adipocyte-secreted protein Acrp30 enhances hepatic insulin action. Nature Medicine *7*, 947–953. https://doi.org/10.1038/90992.

Bianco, A.C., and McAninch, E.A. (2013). The role of thyroid hormone and brown adipose tissue in energy homoeostasis. Lancet Diabetes Endocrinol *1*, 250–258. https://doi.org/10.1016/S2213-8587(13)70069-X.

Blondin, D.P., Labbé, S.M., Tingelstad, H.C., Noll, C., Kunach, M., Phoenix, S., Guérin, B., Turcotte, É.E., Carpentier, A.C., Richard, D., et al. (2014). Increased Brown Adipose Tissue Oxidative Capacity in Cold-Acclimated Humans. The Journal of Clinical Endocrinology & Metabolism *99*, E438–E446. https://doi.org/10.1210/jc.2013-3901.

Blondin, D.P., Labbé, S.M., Noll, C., Kunach, M., Phoenix, S., Guérin, B., Turcotte, É.E., Haman, F., Richard, D., and Carpentier, A.C. (2015). Selective impairment of glucose but not fatty acid or oxidative metabolism in brown adipose tissue of subjects with type 2 diabetes. Diabetes https://doi.org/10.2337/db14-1651.

Blondin, D.P., Frisch, F., Phoenix, S., Guérin, B., Turcotte, É.E., Haman, F., Richard, D., and Carpentier, A.C. (2017). Inhibition of Intracellular Triglyceride Lipolysis Suppresses Cold-Induced Brown Adipose Tissue Metabolism and Increases Shivering in Humans. Cell Metabolism *25*, 438–447. https://doi.org/10.1016/j.cmet.2016.12.005.

Blondin, D.P., Nielsen, S., Kuipers, E.N., Severinsen, M.C., Jensen, V.H., Miard, S., Jespersen, N.Z., Kooijman, S., Boon, M.R., Fortin, M., et al. (2020). Human Brown Adipocyte Thermogenesis Is Driven by β2-AR Stimulation. Cell Metabolism *32*, 287-300.e7. https://doi.org/10.1016/J.CMET.2020.07.005.

Broeders, E.P.M., Nascimento, E.B.M., Havekes, B., Brans, B., Roumans, K.H.M., Tailleux, A., Schaart, G., Kouach, M., Charton, J., Deprez, B., et al. (2015). The Bile Acid Chenodeoxycholic Acid Increases Human Brown Adipose Tissue Activity. Cell Metabolism *22*, 418–426. https://doi.org/10.1016/J.CMET.2015.07.002.

Brychta, R.J., and Chen, K.Y. (2017). Cold-induced thermogenesis in humans. Eur J Clin Nutr *71*, 345. https://doi.org/10.1038/EJCN.2016.223.

Buchwald, H., Estok, R., Fahrbach, K., Banel, D., Jensen, M.D., Pories, W.J., Bantle, J.P., and Sledge, I. (2009). Weight and Type 2 Diabetes after Bariatric Surgery: Systematic Review and Meta-analysis. American Journal of Medicine *122*. https://doi.org/10.1016/j.amjmed.2008.09.041.

Calanna, S., Christensen, M., Holst, J.J., Laferrère, B., Gluud, L.L., Vilsbøll, T., and Knop, F.K. (2013). Secretion of glucose-dependent insulinotropic polypeptide in patients with type 2 diabetes: systematic review and meta-analysis of clinical studies. Diabetes Care *36*, 3346–3352. https://doi.org/10.2337/dc13-0465.

Cannon, B., and Nedergaard, J. (2004). Brown Adipose Tissue: Function and Physiological Significance. Physiological Reviews *84*, 277–359. https://doi.org/10.1152/physrev.00015.2003.

Carmeliet, P., and Tessier-Lavigne, M. (2005). Common mechanisms of nerve and blood vessel wiring. Nature *436*, 193–200. https://doi.org/10.1038/nature03875.

Carpentier, A.C., Blondin, D.P., Virtanen, K.A., Richard, D., Haman, F., and Turcotte, É.E. (2018). Brown adipose tissue energy metabolism in humans. Frontiers in Endocrinology *9*. https://doi.org/10.3389/fendo.2018.00447.

Castellani, J.W., and Young, A.J. (2016). Human physiological responses to cold exposure: Acute responses and acclimatization to prolonged exposure. Autonomic Neuroscience *196*, 63–74. https://doi.org/10.1016/J.AUTNEU.2016.02.009.

Chen, K.Y., Brychta, R.J., Linderman, J.D., Smith, S., Courville, A., Dieckmann, W., Herscovitch, P., Millo, C.M., Remaley, A., Lee, P., et al. (2013). Brown Fat Activation Mediates Cold-Induced Thermogenesis in Adult Humans in Response to a Mild Decrease in Ambient Temperature. The Journal of Clinical Endocrinology & Metabolism *98*, E1218–E1223. https://doi.org/10.1210/jc.2012-4213.

Chen, K.Y., Cypess, A.M., Laughlin, M.R., Haft, C.R., Hu, H.H., Bredella, M.A., Enerbäck, S., Kinahan, P.E., Lichtenbelt, W. van M., Lin, F.I., et al. (2016). Brown Adipose Reporting Criteria in Imaging STudies (BARCIST 1.0): Recommendations for Standardized FDG-PET/CT Experiments in Humans. Cell Metab *24*, 210. https://doi.org/10.1016/J.CMET.2016.07.014.

Chondronikola, M., Volpi, E., Børsheim, E., Porter, C., Annamalai, P., Enerbäck, S., Lidell, M.E., Saraf, M.K., Labbe, S.M., Hurren, N.M., et al. (2014). Brown adipose tissue improves whole-body glucose homeostasis and insulin sensitivity in humans. Diabetes *63*, 4089–4099. https://doi.org/10.2337/db14-0746.

Chondronikola, M., Volpi, E., Børsheim, E., Porter, C., Saraf, M.K., Annamalai, P., Yfanti, C., Chao, T., Wong, D., Shinoda, K., et al. (2016). Brown Adipose Tissue Activation Is Linked to Distinct Systemic Effects on Lipid Metabolism in Humans. Cell Metabolism *23*, 1200–1206. https://doi.org/10.1016/j.cmet.2016.04.029.

Christensen, M., Vedtofte, L., Holst, J.J., Vilsbøll, T., and Knop, F.K. (2011). Glucose-dependent insulinotropic polypeptide: A bifunctional glucose-dependent regulator of glucagon and insulin secretion in humans. Diabetes *60*, 3103–3109. https://doi.org/10.2337/db11-0979.

Cinti, S. (2005). The adipose organ. Prostaglandins Leukot Essent Fatty Acids *73*, 9–15. https://doi.org/10.1016/j.plefa.2005.04.010.

Cohade, C., Osman, M., Pannu, H.K., and Wahl, R.L. (2003). Uptake in supraclavicular area fat ("USA-Fat"): description on 18F-FDG PET/CT. J Nucl Med *44*, 170–176.

Collins, J.M., Neville, M.J., Pinnick, K.E., Hodson, L., Ruyter, B., Dijk, T.H. van, Reijngoud, D.-J., Fielding, M.D., and Frayn, K.N. (2011). De novo lipogenesis in the differentiating human adipocyte can provide all fatty acids necessary for maturation. Journal of Lipid Research *52*, 1683. https://doi.org/10.1194/JLR.M012195.

Coppack, S.W., Evans, R.D., Fisher, R.M., Frayn, K.N., Gibbons, G.F., Humphreys, S.M., Kirk, M.L., Potts, J.L., and Hockaday, T.D.R. (1992). Adipose tissue metabolism in obesity: Lipase action in vivo before and after a mixed meal. *41*, 264–272. https://doi.org/10.1016/0026-0495(92)90269-G.

Coppack, S.W., Fisher, R.M., Humphreys, S.M., Clark, M.L., Pointon, J.J., and Frayn, K.N. (1996). Carbohydrate metabolism in insulin resistance: glucose uptake and lactate production by adipose and forearm tissues in vivo before and after a mixed meal. Clin Sci (Lond) *90*, 409–415. https://doi.org/10.1042/cs0900409.

Cypess, A.M., Lehman, S., Williams, G., Tal, I., Rodman, D., Goldfine, A.B., Kuo, F.C., Palmer, E.L., Tseng, Y.-H., Doria, A., et al. (2009). Identification and Importance of Brown Adipose Tissue in Adult Humans. New England Journal of Medicine *360*, 1509–1517. https://doi.org/10.1056/NEJMoa0810780.

Cypess, A.M., White, A.P., Vernochet, C., Schulz, T.J., Xue, R., Sass, C.A., Huang, T.L., Roberts-Toler, C., Weiner, L.S., Sze, C., et al. (2013). Anatomical localization, gene expression profiling and functional characterization of adult human neck brown fat. Nature Medicine *19*, 635–639. https://doi.org/10.1038/nm.3112.

Czech, M.P., Tencerova, M., Pedersen, D.J., and Aouadi, M. (2013). Insulin signalling mechanisms for triacylglycerol storage. Diabetologia *56*, 949–964. https://doi.org/10.1007/s00125-013-2869-1.

Dadson, P., Hannukainen, J.C., Din, M.U., Lahesmaa, M., Kalliokoski, K.K., Iozzo, P., Pihlajamäki, J., Karlsson, H.K., Parkkola, R., Salminen, P., et al. (2018). Brown adipose tissue lipid metabolism in morbid obesity: Effect of bariatric surgery-induced weight loss. Diabetes, Obesity and Metabolism *20*, 1280–1288. https://doi.org/10.1111/dom.13233.

DeFronzo, R.A., Tobin, J.D., and Andres, R. (1979). Glucose clamp technique: A method for quantifying insulin secretion and resistance. *237*, E214-23. https://doi.org/10.1152/ajpendo.1979.237.3.E214.

Degrado, T.R. (1991). Synthesis of 14 (R,S)-[18F]fluoro-6-thia-heptadecanoic acid (FTHA). Journal of Labelled Compounds and Radiopharmaceuticals *29*, 989–995. https://doi.org/10.1002/jlcr.2580290903.

DeGrado, T.R., Coenen, H.H., and Stöcklin, G. (1991). 14(R,S)-[18F]Fluoro-6-Thia-Heptadecanoic Acid (FTHA): Evaluation in Mouse of a New Probe of Myocardial Utilization of Long Chain Fatty Acids. Journal of Nuclear Medicine *32*.

DeGrado, T.R., Wang, S., and Rockey, D.C. (2000). Preliminary Evaluation of 15-[18F]Fluoro-3-oxa-pentadecanoate as a PET Tracer of Hepatic Fatty Acid Oxidation. Journal of Nuclear Medicine *41*.

Després, J.P., and Lemieux, I. (2006). Abdominal obesity and metabolic syndrome. Nature *444*, 881–887. https://doi.org/10.1038/nature05488.

Eckel, R.H., Fujimoto, W.Y., and Brunzell, J.D. (1979). Gastric Inhibitory Polypeptide Enhanced Lipoprotein Lipase Activity in Cultured Preadipocytes. Diabetes *28*, 1141 LP – 1142. https://doi.org/10.2337/diab.28.12.1141.

Enerbäck, S. (2010). Human Brown Adipose Tissue. Cell Metabolism *11*, 248–252. https://doi.org/10.1016/J.CMET.2010.03.008.

Engel, H., Steinert, H., Buck, A., Berthold, T., Huch Böni, R.A., and von Schulthess, G.K. (1996). Whole-Body PET: Physiological and Artifactual Fluorodeoxyglucose Accumulations. Journal of Nuclear Medicine *37*, 441 LP – 446.

Eriksson, O., Mikkola, K., Espes, D., Tuominen, L., Virtanen, K., Forsbäck, S., Haaparanta-Solin, M., Hietala, J., Solin, O., and Nuutila, P. (2015). The Cannabinoid Receptor-1 Is an Imaging Biomarker of Brown Adipose Tissue. Journal of Nuclear Medicine *56*, 1937 LP – 1941. https://doi.org/10.2967/jnumed.115.156422.

Essen, G. von, Lindsund, E., Cannon, B., Nedergaard, J., von Essen, G., Lindsund, E., Cannon, B., and Nedergaard, J. (2017). Adaptive facultative diet-induced thermogenesis in wild-type but not in UCP1-ablated mice. American Journal of Physiology-Endocrinology and Metabolism *313*, E515–E527. https://doi.org/10.1152/ajpendo.00097.2017.

Falko, J.M., Crockett, S.E., Cataland, S., and Mazzaferri, E.L. (1975). Gastric Inhibitory Polypeptide (GIP) Stimulated by Fat Ingestion in Man. The Journal of Clinical Endocrinology & Metabolism *41*, 260–265. https://doi.org/10.1210/jcem-41-2-260.

Fang, H., and Judd, R.L. (2018). Adiponectin Regulation and Function. Compr Physiol *8*, 1031–1063. https://doi.org/10.1002/CPHY.C170046.

Fang, S., Suh, J.M., Reilly, S.M., Yu, E., Osborn, O., Lackey, D., Yoshihara, E., Perino, A., Jacinto, S., Lukasheva, Y., et al. (2015). Intestinal FXR agonism promotes adipose tissue browning and reduces obesity and insulin resistance. Nat Med *21*, 159. https://doi.org/10.1038/NM.3760.

Fielding, B.A., and Frayn, K.N. (1998). Lipoprotein lipase and the disposition of dietary fatty acids. British Journal of Nutrition *80*, 495–502. https://doi.org/10.1017/S0007114598001585.

Fox, C.S., Massaro, J.M., Hoffmann, U., Pou, K.M., Maurovich-Horvat, P., Liu, C.-Y., Vasan, R.S., Murabito, J.M., Meigs, J.B., Cupples, L.A., et al. (2007). Abdominal Visceral and Subcutaneous Adipose Tissue Compartments. Circulation *116*, 39–48. https://doi.org/10.1161/CIRCULATIONAHA.106.675355.

Frayn, K.N. (2002). Adipose tissue as a buffer for daily lipid flux. Diabetologia *45*, 1201–1210. https://doi.org/10.1007/S00125-002-0873-Y.

Frayn, K.N., and Karpe, F. (2014). Regulation of human subcutaneous adipose tissue blood flow. International Journal of Obesity *38*, 1019–1026. https://doi.org/10.1038/ijo.2013.200.

Frayn, K.N., Karpe, F., Fielding, B.A., Macdonald, I.A., and Coppack, S.W. (2003). Integrative physiology of human adipose tissue. International Journal of Obesity *27*, 875–888. https://doi.org/10.1038/sj.ijo.0802326.

Friedman, J.M., and Halaas, J.L. (1998). Leptin and the regulation of body weight in mammals. Nature *395*, 763–770. https://doi.org/10.1038/27376.

Fu, Y., Luo, N., Klein, R.L., and Timothy Garvey, W. (2005). Adiponectin promotes adipocyte differentiation, insulin sensitivity, and lipid accumulation. Journal of Lipid Research *46*, 1369–1379. https://doi.org/10.1194/jlr.M400373-JLR200.

Gallagher, D., Kelley, D.E., Yim, J.E., Spence, N., Albu, J., Boxt, L., Xavier Pi-Sunyer, F., and Heshka, S. (2009). Adipose tissue distribution is different in type 2 diabetes. American Journal of Clinical Nutrition *89*, 807–814. https://doi.org/10.3945/ajcn.2008.26955.

Geerling, J.J., Boon, M.R., Kooijman, S., Parlevliet, E.T., Havekes, L.M., Romijn, J.A., Meurs, I.M., and Rensen, P.C.N. (2014). Sympathetic nervous system control of triglyceride metabolism: Novel concepts derived from recent studies. Journal of Lipid Research *55*, 180–189. https://doi.org/10.1194/jlr.R045013.

Ghorbani, M., Claus, T.H., and Himms-Hagen, J. (1997). Hypertrophy of brown adipocytes in brown and white adipose tissues and reversal of diet-induced obesity in rats treated with a β3-adrenoceptor agonist. Biochemical Pharmacology *54*, 121–131. https://doi.org/10.1016/S0006-2952(97)00162-7.

Gjedde, A. (1982). Calculation of cerebral glucose phosphorylation from brain uptake of glucose analogs in vivo: a re-examination. Brain Res *257*, 237–274.

Glick, Z., Teague, R.J., and Bray, G.A. (1981). Brown adipose tissue: thermic response increased by a single low protein, high carbohydrate meal. Science *213*, 1125–1127.

Glick, Z., Teague, R.J., Bray, G.A., and Lee, M. (1983). Compositional and metabolic changes in brown adipose tissue following a single test meal. Metabolism *32*, 1146–1150.

Glick, Z., Wickler, S.J., Stern, J.S., and Horwitz, B.A. (1984). Regional blood flow in rats after a single low-protein, high-carbohydrate test meal. The American Journal of Physiology *247*, R160-6.

Glick, Z., Wu, S.Y., Lupien, J., Reggio, R., Bray, G.A., and Fisher, D.A. (1985). Meal-induced brown fat thermogenesis and thyroid hormone metabolism in rats. The American Journal of Physiology *249*, E519-24.

Gloy, V.L., Briel, M., Bhatt, D.L., Kashyap, S.R., Schauer, P.R., Mingrone, G., Bucher, H.C., and Nordmann, A.J. (2013). Bariatric surgery versus non-surgical treatment for obesity: a systematic review and meta-analysis of randomised controlled trials. BMJ *347*. https://doi.org/10.1136/BMJ.F5934.

Gnad, T., Scheibler, S., von Kügelgen, I., Scheele, C., Kilić, A., Glöde, A., Hoffmann, L.S., Reverte-Salisa, L., Horn, P., Mutlu, S., et al. (2014). Adenosine activates brown adipose tissue and recruits beige adipocytes via A2A receptors. Nature *516*, 395–399. https://doi.org/10.1038/nature13816.

Goossens, G.H., and Karpe, F. (2008). Human adipose tissue blood flow and micromanipulation of human subcutaneous blood flow. Methods in Molecular Biology *456*, 97–107. https://doi.org/10.1007/978-1-59745-245-8_7.

Grill, H.J. (2020). A Role for GLP-1 in Treating Hyperphagia and Obesity. Endocrinology *161*, bqaa093. https://doi.org/10.1210/endocr/bqaa093.

Guiducci, L., Grönroos, T., Järvisalo, M.J., Kiss, J., Viljanen, A., Naum, A.G., Viljanen, T., Savunen, T., Knuuti, J., Ferrannini, E., et al. (2007). Biodistribution of the fatty acid analogue 18F-FTHA: Plasma and tissue partitioning between lipid pools during fasting and hyperinsulinemia. Journal of Nuclear Medicine *48*, 455–462.

Guilherme, A., Virbasius, J. V., Puri, V., and Czech, M.P. (2008). Adipocyte dysfunctions linking obesity to insulin resistance and type 2 diabetes. Nature Reviews Molecular Cell Biology *9*, 367–377. https://doi.org/10.1038/nrm2391.

Guilherme, A., Henriques, F., Bedard, A.H., and Czech, M.P. (2019). Molecular pathways linking adipose innervation to insulin action in obesity and diabetes mellitus. Nature Reviews Endocrinology *15*, 207–225. https://doi.org/10.1038/s41574-019-0165-y.

Hanson, R., RE, Pratley, R., Bogardus, C., Narayan, K., Roumain, J., Imperatore, G., Fagot-Campagna, A., Pettitt, D., Bennett, P., and Knowler, W. (2000). Evaluation of simple indices of insulin sensitivity and insulin secretion for use in epidemiologic studies. Am J Epidemiol *151*, 190–198. https://doi.org/10.1093/OXFORDJOURNALS.AJE.A010187.

Hanssen, M.J.W., Hoeks, J., Brans, B., van der Lans, A.A.J.J., Schaart, G., van den Driessche, J.J., Jörgensen, J.A., Boekschoten, M. V, Hesselink, M.K.C., Havekes, B., et al. (2015). Short-term cold acclimation improves insulin sensitivity in patients with type 2 diabetes mellitus. Nature Medicine 2015 21:8 *21*, 863–865. https://doi.org/10.1038/nm.3891.

Hanssen, M.J.W.W., Lans, A.A.J.J. van der, Brans, B., Hoeks, J., Jardon, K.M.C.C., Schaart, G., Mottaghy, F.M., Schrauwen, P., Lichtenbelt, W.D. van M., van der Lans, A.A.J.J., et al. (2016). Short-term Cold Acclimation Recruits Brown Adipose Tissue in Obese Humans. Diabetes *65*, 1179–1189. https://doi.org/10.2337/db15-1372.

Hany, T.F., Gharehpapagh, E., Kamel, E.M., Buck, A., Himms-Hagen, J., and von Schulthess, G.K. (2002). Brown adipose tissue: a factor to consider in symmetrical tracer uptake in the neck and upper chest region. European Journal of Nuclear Medicine and Molecular Imaging *29*, 1393–1398. https://doi.org/10.1007/s00259-002-0902-6.

Harms, M., and Seale, P. (2013). Brown and beige fat: development, function and therapeutic potential. Nature Medicine 2013 19:10 *19*, 1252–1263. https://doi.org/10.1038/nm.3361.

Harms, H.J., Nesterov, S. v, Han, C., Danad, I., Leonora, R., Raijmakers, P.G., Lammertsma, A.A., Knuuti, J., and Knaapen, P. (2014). Comparison of clinical non-commercial tools for automated quantification of myocardial blood flow using oxygen-15-labelled water PET/CT. European Heart Journal - Cardiovascular Imaging *15*, 431–441. https://doi.org/10.1093/ehjci/jet177.

Hassi, J. (1977). The brown adipose tissue in man: Structural and functional aspects in relation to age.

Heaton, J.M. (1972). The distribution of brown adipose tissue in the human. J Anat. *112*:35-39.

Heinonen, I., Bucci, M., Kemppainen, J., Knuuti, J., Nuutila, P., Boushel, R., and Kalliokoski, K.K. (2012). Regulation of subcutaneous adipose tissue blood flow during exercise in humans. Journal of Applied Physiology *112*, 1059–1063. https://doi.org/10.1152/JAPPLPHYSIOL.00732.2011.

Himms-Hagen, J. (1979). Obesity may be due to a malfunctioning of brown fat. Canadian Medical Association Journal *121*, 1361.

Hocking, S., Samocha-Bonet, D., Milner, K.-L., Greenfield, J.R., and Chisholm, D.J. (2013). Adiposity and Insulin Resistance in Humans: The Role of the Different Tissue and Cellular Lipid Depots. Endocrine Reviews *34*, 463–500. https://doi.org/10.1210/ER.2012-1041.

Holland, W.L., Miller, R.A., Wang, Z. V., Sun, K., Barth, B.M., Bui, H.H., Davis, K.E., Bikman, B.T., Halberg, N., Rutkowski, J.M., et al. (2011). Receptor-mediated activation of ceramidase activity initiates the pleiotropic actions of adiponectin. Nature Medicine *17*, 55–63. https://doi.org/10.1038/nm.2277.

Holm, C., Østerlund, T., Laurell, H., and Contreras, J.A. (2000). Molecular Mechanisms Regulating Hormone-Sensitive Lipase and Lipolysis. Annual Review of Nutrition *20*, 365–393. https://doi.org/10.1146/annurev.nutr.20.1.365.

Holstila, M., Pesola, M., Saari, T., Koskensalo, K., Raiko, J., Borra, R.J.H., Nuutila, P., Parkkola, R., and Virtanen, K.A. (2017). MR signal-fat-fraction analysis and T2* weighted imaging measure BAT reliably on humans without cold exposure. Metabolism: Clinical and Experimental *70*. https://doi.org/10.1016/j.metabol.2017.02.001.

Huttunen, P., Hirvonen, J., and Kinnula, V. (1981). The occurrence of brown adipose tissue in outdoor workers. European Journal of Applied Physiology and Occupational Physiology *46*, 339–345. https://doi.org/10.1007/BF00422121.

Ibrahim, M.M. (2010). Subcutaneous and visceral adipose tissue: Structural and functional differences. Obesity Reviews *11*, 11–18. https://doi.org/10.1111/j.1467-789X.2009.00623.x.

Jansson, P.A., Larsson, A., and Lönnroth, P.N. (1998). Relationship between blood pressure, metabolic variables and blood flow in obese subjects with or without non-insulin-dependent diabetes mellitus. Eur J Clin Invest *28*, 813–818. https://doi.org/10.1046/j.1365-2362.1998.00360.x.

Jespersen, N.Z., Larsen, T.J., Peijs, L., Daugaard, S., Homøe, P., Loft, A., De Jong, J., Mathur, N., Cannon, B., Nedergaard, J., et al. (2013). A classical brown adipose tissue mrna signature partly overlaps with brite in the supraclavicular region of adult humans. Cell Metabolism *17*, 798–805. https://doi.org/10.1016/j.cmet.2013.04.011.

Jirapinyo, P., Jin, D.X., Qazi, T., Mishra, N., and Thompson, C.C. (2018). A Meta-Analysis of GLP-1 After Roux-En-Y Gastric Bypass: Impact of Surgical Technique and Measurement Strategy. Obesity Surgery *28*, 615–626. https://doi.org/10.1007/s11695-017-2913-1.

de Jong, J.M.A.A., Sun, W., Pires, N.D., Frontini, A., Balaz, M., Jespersen, N.Z., Feizi, A., Petrovic, K., Fischer, A.W., Bokhari, M.H., et al. (2019). Human brown adipose tissue is phenocopied by classical brown adipose tissue in physiologically humanized mice. Nature Metabolism *1*, 830–843. https://doi.org/10.1038/s42255-019-0101-4.

Kara, K., Boutin, P., Mori, Y., Tobe, K., Dina, C., Yasuda, K., Yamauchi, T., Otabe, S., Okada, T., Eto, K., et al. (2002). Genetic variation in the gene encoding adiponectin is associated with an increased risk of type 2 diabetes in the Japanese population. Diabetes *51*, 536–540. https://doi.org/10.2337/diabetes.51.2.536.

Karpe, F., Fielding, B.A., Ardilouze, J.-L., Ilic, V., Macdonald, I.A., and Frayn, K.N. (2002a). Effects of insulin on adipose tissue blood flow in man. The Journal of Physiology *540*, 1087–1093. https://doi.org/10.1113/JPHYSIOL.2001.013358.

Karpe, F., Fielding, B.A., Ilic, V., Macdonald, I.A., Summers, L.K.M., and Frayn, K.N. (2002b). Impaired postprandial adipose tissue blood flow response is related to aspects of insulin sensitivity. Diabetes *51*, 2467–2473. https://doi.org/10.2337/diabetes.51.8.2467.

Kawamata, Y., Fujii, R., Hosoya, M., Harada, M., Yoshida, H., Miwa, M., Fukusumi, S., Habata, Y., Itoh, T., Shintani, Y., et al. (2003). A G Protein-coupled Receptor Responsive to Bile Acids *. Journal of Biological Chemistry *278*, 9435–9440. https://doi.org/10.1074/JBC.M209706200.

Kersten, S. (2014). Physiological regulation of lipoprotein lipase (Elsevier).

Kety, S.S. (1985). Regional cerebral blood flow: Estimation by means of nonmetabolized diffusible tracers—An overview. Seminars in Nuclear Medicine *15*, 324–328. https://doi.org/10.1016/S0001-2998(85)80010-6.

Kety, S.S., and Schmidt, C.F. (1945). The determination of cerebral blood flow in man by the use of nitrous oxide in low concentrations. Am.J.Physiol. *143*.

Kim, S., and Moustaid-Moussa, N. (2000). Secretory, Endocrine and Autocrine/Paracrine Function of the Adipocyte. The Journal of Nutrition *130*, 3110S-3115S. https://doi.org/10.1093/jn/130.12.3110S.

Kim, W., and Egan, J.M. (2008). The role of incretins in glucose homeostasis and diabetes treatment. Pharmacological Reviews *60*, 470–512. https://doi.org/10.1124/pr.108.000604.

Knapper, J.M.E., Puddicombe, S.M., Morgan, L.M., and Fletcher, J.M. (1995). Investigations into the Actions of Glucose-Dependent Insulinotropic Polypeptide and Glucagon-Like Peptide-1(7–36)amide on Lipoprotein Lipase Activity in Explants of Rat Adipose Tissue. The Journal of Nutrition *125*, 183–188. https://doi.org/10.1093/jn/125.2.183.

Koponen, P., Borodulin, K., Lundqvist, A., Sääksjärvi, K., and Koskinen, S. (2018). FinTerveys 2017 -study.

Koskensalo, K., Raiko, J., Saari, T., Saunavaara, V., Eskola, O., Nuutila, P., Saunavaara, J., Parkkola, R., and Virtanen, K.A.K.A. (2017). Human Brown Adipose Tissue Temperature and Fat Fraction Are Related to Its Metabolic Activity. *102*, 1200–1207. https://doi.org/10.1210/jc.2016-3086.

Kozak, L.P. (2010). Brown Fat and the Myth of Diet-Induced Thermogenesis. Cell Metabolism *11*, 263–267. https://doi.org/10.1016/J.CMET.2010.03.009.

Krishnamoorthy, S., Schmall, J.P., and Surti, S. (2017). PET Physics and Instrumentation. Basic Science of PET Imaging 173–197. https://doi.org/10.1007/978-3-319-40070-9_8.

Kudomi, N., Hirano, Y., Koshino, K., Hayashi, T., Watabe, H., Fukushima, K., Moriwaki, H., Teramoto, N., Iihara, K., and Iida, H. (2013). Rapid quantitative CBF and CMRO(2) measurements from a single PET scan with sequential administration of dual (15)O-labeled tracers. J Cereb Blood Flow Metab *33*, 440–448. https://doi.org/10.1038/JCBFM.2012.188.

Labbé, S., Caron, A., Bakan, I., Laplante, M., Carpentier, A., Lecomte, R., and Richard, D. (2015). In vivo measurement of energy substrate contribution to cold-induced brown adipose tissue thermogenesis. FASEB J *29*, 2046–2058. https://doi.org/10.1096/FJ.14-266247.

Lafontan, M., and Langin, D. (2009). Lipolysis and lipid mobilization in human adipose tissue. Progress in Lipid Research *48*, 275–297. https://doi.org/10.1016/J.PLIPRES.2009.05.001.

Lahesmaa, M., Oikonen, V., Helin, S., Luoto, P., U Din, M., Pfeifer, A., Nuutila, P., and Virtanen, K.A. (2018a). Regulation of human brown adipose tissue by adenosine and A2A receptors – studies with [15O]H2O and [11C]TMSX PET/CT. European Journal of Nuclear Medicine and Molecular Imaging 2018 46:3 *46*, 743–750. https://doi.org/10.1007/S00259-018-4120-2.

Lahesmaa, M., Eriksson, O., Gnad, T., Oikonen, V., Bucci, M., Hirvonen, J., Koskensalo, K., Teuho, J., Niemi, T., Taittonen, M., et al. (2018b). Cannabinoid Type 1 Receptors Are Upregulated During Acute Activation of Brown Adipose Tissue. Diabetes *67*, 1226–1236. https://doi.org/10.2337/DB17-1366.

Lambadiari, V., Triantafyllou, K., and Dimitriadis, G.D. (2015). Insulin action in muscle and adipose tissue in type 2 diabetes: The significance of blood flow. World Journal of Diabetes *6*, 626. https://doi.org/10.4239/WJD.V6.I4.626.

Larsen, O.A., Lassen, N.A., and Quaade, F. (1966). Blood Flow through Human Adipose Tissue Determined with Radioactive Xenon. Acta Physiologica Scandinavica *66*, 337–345. https://doi.org/10.1111/j.1748-1716.1966.tb03208.x.

Lee, J.-Y., Takahashi, N., Yasubuchi, M., Kim, Y.-I., Hashizaki, H., Kim, M.-J., Sakamoto, T., Goto, T., and Kawada, T. (2012). Triiodothyronine induces UCP-1 expression and mitochondrial biogenesis in human adipocytes. American Journal of Physiology-Cell Physiology *302*, C463–C472. https://doi.org/10.1152/ajpcell.00010.2011.

Lee, P., Zhao, J.T., Swarbrick, M.M., Gracie, G., Bova, R., Greenfield, J.R., Freund, J., and Ho, K.K.Y. (2011). High Prevalence of Brown Adipose Tissue in Adult Humans. The Journal of Clinical Endocrinology & Metabolism *96*, 2450–2455. https://doi.org/10.1210/jc.2011-0487.

Lee, P., Smith, S., Linderman, J., Courville, A., Brychta, R., Dieckmann, W., Werner, C., Chen, K., and Celi, F. (2014). Temperature-acclimated brown adipose tissue modulates insulin sensitivity in humans. Diabetes *63*, 3686–3698. https://doi.org/10.2337/DB14-0513.

Lenaz, G. (1998). Role of mitochondria in oxidative stress and ageing. Biochim Biophys Acta *1366*, 53–67. https://doi.org/10.1016/s0005-2728(98)00120-0.

Lidell, M.E., Betz, M.J., Leinhard, O.D., Heglind, M., Elander, L., Slawik, M., Mussack, T., Nilsson, D., Romu, T., Nuutila, P., et al. (2013). Evidence for two types of brown adipose tissue in humans. Nature Medicine *19*, 631–634. https://doi.org/10.1038/nm.3017.

Lidell, M.E., Betz, M.J., and Enerbäck, S. (2014). Two types of brown adipose tissue in humans. Adipocyte *3*, 63–66. https://doi.org/10.4161/adip.26896.

Liu, X., Wang, S., You, Y., Meng, M., Zheng, Z., Dong, M., Lin, J., Zhao, Q., Zhang, C., Yuan, X., et al. (2015). Brown Adipose Tissue Transplantation Reverses Obesity in Ob/Ob Mice. Endocrinology *156*, 2461–2469. https://doi.org/10.1210/EN.2014-1598.

Lowell, B.B., S-Susulic, V., Hamann, A., Lawitts, J.A., Himms-Hagen, J., Boyer, B.B., Kozak, L.P., and Flier, J.S. (1993). Development of obesity in transgenic mice after genetic ablation of brown adipose tissue. Nature *366*, 740–742. https://doi.org/10.1038/366740a0.

Lule, V.K., Garg, S., Gosewade, S.C., Tomar, S.K., and Khedkar, C.D. (2016). Niacin. Encyclopedia of Food and Health 63–72. https://doi.org/10.1016/B978-0-12-384947-2.00483-9.

Lupien, J.R., Glick, Z., Saito, M., and Bray, G.A. (1985). Guanosine diphosphate binding to brown adipose tissue mitochondria is increased after single meal. The American Journal of Physiology *249*, R694-8.

Ma, S.W., and Foster, D.O. (1986). Uptake of glucose and release of fatty acids and glycerol by rat brown adipose tissue in vivo. Can J Physiol Pharmacol *64*, 609–614.

van Marken Lichtenbelt, W.D. (2021). Human Brown Adipose Tissue—A Decade Later. Obesity (Silver Spring) *29*, 1099. https://doi.org/10.1002/OBY.23166.

van Marken Lichtenbelt, W.D., Vanhommerig, J.W., Smulders, N.M., Drossaerts, J.M.A.F.L., Kemerink, G.J., Bouvy, N.D., Schrauwen, P., and Teule, G.J.J. (2009). Cold-Activated Brown Adipose Tissue in Healthy Men. New England Journal of Medicine *360*, 1500–1508. https://doi.org/10.1056/NEJMoa0808718.

Matsuda, M., and DeFronzo, R.A. (1999). Insulin sensitivity indices obtained from oral glucose tolerance testing: Comparison with the euglycemic insulin clamp. Diabetes Care *22*, 1462–1470. https://doi.org/10.2337/diacare.22.9.1462.

Matthews, D.R., Hosker, J.P., Rudenski, A.S., Naylor, B.A., Treacher, D.F., and Turner, R.C. (1985). Homeostasis model assessment: insulin resistance and β-cell function from fasting plasma glucose and insulin concentrations in man. Diabetologia *28*, 412–419. https://doi.org/10.1007/BF00280883.

Melvin, A., and McQuaid, S.E. (2018). In-vivo metabolic studies of regional adipose tissue. Cardiovascular Endocrinology and Metabolism *7*, 75–79. https://doi.org/10.1097/XCE.0000000000000154.

Meriläinen, P.T. (1987). Metabolic monitor. International Journal of Clinical Monitoring and Computing *4*, 167–177. https://doi.org/10.1007/BF02915904.

Merlotti, C., Ceriani, V., Morabito, A., and Pontiroli, A.E. (2017). Subcutaneous fat loss is greater than visceral fat loss with diet and exercise, weight-loss promoting drugs and bariatric surgery: A critical review and meta-analysis. International Journal of Obesity *41*, 672–682. https://doi.org/10.1038/ijo.2017.31.

Mihalopoulos, N.L., Yap, J.T., Beardmore, B., Holubkov, R., Nanjee, M.N., and Hoffman, J.M. (2020). Cold-Activated Brown Adipose Tissue is Associated with Less Cardiometabolic Dysfunction in Young Adults with Obesity. Obesity *28*, 916–923. https://doi.org/https://doi.org/10.1002/oby.22767.

Mills, E.L., Pierce, K.A., Jedrychowski, M.P., Garrity, R., Winther, S., Vidoni, S., Yoneshiro, T., Spinelli, J.B., Lu, G.Z., Kazak, L., et al. (2018). Accumulation of succinate controls activation of adipose tissue thermogenesis. Nature *560*, 102. https://doi.org/10.1038/S41586-018-0353-2.

Montez, J.M., Soukas, A., Asilmaz, E., Fayzikhodjaeva, G., Fantuzzi, G., and Friedman, J.M. (2005). Acute leptin deficiency, leptin resistance, and the physiologic response to leptin withdrawal. Proc Natl Acad Sci U S A *102*, 2537–2542. https://doi.org/10.1073/pnas.0409530102.

Morigny, P., Boucher, J., Arner, P., and Langin, D. (2021). Lipid and glucose metabolism in white adipocytes: pathways, dysfunction and therapeutics. Nature Reviews Endocrinology 1–20. https://doi.org/10.1038/s41574-021-00471-8.

Morrison, S.F., and Nakamura, K. (2019). Central Mechanisms for Thermoregulation. Annual Review of Physiology *81*, 285–308. https://doi.org/10.1146/annurev-physiol-020518-114546.

Morrison, S.F., Madden, C.J., and Tupone, D. (2012). Central control of brown adipose tissue thermogenesis. Frontiers in Endocrinology *3*. https://doi.org/10.3389/fendo.2012.00005.

Moses, W.W. (2011). Fundamental Limits of Spatial Resolution in PET. Nucl Instrum Methods Phys Res A *648 Supplement 1*, S236. https://doi.org/10.1016/J.NIMA.2010.11.092.

Müller, T.D., Finan, B., Bloom, S.R., D'Alessio, D., Drucker, D.J., Flatt, P.R., Fritsche, A., Gribble, F., Grill, H.J., Habener, J.F., et al. (2019). Glucagon-like peptide 1 (GLP-1). Molecular Metabolism *30*, 72–130. https://doi.org/10.1016/j.molmet.2019.09.010.

Murphy, M.P., and O'Neill, L.A.J. (2018). Krebs Cycle Reimagined: The Emerging Roles of Succinate and Itaconate as Signal Transducers. Cell *174*, 780–784. https://doi.org/10.1016/j.cell.2018.07.030.

Muzik, O., Mangner, T.J., and Granneman, J.G. (2012). Assessment of Oxidative Metabolism in Brown Fat Using PET Imaging. Frontiers in Endocrinology *3*, 15. https://doi.org/10.3389/fendo.2012.00015.

Nakamura, K., and Morrison, S.F. (2007). Central efferent pathways mediating skin cooling-evoked sympathetic thermogenesis in brown adipose tissue. American Journal of Physiology - Regulatory Integrative and Comparative Physiology *292*, 127–136. https://doi.org/10.1152/ajpregu.00427.2006.

Nannipieri, M., Baldi, S., Mari, A., Colligiani, D., Guarino, D., Camastra, S., Barsotti, E., Berta, R., Moriconi, D., Bellini, R., et al. (2013). Roux-en-Y Gastric Bypass and Sleeve Gastrectomy: Mechanisms of Diabetes Remission and Role of Gut Hormones. The Journal of Clinical Endocrinology & Metabolism *98*, 4391–4399. https://doi.org/10.1210/jc.2013-2538.

Nauck, M.A., and Meier, J.J. (2018). Incretin hormones: Their role in health and disease. Diabetes, Obesity and Metabolism *20*, 5–21. https://doi.org/10.1111/dom.13129.

Nauck, M.A., Heimesaat, M.M., Orskov, C., Holst, J.J., Ebert, R., and Creutzfeldt, W. (1993). Preserved incretin activity of glucagon-like peptide 1 [7-36 amide] but not of synthetic human gastric inhibitory polypeptide in patients with type-2 diabetes mellitus. J Clin Invest *91*, 301–307. https://doi.org/10.1172/JCI116186.

Nedergaard, J., and Cannon, B. (2010). The Changed Metabolic World with Human Brown Adipose Tissue: Therapeutic Visions. Cell Metabolism *11*, 268–272. https://doi.org/https://doi.org/10.1016/j.cmet.2010.03.007.

Nedergaard, J., Bengtsson, T., and Cannon, B. (2007). Unexpected evidence for active brown adipose tissue in adult humans. American Journal of Physiology.Endocrinology and Metabolism *293*, E444-52. https://doi.org/00691.2006 [pii].

Nedergaard, J., Bengtsson, T., and Cannon, B. (2010). Three years with adult human brown adipose tissue. Ann N Y Acad Sci *1212*, E20–E36. https://doi.org/10.1111/j.1749-6632.2010.05905.x.

Nesterov, S. v., Deshayes, E., Sciagrà, R., Settimo, L., Declerck, J.M., Pan, X.-B., Yoshinaga, K., Katoh, C., Slomka, P.J., Germano, G., et al. (2014). Quantification of Myocardial Blood Flow in Absolute Terms Using 82Rb PET Imaging. JACC: Cardiovascular Imaging *7*, 1119–1127. https://doi.org/10.1016/j.jcmg.2014.08.003.

Nesterov, S. v., Turta, O., Han, C., Maki, M., Lisinen, I., Tuunanen, H., and Knuuti, J. (2015). C-11 acetate has excellent reproducibility for quantification of myocardial oxidative metabolism. European Heart Journal - Cardiovascular Imaging *16*, 500–506. https://doi.org/10.1093/ehjci/jeu289.

Nicholls, D.G., and Locke, R.M. (1984). Thermogenic mechanisms in brown fat. Physiological Reviews *64*, 1–64. https://doi.org/10.1152/physrev.1984.64.1.1.

Ohashi, K., Parker, J.L., Ouchi, N., Higuchi, A., Vita, J.A., Gokce, N., Pedersen, A.A., Kalthoff, C., Tullin, S., Sams, A., et al. (2010). Adiponectin promotes macrophage polarization toward an anti-inflammatory phenotype. Journal of Biological Chemistry *285*, 6153–6160. https://doi.org/10.1074/jbc.M109.088708.

Oikonen, V. (2014). TPC - Model for radiowater. WWW-document, accessed 5.10.2021 http://www.turkupetcentre.net/petanalysis/model_radiowater.html

Orava, J., Nuutila, P., Lidell, M.E., Oikonen, V., Noponen, T., Viljanen, T., Scheinin, M., Taittonen, M., Niemi, T., Enerback, S., et al. (2011). Different metabolic responses of human brown adipose tissue to activation by cold and insulin. Cell Metab *14*, 272–279. https://doi.org/10.1016/j.cmet.2011.06.012.

Orava, J., Nuutila, P., Noponen, T., Parkkola, R., Viljanen, T., Enerbäck, S., Rissanen, A., Pietiläinen, K.H., and Virtanen, K.A. (2013). Blunted metabolic responses to cold and insulin stimulation in brown adipose tissue of obese humans. Obesity *21*, 2279–2287. https://doi.org/10.1002/oby.20456.

Ouchi, N., Parker, J.L., Lugus, J.J., and Walsh, K. (2011a). Adipokines in inflammation and metabolic disease. Nature Reviews Immunology *11*, 85–97. https://doi.org/10.1038/nri2921.

Ouchi, N., Parker, J.L., Lugus, J.J., and Walsh, K. (2011b). Insulin resistance Adipokines in inflammation and metabolic disease. https://doi.org/10.1038/nri2921.

Ouellet, V., Labbé, S.M., Blondin, D.P., Phoenix, S., Guérin, B., Haman, F., Turcotte, E.E., Richard, D., and Carpentier, A.C. (2012). Brown adipose tissue oxidative metabolism contributes to energy expenditure during acute cold exposure in humans. Journal of Clinical Investigation *122*, 545–552. https://doi.org/10.1172/JCI60433.

Park, J., Kim, M., Sun, K., An, Y.A., Gu, X., and Scherer, P.E. (2017). VEGF-A–Expressing Adipose Tissue Shows Rapid Beiging and Enhanced Survival After Transplantation and Confers IL-4–Independent Metabolic Improvements. Diabetes *66*, 1479–1490. https://doi.org/10.2337/db16-1081.

Parks, D., Blanchard, S., Bledsoe, R., Chandra, G., Consler, T., Kliewer, S., Stimmel, J., Willson, T., Zavacki, A., Moore, D., et al. (1999). Bile acids: natural ligands for an orphan nuclear receptor. Science *284*, 1365–1368. https://doi.org/10.1126/SCIENCE.284.5418.1365.

Patlak, C.S., Blasberg, R.G., and Fenstermacher, J.D. (1983). Graphical Evaluation of Blood-to-Brain Transfer Constants from Multiple-Time Uptake Data. Journal of Cerebral Blood Flow & Metabolism *3*, 1–7. https://doi.org/10.1038/jcbfm.1983.1.

Peterson, C.M., Orooji, M., Johnson, D.N., Naraghi-Pour, M., and Ravussin, E. (2017). Brown adipose tissue does not seem to mediate metabolic adaptation to overfeeding in men. Obesity *25*, 502–505. https://doi.org/10.1002/OBY.21721.

Ravussin, E., and Galgani, J.E. (2011). The Implication of Brown Adipose Tissue for Humans. Annual Review of Nutrition *31*, 33–47. https://doi.org/10.1146/annurev-nutr-072610-145209.

Revelli, J.P., Muzzin, P., and Giacobino, J.P. (1992). Modulation in vivo of beta-adrenergic-receptor subtypes in rat brown adipose tissue by the thermogenic agonist Ro 16-8714. Biochemical Journal *286*, 743. https://doi.org/10.1042/BJ2860743.

Rezai-Zadeh, K., and Münzberg, H. (2013). Integration of sensory information via central thermoregulatory leptin targets. Physiology and Behavior *121*, 49–55. https://doi.org/10.1016/j.physbeh.2013.02.014.

Ricquier, D. (2005). Respiration uncoupling and metabolism in the control of energy expenditure. Proceedings of the Nutrition Society *64*, 47–52. https://doi.org/10.1079/pns2004408.

Rothwell, N.J., Stock, M.J., and Sudera, D.K. (1985). Beta-adrenoreceptors in rat brown adipose tissue: proportions of beta 1- and beta 2-subtypes. American Journal of Physiology - Endocrinology and Metabolism *11*. https://doi.org/10.1152/AJPENDO.1985.248.4.E397.

Rutland, M.D. (1979). A single injection technique for subtraction of blood background in 131 I-hippuran renograms. The British Journal of Radiology *52*, 134–137. https://doi.org/10.1259/0007-1285-52-614-134.

Saito, M., Minokoshi, Y., and Shimazu, T. (1989). Metabolic and sympathetic nerve activities of brown adipose tissue in tube-fed rats. American Journal of Physiology - Endocrinology and Metabolism *257*. https://doi.org/10.1152/AJPENDO.1989.257.3.E374.

Saito, M., Okamatsu-Ogura, Y., Matsushita, M., Watanabe, K., Yoneshiro, T., Nio-Kobayashi, J., Iwanaga, T., Miyagawa, M., Kameya, T., Nakada, K., et al. (2009). High Incidence of Metabolically Active Brown Adipose Tissue in Healthy Adult Humans. Diabetes *58*, 1526–1531. https://doi.org/10.2337/db09-0530.

Samra, J.S., Simpson, E.J., Clark, M.L., Forster, C.D., Humphreys, S.M., Macdonald, I.A., and Frayn, K.N. (1996). Effects of epinephrine infusion on adipose tissue: Interactions between blood flow and lipid metabolism. American Journal of Physiology - Endocrinology and Metabolism *271*. https://doi.org/10.1152/ajpendo.1996.271.5.e834.

Savisto, N., Viljanen, T., Kokkomäki, E., Bergman, J., and Solin, O. (2018). Automated production of [18F]FTHA according to GMP. Journal of Labelled Compounds and Radiopharmaceuticals *61*, 84–93. https://doi.org/10.1002/jlcr.3589.

Schlichtkrull, J., Munck, O., and Jersild, M. (1965). The M-value, an index of blood sugar control in diabetics. Acta Med Scand *177*, 95–102. https://doi.org/10.1111/J.0954-6820.1965.TB01810.X.

Schweitzer, L., Geisler, C., Pourhassan, M., Braun, W., Glüer, C.C., Bosy-Westphal, A., and Müller, M.J. (2015). What is the best reference site for a single MRI slice to assess whole body skeletal muscle and adipose tissue volumes in healthy adults? American Journal of Clinical Nutrition *102*, 58–65. https://doi.org/10.3945/ajcn.115.111203.

Seltzer, H., Allen, E., Herron, A., and Brennan, M. (1967). Insulin secretion in response to glycemic stimulus: relation of delayed initial release to carbohydrate intolerance in mild diabetes mellitus. J Clin Invest *46*, 323–335. https://doi.org/10.1172/JCI105534.

Sharp, L.Z., Shinoda, K., Ohno, H., Scheel, D.W., Tomoda, E., Ruiz, L., Hu, H., Wang, L., Pavlova, Z., Gilsanz, V., et al. (2012). Human BAT Possesses Molecular Signatures That Resemble Beige/Brite Cells. PLoS ONE *7*, e49452. https://doi.org/10.1371/journal.pone.0049452.

Shin, H., Ma, Y., Chanturiya, T., Cao, Q., Wang, Y., Kadegowda, A.K.G., Jackson, R., Rumore, D., Xue, B., Shi, H., et al. (2017). Lipolysis in Brown Adipocytes Is Not Essential for Cold-Induced Thermogenesis in Mice. Cell Metabolism *26*, 764-777.e5. https://doi.org/https://doi.org/10.1016/j.cmet.2017.09.002.

Singla, P. (2010). Metabolic effects of obesity: A review. World Journal of Diabetes *1*, 76. https://doi.org/10.4239/wjd.v1.i3.76.

Sjöström, L., Lindroos, A.-K., Peltonen, M., Torgerson, J., Bouchard, C., Carlsson, B., Dahlgren, S., Larsson, B., Narbro, K., Sjöström, C.D., et al. (2004). Lifestyle, diabetes, and cardiovascular risk factors 10 years after bariatric surgery. N Engl J Med *351*, 2683–2693. https://doi.org/10.1056/NEJMoa035622.

Slavin, B.G., and Ballard, K.W. (1978). Morphological studies on the adrenergic innervation of white adipose tissue. The Anatomical Record *191*, 377–389. https://doi.org/10.1002/ar.1091910310.

Stahl, A., Evans, J.G., Pattel, S., Hirsch, D., and Lodish, H.F. (2002). Insulin Causes Fatty Acid Transport Protein Translocation and Enhanced Fatty Acid Uptake in Adipocytes. Developmental Cell *2*, 477–488. https://doi.org/10.1016/S1534-5807(02)00143-0.

Stumvoll, M., Tschritter, O., Fritsche, A., Staiger, H., Renn, W., Weisser, M., Machicao, F., and Häring, H. (2002). Association of the T-G polymorphism in adiponectin (Exon 2) with obesity and insulin sensitivity: Interaction with family history of type 2 diabetes. Diabetes *51*, 37–41. https://doi.org/10.2337/diabetes.51.1.37.

Summers, L.K.M., Samra, J.S., Humphreys, S.M., Morris, R.J., and Frayn, K.N. (1996). Subcutaneous abdominal adipose tissue blood now: Variation within and between subjects and relationship to obesity. Clinical Science *91*, 679–683. https://doi.org/10.1042/cs0910679.

Sun, K., Kusminski, C.M., and Scherer, P.E. (2011). Adipose tissue remodeling and obesity. Journal of Clinical Investigation *121*, 2094–2101. https://doi.org/10.1172/JCI45887.

Sun, K., Asterholm, I.W., Kusminski, C.M., Bueno, A.C., Wang, Z. V., Pollard, J.W., Brekken, R.A., and Scherer, P.E. (2012). Dichotomous effects of VEGF-A on adipose tissue dysfunction. Proc Natl Acad Sci U S A *109*, 5874–5879. https://doi.org/10.1073/pnas.1200447109.

Sung, H.K., Doh, K.O., Son, J.E., Park, J.G., Bae, Y., Choi, S., Nelson, S.M.L., Cowling, R., Nagy, K., Michael, I.P., et al. (2013). Adipose vascular endothelial growth factor regulates metabolic homeostasis through angiogenesis. Cell Metabolism *17*, 61–72. https://doi.org/10.1016/j.cmet.2012.12.010.

Thondam, S.K., Daousi, C., Wilding, J.P.H., Holst, J.J., Ameen, G.I., Yang, C., Whitmore, C., Mora, S., and Cuthbertson, D.J. (2017). Glucose-dependent insulinotropic polypeptide promotes lipid deposition in subcutaneous adipocytes in obese type 2 diabetes patients: a maladaptive response. American Journal of Physiology-Endocrinology and Metabolism *312*, E224–E233. https://doi.org/10.1152/ajpendo.00347.2016.

Thondam, S.K., Cuthbertson, D.J., and Wilding, J.P.H. (2020). The influence of Glucose-dependent Insulinotropic Polypeptide (GIP) on human adipose tissue and fat metabolism: Implications for obesity, type 2 diabetes and Non-Alcoholic Fatty Liver Disease (NAFLD). Peptides (N.Y.) *125*, 170208. https://doi.org/10.1016/j.peptides.2019.170208.

Thörne, A., and Wahren, J. (1989). Beta-adrenergic blockade does not influence the thermogenic response to a mixed meal in man. Clinical Physiology *9*, 321–332. https://doi.org/10.1111/J.1475-097X.1989.TB00986.X.

Tilg, H., and Moschen, A.R. (2006). Adipocytokines: Mediators linking adipose tissue, inflammation and immunity. Nature Reviews Immunology *6*, 772–783. https://doi.org/10.1038/nri1937.

Toro-Ramos, T., Goodpaster, B.H., Janumala, I., Lin, S., Strain, G.W., Thornton, J.C., Kang, P., Courcoulas, A.P., Pomp, A., and Gallagher, D. (2015). Continued loss in visceral and intermuscular adipose tissue in weight-stable women following bariatric surgery. Obesity *23*, 62–69. https://doi.org/10.1002/oby.20932.

Trouwborst, I., Bowser, S.M., Goossens, G.H., and Blaak, E.E. (2018). Ectopic Fat Accumulation in Distinct Insulin Resistant Phenotypes; Targets for Personalized Nutritional Interventions. Frontiers in Nutrition *5*, 77. https://doi.org/10.3389/FNUT.2018.00077.

Turer, A.T., and Scherer, P.E. (2012). Adiponectin: Mechanistic insights and clinical implications. Diabetologia *55*, 2319–2326. https://doi.org/10.1007/s00125-012-2598-x.

U Din, M., Raiko, J., Saari, T., Kudomi, N., Tolvanen, T., Oikonen, V., Teuho, J., Sipilä, H., Savisto, N., Parkkola, R., et al. (2016). Human brown adipose tissue [15O]O2 PET imaging in the presence and absence of cold stimulus. European Journal of Nuclear Medicine and Molecular Imaging *43*, 1878.

U Din, M., Raiko, J., Saari, T., Saunavaara, V., Kudomi, N., Solin, O., Parkkola, R., Nuutila, P., and Virtanen, K.A. (2017). Human Brown Fat Radiodensity Indicates Underlying Tissue Composition and Systemic Metabolic Health. *102*, 2258–2267. https://doi.org/10.1210/jc.2016-2698.

Valassi, E., Scacchi, M., and Cavagnini, F. (2008). Neuroendocrine control of food intake. Nutrition, Metabolism and Cardiovascular Diseases *18*, 158–168. https://doi.org/10.1016/j.numecd.2007.06.004.

Vijgen, G.H.E.J., Bouvy, N.D., Teule, G.J.J., Brans, B., Schrauwen, P., and van Marken Lichtenbelt, W.D. (2011). Brown adipose tissue in morbidly obese subjects. PLoS One *6*, e17247. https://doi.org/10.1371/journal.pone.0017247.

Vijgen, G.H.E.J., Bouvy, N.D., Teule, G.J.J., Brans, B., Hoeks, J., Schrauwen, P., and van Marken Lichtenbelt, W.D. (2012). Increase in Brown Adipose Tissue Activity after Weight Loss in Morbidly Obese Subjects. The Journal of Clinical Endocrinology & Metabolism *97*, E1229–E1233. https://doi.org/10.1210/JC.2012-1289.

Virtanen, K.A., Lidell, M.E., Orava, J., Heglind, M., Westergren, R., Niemi, T., Taittonen, M., Laine, J., Savisto, N.-J., Enerbäck, S., et al. (2009). Functional Brown Adipose Tissue in Healthy Adults. New England Journal of Medicine *360*, 1518–1525. https://doi.org/10.1056/NEJMoa0808949.

Vosselman, M.J., Brans, B., van der Lans, A.A., Wierts, R., van Baak, M.A., Mottaghy, F.M., Schrauwen, P., and van Marken Lichtenbelt, W.D. (2013). Brown adipose tissue activity after a high-calorie meal in humans. The American Journal of Clinical Nutrition *98*, 57–64. https://doi.org/10.3945/ajcn.113.059022.

Vrieze, A., Schopman, J.E., Admiraal, W.M., Soeters, M.R., Nieuwdorp, M., Verberne, H.J., and Holleman, F. (2012). Fasting and postprandial activity of brown adipose tissue in healthy men. J Nucl Med *53*, 1407–1410. https://doi.org/10.2967/jnumed.111.100701.

Waldén, T.B., Hansen, I.R., Timmons, J.A., Cannon, B., and Nedergaard, J. (2012). Recruited vs. nonrecruited molecular signatures of brown, "brite," and white adipose tissues. American Journal of Physiology-Endocrinology and Metabolism *302*, E19–E31. https://doi.org/10.1152/ajpendo.00249.2011.

Walker, G.E., Marzullo, P., Ricotti, R., Bona, G., and Prodam, F. (2014). The pathophysiology of abdominal adipose tissue depots in health and disease. Hormone Molecular Biology and Clinical Investigation *19*, 57–74. https://doi.org/10.1515/hmbci-2014-0023.

Weinstock, P.H., Levak-Frank, S., Hudgins, L.C., Radner, H., Friedman, J.M., Zechner, R., and Breslow, J.L. (1997). Lipoprotein lipase controls fatty acid entry into adipose tissue, but fat mass is preserved by endogenous synthesis in mice deficient in adipose tissue lipoprotein lipase. Proceedings of the National Academy of Sciences *94*, 10261–10266. https://doi.org/10.1073/PNAS.94.19.10261.

Weir, J.B. de V. (1949). New methods for calculating metabolic rate with special reference to protein metabolism. The Journal of Physiology *109*, 1–9. https://doi.org/10.1113/jphysiol.1949.sp004363.

Weir, G., Ramage, L.E., Akyol, M., Rhodes, J.K., Kyle, C.J., Fletcher, A.M., Craven, T.H., Wakelin, S.J., Drake, A.J., Gregoriades, M.-L., et al. (2018). Substantial Metabolic Activity of Human Brown Adipose Tissue during Warm Conditions and Cold-Induced Lipolysis of Local Triglycerides. Cell Metab *27*, 1348-1355.e4. https://doi.org/10.1016/j.cmet.2018.04.020.

WHO (2019). Eurohealth: addressing obesity in Europe (Copenhagen PP - Copenhagen: World Health Organization. Regional Office for Europe).

Wickremesekera, K., Miller, G., Naotunne, T.D., Knowles, G., and Stubbs, R.S. (2005). Loss of Insulin Resistance after Roux-en-Y Gastric Bypass Surgery: a Time Course Study. Obesity Surgery *15*, 474–481. https://doi.org/10.1381/0960892053723402.

William, W.N., Ceddia, R.B., and Curi, R. (2002). Leptin controls the fate of fatty acids in isolated rat white adipocytes. Journal of Endocrinology *175*, 735–744. https://doi.org/10.1677/joe.0.1750735.

Williams, G., and Kolodny, G.M. (2008). Method for Decreasing Uptake of 18 F-FDG by Hypermetabolic Brown Adipose Tissue on PET. American Journal of Roentgenology *190*, 1406–1409. https://doi.org/10.2214/AJR.07.3205.

Wu, J., Boström, P., Sparks, L.M., Ye, L., Choi, J.H., Giang, A.-H., Khandekar, M., Virtanen, K.A., Nuutila, P., Schaart, G., et al. (2012). Beige Adipocytes Are a Distinct Type of Thermogenic Fat Cell in Mouse and Human. Cell *150*, 366–376. https://doi.org/10.1016/j.cell.2012.05.016.

Wu, X., Motoshima, H., Mahadev, K., Stalker, T.J., Scalia, R., and Goldstein, B.J. (2003). Involvement of AMP-activated protein kinase in glucose uptake stimulated by the globular domain of adiponectin in primary rat adipocytes. Diabetes *52*, 1355–1363. https://doi.org/10.2337/diabetes.52.6.1355.

Xue, B., Coulter, A., Rim, J.S., Koza, R.A., and Kozak, L.P. (2005). Transcriptional Synergy and the Regulation of Ucp1 during Brown Adipocyte Induction in White Fat Depots. Molecular and Cellular Biology *25*, 8311. https://doi.org/10.1128/MCB.25.18.8311-8322.2005.

Xue, B., Rim, J.-S., Hogan, J.C., Coulter, A.A., Koza, R.A., and Kozak, L.P. (2007). Genetic variability affects the development of brown adipocytes in white fat but not in interscapular brown fats. Journal of Lipid Research *48*, 41–51. https://doi.org/10.1194/JLR.M600287-JLR200.

Yamauchi, T., Kamon, J., Minokoshi, Y., Ito, Y., Waki, H., Uchida, S., Yamashita, S., Noda, M., Kita, S., Ueki, K., et al. (2002). Adiponectin stimulates glucose utilization and fatty-acid oxidation by activating AMP-activated protein kinase. Nature Medicine *8*, 1288–1295. https://doi.org/10.1038/nm788.

Yamauchi, T., Kamon, J., Ito, Y., Tsuchida, A., Yokomizo, T., Kita, S., Sugiyama, T., Miyagishi, M., Hara, K., Tsunoda, M., et al. (2003). Cloning of adiponectin receptors that mediate antidiabetic metabolic effects. Nature *423*, 762–769. https://doi.org/10.1038/nature01705.

Yao, X., Shan, S., Zhang, Y., and Ying, H. (2011). Recent progress in the study of brown adipose tissue. Cell & Bioscience *1*, 35. https://doi.org/10.1186/2045-3701-1-35.

Yeung, H.W.D., Grewal, R.K., Gonen, M., Schöder, H., and Larson, S.M. (2003). Patterns of 18F-FDG Uptake in Adipose Tissue and Muscle: A Potential Source of False-Positives for PET. Journal of Nuclear Medicine *44*, 1789 LP – 1796.

Yip, R.G.-C., Boylan, M.O., Kieffer, T.J., and Wolfe, M.M. (1998). Functional GIP Receptors Are Present on Adipocytes. Endocrinology *139*, 4004–4007. https://doi.org/10.1210/endo.139.9.6288.

Zechner, R., Zimmermann, R., Eichmann, T.O., Kohlwein, S.D., Haemmerle, G., Lass, A., and Madeo, F. (2012). FAT SIGNALS - Lipases and Lipolysis in Lipid Metabolism and Signaling. Cell Metabolism *15*, 279. https://doi.org/10.1016/J.CMET.2011.12.018.

Zhou, H., Yamada, Y., Tsukiyama, K., Miyawaki, K., Hosokawa, M., Nagashima, K., Toyoda, K., Naitoh, R., Mizunoya, W., Fushiki, T., et al. (2005). Gastric inhibitory polypeptide modulates adiposity and fat oxidation under diminished insulin action. Biochemical and Biophysical Research Communications *335*, 937–942. https://doi.org/10.1016/j.bbrc.2005.07.164.

Zingaretti, M.C., Crosta, F., Vitali, A., Guerrieri, M., Frontini, A., Cannon, B., Nedergaard, J., and Cinti, S. (2009). The presence of UCP1 demonstrates that metabolically active adipose tissue in the neck of adult humans truly represents brown adipose tissue. The FASEB Journal *23*, 3113–3120. https://doi.org/10.1096/fj.09-133546.

Zoico, E., Rubele, S., De Caro, A., Nori, N., Mazzali, G., Fantin, F., Rossi, A., and Zamboni, M. (2019). Brown and Beige Adipose Tissue and Aging. Front Endocrinol (Lausanne) *10*, 368. https://doi.org/10.3389/fendo.2019.00368.

Zwick, R.K., Guerrero-Juarez, C.F., Horsley, V., and Plikus, M. V (2018). Anatomical, Physiological, and Functional Diversity of Adipose Tissue. Cell Metabolism *27*, 68–83. https://doi.org/https://doi.org/10.1016/j.cmet.2017.12.002.

TURUN
YLIOPISTO
UNIVERSITY
OF TURKU

Painosalama, Turku, Finland 2022

ISBN 978-951-29-8883-9 (PRINT)
ISBN 978-951-29-8884-6 (PDF)
ISSN 0355-9483 (Print)
ISSN 2343-3213 (Online)